



**Università degli Studi della Calabria**

**Dottorato di Ricerca in Ingegneria Chimica e dei Materiali**  
*SCUOLA DI DOTTORATO " PITAGORA " IN SCIENZE INGEGNERISTICHE*

**Tesi**

**Preparation of Organic Solvent Resistant  
Polymeric Membranes for Applications  
in Non-aqueous Systems**

**Settore Scientifico Disciplinare CHIM07 – Fondamenti chimici delle tecnologie**

*Supervisori*

Ch.mo Prof. Enrico DRIOLI

*Candidato*

Eun Woo LEE

Ciclo XXIV

*Il Coordinatore del Corso di Dottorato*

Ch.mo Prof. Raffaele MOLINARI

---

*A.A. 2010-2011*

## List of contents

Summary.....	I
Sommario.....	IV
Acknowledgements .....	VII
<b>Chapter 1 An introduction on membrane technology.....</b>	<b>1</b>
1.1. Introduction .....	1
1.2. Membrane and membrane separation.....	3
1.2.1. Membrane materials.....	3
1.2.2. Membrane structures .....	4
1.2.3. Membrane modules.....	6
1.3. Membrane processes.....	10
1.4. Preparation of synthetic membranes .....	13
1.4.1. Phase inversion.....	13
1.4.1.1. Principle of membrane formation by phase inversion.....	15
1.5. Influence of various parameters on membrane morphology.....	21
1.6. Membrane characterization.....	25
1.6.1. Morphological analysis .....	25
1.6.2. Physicochemical parameters .....	27
1.6.3. Performance parameters .....	27
1.7. Transport mechanism.....	29
References .....	36
<b>Chapter 2 Solvent resistant membranes .....</b>	<b>41</b>
2.1. Solvent resistant nanofiltration membranes .....	41

2.1.1. Materials .....	45
2.1.2. Commercial membranes .....	48
2.1.3. Applications for industry .....	51
2.1.3.1. Food applications .....	51
2.1.3.2. Catalytic applications .....	52
2.1.3.3. Petrochemical applications .....	53
2.1.3.4. Pharmaceutical applications .....	55
2.1.4. Transport models for SRNF membranes in non-aqueous systems .....	55
2.2. Scope and outline of this study .....	61
References .....	64
<b>Chapter 3 Porous PDMS membranes .....</b>	<b>71</b>
3.1. Introduction .....	71
3.2. Experimental .....	73
3.2.1. Materials .....	73
3.2.2. Preparation of porous PDMS membranes .....	75
3.2.2.1. PDMS/Alcohols system .....	75
3.2.2.2. PDMS/Dioxane system .....	76
3.2.3. Membrane characterization .....	77
3.3. Results and discussion .....	78
3.3.1. PDMS/Alcohols system .....	78
3.3.1.1. Screening of effective additives .....	78
3.3.1.2. Effect of EG concentration .....	79
3.3.1.3. Effects of temperature of casting solution and the thermal post- treatment .....	81

3.3.2. PDMS/Dioxane system .....	84
3.3.2.1. Effect of Dioxane content .....	84
3.4. Conclusions .....	90
References .....	93

**Chapter 4 Polyimide asymmetric membranes**..... 95

4.1. Introduction .....	95
4.2. Experimental.....	96
4.2.1. Materials .....	96
4.2.2. Membranes preparation.....	99
4.2.3. Membrane permeation experiments.....	101
4.2.4. Membrane characterization.....	102
4.2.5. Ternary phase diagrams.....	103
4.3. Results and discussion.....	103
4.3.1. Effect of the polymer concentration .....	103
4.3.2. Effect of the concentration of volatile co-solvent.....	105
4.3.3. Permeation flux of pure solvents .....	109
4.3.4. Effect of the ionic charge, molecular weight and solvent type on membrane rejection .....	111
4.3.5. Effect of solvent type in the casting solution .....	113
4.3.6. Effect of non-solvent additives .....	118
4.3.7. Effect of different crosslinking conditions .....	123
4.4. Conclusions .....	127
References .....	129

**Chapter 5 Solvent resistant hollow fiber membranes**..... 133

5.1. Introduction .....	133
5.2. Experimental.....	135
5.2.1. Materials .....	135
5.2.2. Spinning of hollow fiber membranes .....	136
5.2.3. Chemical crosslinking (post-treatment) and module preparation .....	139
5.2.4. Characterization of hollow fiber membranes .....	139
5.2.4.1. Membrane morphology and chemical/mechanical properties .....	139
5.2.4.2. Nanofiltration test .....	140
5.3. Results and Discussion.....	142
5.3.1. Membrane morphology .....	142
5.3.2. Chemical and mechanical properties.....	145
5.3.3. Permeation properties .....	149
5.4. Conclusions .....	153
References .....	155
General conclusions.....	158

## Summary

Nowadays, membrane processes are used in a wide range of separation applications and the number of such applications is still rapidly growing. Since, today, environmental concerns have added impetus to the search for highly energy efficient and environmentally safe separation technologies. One of such technology which can meet these needs is the membrane separation, which offers significant reductions in energy consumption and eco-friendly process in comparison with conventional separation techniques.

The membrane processes which can operate in liquid non-aqueous environments have grown not only in academic interests but also in industrial applications. However, the transport mechanism of molecules of solvents and solutes through the polymeric membranes in non-aqueous system is much more complicated than that of in aqueous system. In non-aqueous system, the physical and chemical interaction between membrane, solute and solvents has to be taken into account. Even the transport mechanism is not fully understood it should be noted, however, that the recent intensive study on the development of new membranes and materials has resulted in commercially available membrane for organic solvent nanofiltration (OSN).

This study is focused on the preparation and characterization of polymeric membranes for uses in non-aqueous system. Polymeric membranes were prepared from poly(dimethyl siloxane) (PDMS) or copolyimide (P84, PI). To control the pore size and pore size distribution, optimum procedures and manufacturing parameters were established.

More detailed experimental conditions and results will be discussed in the following individual chapters.

Chapter 1 gives a general introduction on membrane and membrane process. In addition, the basic principles of membrane technology and theories necessary for understanding transport phenomena are discussed in this chapter.

In Chapter 2, more detailed background and review of literature on the organic solvent resistant membranes are discussed. Finally, clear scope and outline of this thesis will be covered in this chapter.

The fabrication and evaluation of the flat sheet poly(dimethyl siloxane) (PDMS) membranes are described in Chapter 3. Two different methods were used for the porous PDMS membranes. The first method was using chemical pore forming agent, alcohols (isopropanol, methanol, ethanol and ethylene glycol) and water, which can react with hydrogen molecule in crosslinker of PDMS to form hydrogen ( $H_2$ ) gas. Here, crosslinking speed of PDMS and reaction ( $H_2$  formation) and diffusion rate of  $H_2$  gas govern the structure and porosity of the membrane. The second method was using physical pore forming agent, 1,4-Dioxane, which was dispersed in PDMS solution then washed out after the film formation.

In Chapter 4, asymmetric P84<sup>®</sup> co-polyimide membranes in flat sheet configuration have been prepared and characterized. The effects of polymer concentration and solvent type on the performance and morphology of polyimide membranes have been intensively investigated. Furthermore, volatile co-solvent additive (1,4-Dioxane) and non-solvent

additives (water and ethanol) were used to prepare ternary mixture of casting solution and the effect on the membrane morphology and permeation properties were also investigated. The membrane performances were evaluated by organic solvents permeation experiments and rejection test using dyes which have different physical and chemical properties (molecular weight and charge).

The results evidenced that the morphology and also the membrane performances can be influenced by thermodynamic and kinetic effects during phase inversion process.

After membrane formation, to improve the chemical stability of the membrane, chemical crosslinking was conducted using 1,5-Diamino-2-methylpentane (DAMP). Crosslinking conditions were also optimized by controlling the concentration of crosslinker and crosslinking time. Crosslinked membranes were highly stable in numerous organic solvents including aprotic solvents (DMAc, DMF and NMP) in which the original polymer was soluble.

In Chapter 5, solvent resistant nanofiltration (SRNF) hollow fiber membranes were prepared from P84<sup>®</sup> co-polyimide by wet or dry-wet phase inversion methods. Furthermore, innovative in-line chemical crosslinking was carried out by introducing aqueous diamine (DAMP) solution as the bore fluid. Chemical and mechanical properties were analyzed by FT-IR/ATR and tensile strength measurement, respectively. In addition, permeation properties of the hollow fiber membranes were characterized by solvent flux and solute (Rhodamine B) rejection in acetonitrile and ethanol.



## Sommario

Operazioni a membrana sono oggi usate in numerosi processi di separazione e il numero di applicazioni è in rapida crescita anche grazie alla necessità di sviluppare nuovi processi sempre più eco-sostenibili. Le operazioni a membrana sono infatti caratterizzate da una più elevata efficienza energetica e minore impatto ambientale rispetto ai processi tradizionali di separazione.

In particolare, è evidente un crescente interesse sia accademico che industriale verso processi di separazione a membrana in fase liquida non acquosa. Tuttavia i meccanismi di trasporto del soluto attraverso membrane polimeriche in ambiente organico, sono molto più complicati che in fase acquosa a causa delle forti interazioni fisiche e chimiche tra membrana, soluto e solvente.

Nonostante i meccanismi di trasporto non siano stati completamente chiariti, sono attualmente disponibili membrane commerciali per nanofiltrazione in solventi organici (OSN).

Questo lavoro ha avuto come obiettivo la preparazione e caratterizzazione di membrane polimeriche da impiegare in separazioni in solventi organici.

Sono state preparate membrane polimeriche a base di polidimetilsilossano (PDMS) e un co-polimero della polimide (P84, PI).

Al fine di controllare la dimensione e distribuzione dei pori, è stato investigato l'effetto dei diversi parametri di preparazione e i dettagli sperimentali sono forniti nei capitoli seguenti

Nel Capitolo 1 è presentata una introduzione generale sulle membrane e i processi a membrana.

Nel Capitolo 2 è presentata una overview sullo stato dell'arte delle membrane polimeriche per separazioni in solventi organici, con particolare attenzione alle membrane da nanofiltrazione (SRNF).

Nel Capitolo 3 è descritta la preparazione di membrane piane porose a base di PDMS. Due differenti metodi sono stati seguiti: nel primo, per formare i pori delle membrane, sono state usate specie chimiche quali acqua, iso-propanolo, metanolo, etanolo e glicole etilenico, che producono idrogeno gassoso in situ mediante reazione con i gruppi Si-H del crosslinker usato per preparare il PDMS (polimero formato da reazione di idrosililazione fra un pre-polimero e un crosslinker). Nel secondo metodo è stato usato l'1,4-diossano come additivo in grado di formare i pori successivamente alla sua rimozione dalla membrana.

Nel Capitolo 4, è stata descritta la preparazione e caratterizzazione di membrane asimmetriche piane della co-polimide P84<sup>®</sup>. E' stato studiato l'effetto della concentrazione del polimero e del tipo del solvente sulla morfologia e proprietà di trasporto delle membrane.

E' stato inoltre investigato l'effetto della presenza di diverse concentrazioni di un co-solvente (1,4-diossano) o un non-solvente (acqua ed etanolo) nella soluzione polimerica.

Le proprietà di trasporto delle membrane sono state valutate in test di permeazione con solventi organici e di reiezione nei medesimi solventi con molecole modello quali coloranti a diversa massa molare e carica

Le membrane di P84<sup>®</sup> sono state reticolate, al fine di aumentarne la

stabilità, mediante reazione con 1,5-diamino-2-metilpentano (DAMP). Le condizioni di reticolazione sono state ottimizzate variando la concentrazione del reagente e il tempo di reazione. Le membrane reticolate sono risultate completamente stabili in numerosi solventi organici inclusi solventi come DMAc, DMF e NMP, in cui il polimero di partenza era solubile.

Nel Capitolo 5 è stata descritta la preparazione di fibre cave SRNF mediante inversione di fase indotta da non solvente, preceduta o meno, da una parziale evaporazione del solvente.

Inoltre è stata realizzata una innovativa procedura di reticolazione in cui durante la filatura il DAMP è stato introdotto nel fluido interno.

Le proprietà chimiche e meccaniche delle fibre sono state analizzate rispettivamente mediante FT-IR/ATR e test di elongazione. Inoltre sono stati condotti test di permeazione e reiezione usando la Rodamina B in acetonitrile ed etanolo.

## **Acknowledgements**

The research leading to these results has received funding from the European Community's Seventh Framework Programme [FP7/2007-2013] under grant agreement n° ITN 214226 NEMOPUR.

# **Chapter 1 An introduction to membrane technology**

## **1.1. Introduction**

Membrane technology has been used in numerous industrial applications. Membrane separation processes provide the following advantages [1-4] compared to conventional separation processes like distillation, crystallization, extraction, absorption and adsorption;

1. Membrane processes, in general, do not require phase changes during the transfer across membrane (except membrane distillation). As a result, energy requirements are relatively low.
2. Flexibility in equipment design and operations because the membrane systems are modular. Depending on the requirements, it is possible to increase and/or decrease the number of membrane modules (membrane area) to achieve target goals in a given separation.
3. The modular design of membrane process provides a compact footprint which minimizes space requirement and lower maintenance costs as well.
4. Membrane processes are eco-friendly process since they do not generate any second pollutants and do not need any additional chemicals for separation.
5. Membranes can be produced with high selectivity for the components to be separated. In some application, these values are much higher than conventional processes.

6. Membrane processes are able to recover minor but valuable components from a main stream without substantial energy costs.

In order to develop successful membrane processes, all individual core R&D factors (shown in Figure 1.1) starting from the selection of an appropriate material to process optimization and evaluation, including economic analysis, should be well integrated and perfectly optimized. Especially, material selection and preparation of membrane and modules with the optimum separation characteristics are the most important part in the whole process.

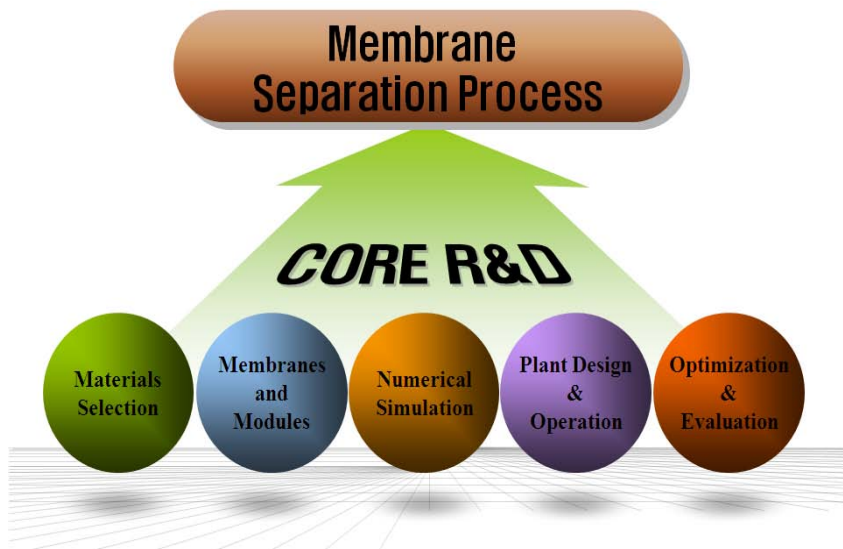


Figure 1.1. Core R&D factors for development of successful membrane process.

## **1.2. Membrane and membrane separation**

Although it is difficult to give an exact definition of a membrane, membrane can be defined as a selective or non-selective barrier that separates and/or contacts two adjacent phases and allows or promotes the exchange of matter and/or energy between the phases.

Separation through the membrane can be achieved by transporting certain component more rapidly than others by physicochemical affinity or interaction between membrane and species, applying appropriate driving forces such as concentration, pressure, temperature and electrical potential gradients, etc. [3].

### **1.2.1. Membrane materials**

Membranes can be classified by their nature, i.e. biological or synthetic membranes [1]. Synthetic membranes are further subdivided into organic (polymeric), inorganic (ceramics, metals and glass) and liquids [4].

Inorganic membranes have several useful properties such as their high mechanical stability and elevated resistance at high operating temperature with superior chemical resistance [5]. The long-term stability at high temperature makes these materials very attractive for gas separation at high temperature, especially in combination with a chemical reaction where the membrane is used as catalysts as well as a selective barrier to improve conversion rate by removing one of the components produced by reaction (membrane reactor). However, despite these beneficial properties, the most utilized membrane material is still

polymeric, since inorganic membranes are fairly brittle and much more expensive with respect to the membrane area compared to membranes produced from organic materials. Furthermore, high capital cost and sealing problem at high temperature should be solved [3].

As mentioned above, most commercially available membranes are prepared from polymeric materials. Basically, all polymers can be used as membrane material but the physical and chemical properties differ so much that only a limited number will be used in practice. The polymer materials not only have to resist acids, bases, oxidants or reductants, high pressures and high temperatures, but also must have appropriate chemical properties for realizing high flux and high selectivity membranes for the various applications. Furthermore, with polymeric membranes good processability, inexpensive production and easy modular design can be obtained. Therefore, it is important to understand the polymer properties such as structural factors - chain flexibility, molecular weight and chain interaction - that determine the thermal, chemical and mechanical characteristics of polymers [4].

### **1.2.2. Membrane structures**

Other than for the type of materials, with regard to the membrane morphology or structure, membranes can also be classified into symmetric and asymmetric membranes (Figure 1.2). Further, these classes can be categorized into porous and dense (non-porous) membranes.

The symmetric membrane can be cylindrical porous, porous and non-porous. The thickness of symmetric membranes ranges roughly from 10



to 200  $\mu\text{m}$ . The structure and the transport properties of symmetric membrane are identical over the entire cross-section and the thickness of the entire membrane determines the flux [3].

The asymmetric membranes can be 1) porous, 2) integrally skinned or 3) composite, that is consisting of a porous support layer and a dense top selective layer. The asymmetric membranes refer to the formation of a thin (typically 0.1-1.0  $\mu\text{m}$  in thickness) dense or porous layer which is bonded to a thick, porous substructure (100-200  $\mu\text{m}$  in thickness). In asymmetric membranes, porous substructure provides mechanical strength of the membrane while the separation takes place in selective porous or dense layer. It should be noted that the integrally skinned membrane uses same material for selective (dense) layer and sublayer. However, in composite membranes, the selective layer and support layer originate from different materials and each layer can be optimized independently.

Most porous membranes had been developed for size-based separation of mixtures in liquid phase, driven by a pressure difference or concentration difference. Based on its pore size, a porous membrane should be classified into microfiltration (MF: from 1.0 to 0.05  $\mu\text{m}$ ), ultrafiltration (UF: from 50 to 2 nm) and nanofiltration (NF: less than 2 nm) [3, 6]. In a dense membrane, the separation occurs through fluctuating free volume and a mixture of molecules is transported by concentration or electrical potential gradient. Dense membranes are mainly used to separate components which have similar size but have different chemical/physical nature in process such as reverse osmosis (RO), gas separation (GS), vapor permeation (VP) and pervaporation

(PV).

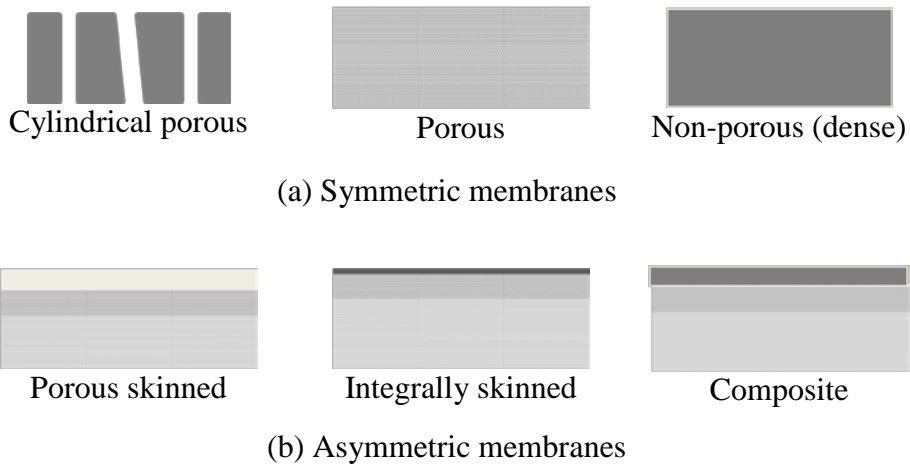


Figure 1.2. Schematic representation of various membrane structures.

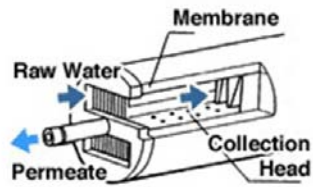
### 1.2.3. Membrane modules

The membranes can be fabricated as flat sheets, hollow fibers or capillaries and tubular membranes. Then, in order to use the prepared membranes on a practical scale, large membrane areas are normally required. The smallest unit in which a certain membrane area is packed is called a module. Modules are the smallest, replaceable unit in a membrane system, and housed in any appropriate cartridge or vessel configuration. The most commonly used module configurations for industrial applications are illustrated in Figure 1.3 [1, 7].

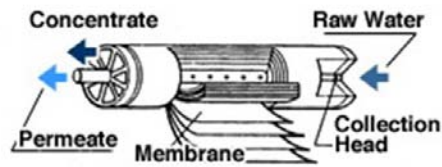
Flat sheet membranes are mainly installed in plate and frame or spiral-wound module configuration. In plate and frame module, the membranes, porous membrane support plates, and spacers are clamped together and

stacked layer by layer. In this module configuration, the membranes can easily be changed and the housings and other components are made from stainless steel so that the module can be steam sterilized. It makes this module configuration suitable for pharmaceutical, bio products, or fine chemicals applications. However, this unit is relatively expensive and the change of the membranes is labor intensive.

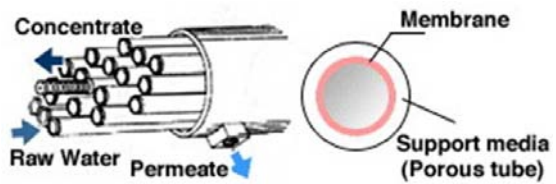
Spiral-wound module is widely used today in reverse osmosis, ultrafiltration, and gas/vapor separation. Commercial modules are about 1 meter length and have a diameter of 10 to 60 cm. The membrane area of these spiral-wound elements is 3 to 60 m<sup>2</sup> and 2 to 6 elements are placed in series in a pressure vessel. This module configuration provides a relatively large membrane area per unit volume. The large-scale production is quite cost effective and module cost per membrane area is quite low. Disadvantages of this module configuration are (a) quite sensitive to fouling, (b) the feed channels can easily be blocked, requiring additional care for pretreatment, and (c) the presence of spacer has a large influence on mass transfer and the pressure drop.



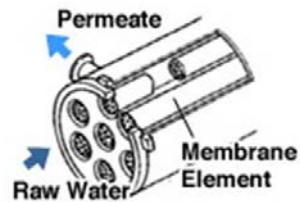
(a) Plate and frame module



(b) Spiral-wound module



(c) Tubular module



(d) Hollow fiber module

Figure 1.3. Schematic drawings and photos of various membrane module configurations.

In contrast to hollow fibers, tubular membranes are not self-supporting. Therefore, tubular membranes are placed into porous stainless steel or ceramic and fiberglass reinforced plastic pipes. The pressurized feed introduced through the bore and permeates are collected on the outer side of the porous support pipe. The main advantages of this module configuration are that concentration polarization and membrane fouling can be easily controlled. In addition, plugging of membrane module is avoided even with feed solution contains high concentration of solid matters or with high viscous systems. However, low packing density which leads to low membrane area and high cost remain a disadvantages.

The hollow fiber and capillary membrane modules have the highest packing density of all module configurations available on the market today. The diameter of the fibers varies over a wide range, from 50 to 3000  $\mu\text{m}$ . Particularly, fibers with a diameter greater than 500  $\mu\text{m}$  are called capillary fibers. Feed stream can flow through the lumen side (or inside) (inside to out) of the fiber or on the shell side (or outside) (outside to in). However, the main disadvantages of hollow fiber module configuration are the difficult control of concentration polarization and membrane fouling. Therefore, pretreatment processes are required and as a consequence main application of the hollow fiber membrane module configuration is in desalination of seawater, in gas separation and pervaporation in which the feed stream is relatively clean [1, 3].

Table 1.1 Advantages and disadvantages of module configuration [2, 8].

Module	Chanel spacing (cm)	Packing density ( $\text{m}^2/\text{m}^3$ )	Energy costs (pumping)	Particulate plugging	Ease of cleaning
Flat sheet	0.03-0.25	300	moderate	moderate	good
Spiral wound	0.03-0.1	600	low	very high	poor-fair
Tubular	1.0-2.5	60	high	low	excellent
Hollow fiber	0.02-0.25	1200	low	high	fair

### 1.3. Membrane processes

In the last few decades, numerous research papers have been reported on new membrane materials which have improved separation properties (high flux and high selectivity). These scientific efforts make that membrane operations can successfully substitute and/or integrate with conventional separation processes. In the early 1960's, a major breakthrough was achieved by the development of high performance asymmetric cellulose acetate membranes by Loeb and Sourirajan [9].

Today, 50 years later, membranes and membrane processes have indeed become valuable tools for the separation of molecular mixtures.

Membrane processes can be classified according to the driving forces into [1, 3, 10];

1) Pressure: microfiltration (MF), ultrafiltration (UF), nanofiltration (NF), reverse osmosis (RO), gas separation (GS).

2) Concentration gradient: gas separation (GS), vapor permeation (VP), pervaporation (PV), forward osmosis (FO) [11], pressure retarded osmosis (PRO) [12-13], membrane contactor (MC) and liquid membrane (accompanying reaction).

3) Electrical potential: electro dialysis (ED), electro-osmosis, electrophoresis.

4) Temperature difference: membrane distillation (MD).

However, it should be noted that in many membrane processes more than one driving force can work at the same time, and all these parameters (pressure, concentration, etc.) can be expressed by the electro-chemical potential.

Now, membrane processes are extending their application in a wide range of industrial processes [10]. For instance, seawater and brackish water desalination using reverse osmosis and electrodialysis are energy efficient and highly economic processes for large-scale production of potable water. Micro- and ultrafiltration are used for the production of high-quality industrial water and for the treatment of industrial effluents. In addition, membrane processes have found a multitude of applications in chemical and pharmaceutical industries as well as in food processing and biotechnology. They are used on a large scale in gas separation, vapor permeation and pervaporation. The development of membranes with improved properties will most likely increase the importance of membranes and membrane processes in a growing number of applications for the sustainable growth of modern industrial societies.

Table 1.2 Classification of membrane process and their applications[3].

Separation process	Membrane Type	Driving force	Method of separation	Range of application
Microfiltration	symmetric macroporous, 0.1-10 $\mu\text{m}$ pore radius	hydrostatic pressure difference 0.1-1 bar	sieving mechanism convection	water purification, sterilization
Ultrafiltration	asymmetric macroporous, 1-10 $\mu\text{m}$ pore radius	hydrostatic pressure difference (0.5-5 bar)	sieving mechanism convection	separation of molecular mixtures
Nanofiltration	asymmetric mesoporous, 0.5-2 nm	hydrostatic pressure (5-20 bar)	sieving mechanism diffusion Donnan exclusion	separation of molecular mixtures and ions
Reverse osmosis	integrally skinned asymmetric membrane or thin film composite (TFC)	hydrostatic pressure (20-100 bar)	solution-diffusion	separation of salts and microsolute from solutions
Dialysis	symmetric microporous, 0.1-10 $\mu\text{m}$ pore radius	concentration gradient	diffusion in convection free layer	separation of salts and microsolute from macromolecular solutions
Electro dialysis	symmetric ion exchange membranes	electrical potential gradient	Donnan exclusion	desalting of ionic solutions
Gas and vapor separation	dense homogeneous or porous polymer	gas and vapor pressure	solubility and diffusion, Knudsen diffusion	separation of gas mixture, vapors and isotopes
Pervaporation	dense homogeneous asymmetric	vapor pressure	solution-diffusion	separation of azeotropic mixtures



However, an important issue in membrane technology is not only improving the transport properties but also to achieve a high physical, chemical and thermal stability. That is why among the available polymeric materials only few are used for the preparation of commercial membranes [14].

#### **1.4. Preparation of synthetic membranes**

To obtain a membrane structure with morphology appropriate for a specific application, several techniques have been used for preparation of synthetic membranes. The most important techniques are sintering, track etching, stretching and phase separation processes. In particular, for the preparation of polymeric membranes related to this study, the phase inversion method will be introduced in detail.

##### **1.4.1. Phase inversion**

‘Phase inversion’ refers to the process in which a homogenous solution of a polymer in a solvent (or solvent mixture) inverts from a single phase into a two-phase system by a demixing process. The two-phase system consists of a polymer-rich phase which will form the membrane structure and a polymer-lean phase which will form the pores in the final membrane.

The phase separation of polymer solutions can be induced as follows [1, 4]:

1) Evaporation induced phase inversion (EIPS) - Precipitation by solvent evaporation:

In this method a polymer is dissolved in a solvent or a mixture of volatile solvent and a less volatile solvent. Then, the polymer solution is cast on a support. As the solvent evaporates from a cast film, the polymer rich phase develops and leads to the precipitation of the polymer (formation of skinned membrane).

2) Vapour induced phase inversion (VIPS) - Precipitation by absorption of non-solvent from the vapour phase:

A cast film, consisting of a polymer and a solvent, is placed in a vapour environment saturated with the non-solvent. The high concentration of the solvent in the vapour phase prevents evaporation of the solvent from the cast film and precipitation takes place when the non-solvent vapour penetrates into the film. Membrane formation occurs because of the diffusion of non-solvent into the cast film. This leads to a porous membrane without top-layer.

3) Thermally induced phase inversion (TIPS) - Precipitation by cooling:

A polymer melts in appropriate diluents at a temperature close to the melting point of the polymer increase of temperature. Demixing is induced when the temperature is decreased. After phase inversion, the diluent is removed by extraction, evaporation or freeze drying [15-16].

4) Non-solvent induced phase inversion (NIPS) - Precipitation in a non-solvent:

A polymer solution is cast on a suitable support and immersed in a coagulation bath containing a non-solvent. The prerequisite for this

method is that the solvent of the polymer and the non-solvent must be thoroughly miscible, while the polymer should not dissolve in the non-solvent. The exchange of solvent and non-solvent induces the precipitation of the polymer. This technique has widely used in preparation of commercially available flat sheet and hollow fiber membranes.

In the following sections, more details on the phase inversion mechanism will be discussed.

#### **1.4.1.1. Principle of membrane formation by phase inversion**

During the phase inversion process, the combination of steps leading to a given membrane structure involves a complex interaction of thermodynamic and mass transfer processes. Thermodynamic characteristics of the initial polymer solution and the immersion medium, combined with the kinetic effects of solvent/non-solvent mass transfer, thus determine the ultimate membrane structure in a complex way [17-18].

##### 1) Thermodynamics

All of the possible combination of three components - polymer, solvent and non-solvent - can be plotted in a ternary diagram. The corners represent the each pure component and three axes indicate three possible binary mixtures while a point in the triangle a ternary composition as shown in Figure 1.4 and Figure 1.5. A ternary phase diagram is very useful in the description of the thermodynamic

properties of a polymer/solvent/non-solvent system.

In the immersion precipitation process the cast layer becomes thermodynamically unstable (or metastable) and phase separation occurs. The three main demixing mechanisms are (Liquid-Liquid, L-L) binodal demixing (nucleation and growth), (Liquid-Liquid, L-L) spinodal decomposition and (Solid-Liquid, S-L) gelation (aggregation formation).

#### a) Binodal demixing (Liquid - Liquid)

In most phase inversion process, liquid-liquid demixing occurs when a system lower its free enthalpy of mixing by separating into two liquid phases [1, 19]. During membrane formation the composition changes from composition A, which represents the initial casting solution composition, to a composition C, which represents the final membrane composition. The position of composition C on polymer/non-solvent axis determines the overall porosity of the membrane. At composition C the two phases are in equilibrium: a polymer-rich phase, which forms the structure of the final membrane, represented by point S, and a polymer-lean phase, which constitutes the membrane pores filled with precipitant, represented by point L. The point B represents the concentration at which the polymer initially precipitates.

The line connecting all compositions with a common tangent plane to the Gibbs free energy of mixing is called the binodal. The binodal curve divides the system into two phases: one-phase region and two-phase region. When the coagulation path crosses the binodal curve, the system starts to separate through nucleation and growth mechanism or spinodal decomposition. The polymer solution phase separates by nucleation and

growth mechanism into polymer-rich phase (S in Figure 1.4) and polymer-lean phase (L in Figure 1.4) [20].

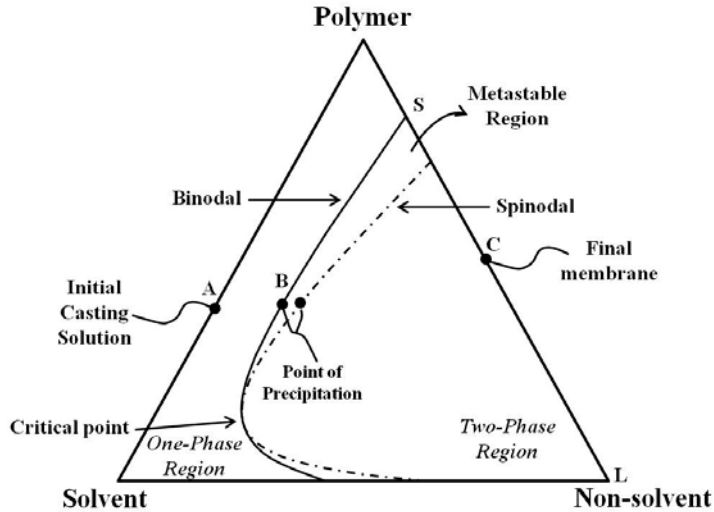


Figure 1.4. Three components phase diagram of isothermal immersion precipitation process [7].

In Figure 1.5, the phase diagram is divided into a homogeneous region (one-phase region) and an area representing a liquid-liquid demixing gap [16]. The liquid-liquid demixing gap is entered when a sufficient amount of non-solvent is added in the solution [21]. Phase inversion within the metastable area between binodal and spinodal (path A and C in Figure 1.5) is different from the inversion inside the unstable area (path B). The mechanism following path A or C is called nucleation and growth process (NG) and that following B is called spinodal decomposition (SD).

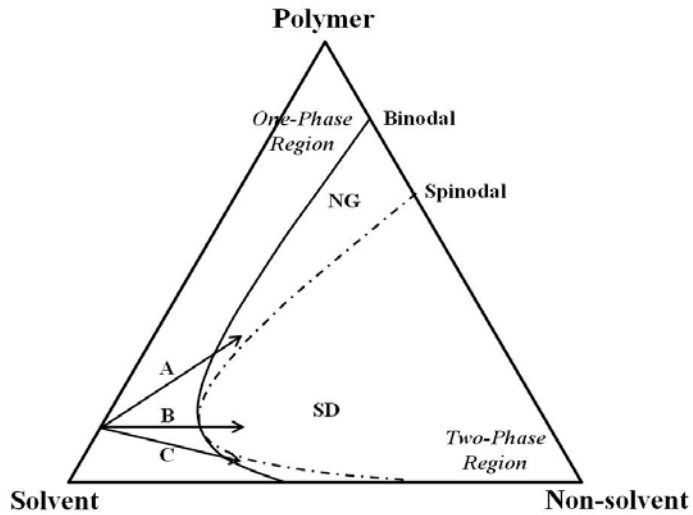


Figure 1.5. Different pathways of a binary casting solution into the miscibility gap of a ternary membrane forming system [2, 22].

When the precipitation pathway enters the two-phase region of the phase diagram above the critical point at which the binodal and spinodal lines intersect, precipitation will occur as growth of polymer-rich phase (path A). If very low concentration of polymer solution is used, in which the precipitation pathway enters the two-phase region of the phase diagram below the critical point, precipitation produces polymer gel particles in a continuous liquid phase. The membrane that forms has little mechanical strength (path C). It thus has to be recognized that only path A is convenient to give membranes [1, 7].

For thermodynamic evaluations of a membrane-forming system, the Flory-Huggins theory of polymer solutions [23], which has been extended to a ternary system containing non-solvent/solvent/polymer by Tompa [24], is usually used. Finally, binary interaction parameters of solvent/non-solvent, polymer/solvent and polymer/non-solvent

calculated from the Flory-Huggins relation is used to understand the structure and performance of a membrane prepared by immersion precipitation.

#### b) Spinodal demixing (Liquid - Liquid)

The mechanism, following the path B in Figure 1.5, is called spinodal decomposition (SD). This occurs whenever the homogeneous polymer solution directly moves to the thermodynamically unstable zone within the spinodal. Again, two different phases are formed, but instead of developing well-defined nuclei, two co-continuous phases will be formed [2, 25].

Spinodal decomposition is often believed to occur when large temperature gradients induce phase separation [26]. When phase separation is predominately induced via mass transfer it has previously been suggested that it cannot occur via spinodal decomposition [26-27].

#### c) Gelation (Solid - Liquid)

Gelation is a mechanism for fixing the membrane structure during membrane formation, especially for the formation of the top layer. (On the other hand, the porous sublayer is the result of liquid-liquid phase separation by nucleation and growth.)

A typical (S-L) demixing occurring in membrane formation involves crystallization of semi-crystalline polymers in the presence of a liquid phase. This process is referred to as gelation (or aggregation). The factor determining the type of phase separation at any point in the cast film is the local polymer concentration at the moment of precipitation. After

immersion there is a rapid depletion of solvent from the film and a relatively small penetration of non-solvent. This means that the polymer concentration at the film/bath interface increases and that the gel boundary is crossed [28].

## 2) Kinetic

Kinetics of phase separation can be explained by diffusion rate (exchange rate) between the solvent and non-solvent in polymer solution and coagulation bath [28-29].

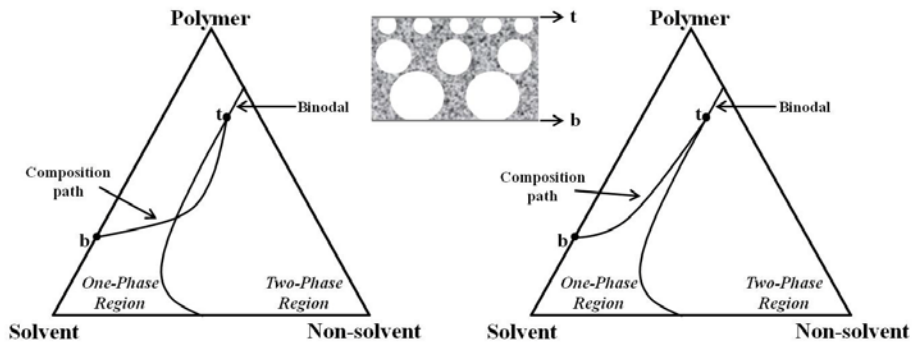


Figure 1.6. Schematic composition path of the cast film by the instantaneous demixing (left) and delaying demixing (right). t: the top of the film, b: the bottom of the film [1].

### a) Instantaneous and delayed demixing processes

Figure 1.6 shows the composition path of a polymer film immediately immersed in non-solvent bath after casting. After immersion of cast film, diffusion process between solvent and non-solvent starts from the top of the film (point t). In Figure 1.6 (left), the composition path from 'point t' already crossed the binodal, indicating that liquid-liquid demixing occur



immediately. It is called the instantaneous demixing.

In contrast, Figure 1.6 (right) indicates that composition path started from point t remains in the one-phase region of the phase diagram. This means that the no demixing starts immediately after immersion and it takes some time before the membrane is formed [18].

Two type of demixing process leads to different types of membrane morphology. When instantaneous demixing occurs, membrane can be formed very thin top layer and/or porous top layer with a sublayer of a lot of macrovoids. On the other hand, the membrane formed by delayed demixing has with very dense and thick top layer [1, 16].

### **1.5. Influence of various parameters on membrane morphology**

Membrane morphology is strongly influenced by the several factors such as the polymer type, composition of polymer solution and casting (or spinning) conditions including evaporation time, relative humidity and temperature of the air. Also, the compositions of coagulant and coagulation temperature are critical factors which can determine the membrane structure. More details on the effects of 1) the choice of solvent and non- solvent and 2) the composition of the polymer solution on membrane morphology will be discussed below.

#### **1) Choice of solvent and non-solvent**

In order to prepare membranes by immersion precipitation, not only perfect solubility of polymer in the solvent, but also the complete miscibility of the solvent and the non-solvent are the most important

factors must take into account.

When the mutual affinity (or miscibility) between the solvent and non-solvent is high, rapid solvent and non-solvent exchange occurs during the phase inversion process. It results in instantaneous demixing and forming the morphology with a thin top layer and a finger-like structure [30].

Conversely if there is low affinity between the solvent and non-solvent, then low miscibility will delay the onset of demixing and finally forming a dense and thick top layer. Ways to delay the onset of demixing includes the addition of solvent and/or additives into the coagulation bath or the introduction of additives to the dope solution. Polymeric, inorganic salts or even non-solvents of the polymer can be used as the additives for this purpose. In addition, an increase of the temperature in the coagulation bath leads to a higher exchange rate and a higher porosity. Also, the tendency to form macrovoids will be higher.

## 2) Composition of the polymer solution

### a) Concentration of the polymer

Increasing the initial polymer concentration in the polymer solution, a much higher polymer concentration at the polymer/non-solvent interface is obtained. Non-solvent inward diffusion is thus lowered and demixing delayed. Denser skins with increased thickness, low porosity of sublayer and lower fluxes is obtained. However, a low polymer concentration in the polymer solution causes a typical finger like structure implying that the volume fraction of polymer decreases due to instantaneous liquid-liquid demixing.

#### b) Pore forming additives

Membrane morphology can be controlled by the addition of pore forming additives like ionic salts (LiCl, ZnCl<sub>2</sub>) [31-32], organic acid (acetic acid, propionic acid) [33-35] and polymeric additive (poly(vinyl pyrrolidone) (PVP) [29, 31, 36], poly(ethylene glycol) (PEG) [35, 37]. These additives can also be added to control the viscosity of polymer solution and the evaporation rate. As a result, pore size and porosity of membrane will be modulated, as reflected in the solvent flux and the rejection. For example, the addition of ionic salts such as LiCl, ZnCl<sub>2</sub> and organic acid such as acetic acid, propionic acid causes macrovoid formation. The PVP affects the porosity increased and the macrovoids formation disappeared as adding to casting solution. It should be noted that the molecular weight of the polymeric additives also useful tool to control pore size of the membranes.

#### c) Addition of non-solvents

Non-solvents or low solubility solvents can be used to control the membrane porosity. By adding the non-solvents to the polymer solution, the film will become unstable. Hence, phase separation will occur quickly and equally throughout the film, thus formation of macrovoids [30, 38-41]. On the contrary, non-solvent additive could also suppress macrovoids formation and pores become very well interconnected due to fast diffusion of solvents from the casting film into the coagulation bath [42]. The amount of non-solvent additive should be controlled because amount of non-solvent added must be in the homogeneous region such that demixing does not occur and all the components should be

completely miscible with each other.

d) Addition of volatile (non-)solvents

To prepare integrally skinned asymmetric membranes with the dry-wet phase inversion, the evaporation step is decisive factor [43]. Addition of volatile solvent in the polymer solution occur an instantaneous destabilization in the outer most surface of the nascent film, resulting in a defect-free region with locally elevated polymer concentration. Accordingly, lower solvent permeances and higher rejections through membrane produced will be obtained.

Based on the factors reviewed above, it can be concluded that each specific membrane can be prepared by following the below instructions;

For MF and UF membranes,

- Low polymer concentration
- High mutual affinity between solvent and non-solvent
- Addition of non-solvent into the polymer solution
- Addition of the additives in the polymer solution

For NF membranes,

- Relatively higher polymer concentration than MF and UF
- Increase of evaporation time with addition of volatile solvent
- Decrease of exchange rate between solvent and non-solvent by reducing mutual affinity
- Controlling composition of coagulation bath with weak non-solvents

## **1.6. Membrane characterization**

Membrane process can be used in a wide range of separation applications with a specific membrane being required for every application. Thus, depend on the application, membranes may differ significantly in their structure, physical/chemical properties and permeation properties. Therefore, characterization of the membrane is one of the most important steps in membrane research and development.

In order to evaluate the membrane properties, different instrumental analysis methods can be adopted and each technique has unique power to characterize the membrane property. However, they can be divided into following three categories.

### **1.6.1. Morphological analysis**

#### **1) Microscopic techniques**

The main advantage of microscopic analysis is that direct visual information of the membrane morphology is obtained. Most commonly used technique is Scanning Electron Microscopy (SEM). SEM is a very convenient and simple method to obtain an image of the membrane structure by radiation of the sample with an electron beam. SEM has a resolution of up to 5 nm and provides good information on the structures including pore sizes and pore shape. Back-scattered electrons (BSE) are different image mode of SEM and beam electrons that are reflected from the sample by elastic scattering. Since heavy elements having high atomic number backscatter electrons more strongly than light elements (low atomic number), and thus appear brighter in the image, BSE images

can provide information about the distribution of different elements in the sample. In addition, Transmission Electron Microscopy (TEM) and Atomic Force Microscopy (AFM) are also frequently used to study membrane structure.

## 2) Pore size distribution or porometry

The pore size and pore size distribution of membrane are determined by bubble-point test, mercury intrusion method, BET (Brunauer-Emmett-Teller) and porometry method. These methods are very useful for porous membranes both polymeric and inorganic. Especially, the porometry method is measured the diameter of a pore at its most constricted part, the largest pore diameter, the mean pore diameter, the pore distribution, and gas permeability in a porous material. The pores in the sample are spontaneously filled with a wetting liquid. Pressure of an inert gas is slowly increased to remove liquid from pores and permits gas flow through the pores. Measured differential pressures and flow rates of inert gas through wet and dry conditions of the sample are used to compute the number of pores with a certain size. The mean pore size is given the point where the 50% 'dry' flow curve crosses the 'wet' flow curve [3].

## 3) FT-IR

Fourier Transform Infrared Spectroscopy (FT-IR) is frequently used for surface analysis and detects absorptions in the infrared region (4000-400  $\text{cm}^{-1}$ ). Especially this technique can be used to determine the functional chemistry of membrane surface. Functional groups in the

sample absorb energy at specific wavelengths, which results in an attenuated signal at the infrared detector. The infrared spectrum is measured interferometrically using a FT-IR spectrometer. The resulting absorption spectrum is a unique fingerprint of a compound [2].

### **1.6.2. Physicochemical parameters**

#### 1) Swelling

Swelling of membrane uses to know membrane porosity and provides significant influence for permeation performances of membrane. The swelling in dense membranes is evidenced by large permeate fluxes, whilst in porous membranes it could cause a low solvent permeation [44]. Because swelling under pressure would indicate the interaction between solvent and membrane thus polymer chain mobility, which usually results in compaction [45].

#### 2) Mechanical strength measurement

The tensile strength of the membrane is the stress needed to break the sample. After measuring the elongation of the sample at each stress level, tensile modulus can confirm through plot of stress-strain. If the slope is steep, the sample has a high tensile modulus, which means it resists deformation and is hard and brittle. If the slope is gentle, then the sample has a low tensile modulus, which means it is easily deformed and is ductile and tough [1].

### **1.6.3. Performance parameters**

The functional performance of a membrane can be defined by the flux

and rejection.

#### 1) Water and solvent permeation measurement

The simplest characterization experiment is the determination of the pure solvent flux. The solvent flux ( $J$ ,  $l/m^2/h$  or  $LMH$ ) through the membrane can be calculated from the correlation between the volumetric permeate ( $V$ ,  $l$ ) and membrane area ( $A$ ,  $m^2$ ) and unit time ( $t$ ,  $h$ ).

$$J = \frac{V}{A \times t} \quad (1.1)$$

However, compaction phenomena affect the flux declines as increasing pressure.

#### 2) Solute rejection measurements

Molecular weight cut-off (MWCO) is defined as the molecular weight which is 90 % rejected by the membrane. However, it is not absolute definition for the pore size of membrane, since the retention depends on a number of factors e.g. shape and flexibility of the solute, the interaction of solute with the membrane material, polarization phenomena and different test conditions (pressure, temperature, solvent type, concentration and type of solute), etc. [1].

The rejection ( $R$ ) is calculated by one of the following two equations [46].

$$R (\%) = \left( 1 - \frac{C_p}{C_r} \right) \times 100 \quad (1.2)$$



$$R (\%) = \left( 1 - \frac{C_p}{C_f} \right) \times 100 \quad (1.3)$$

where  $C_f$ ,  $C_p$  and  $C_r$  represent the concentration of solute in feed, permeate and retentate, respectively [47-48].

### 1.7. Transport mechanism

The principal property of membranes used in separation applications is their ability to control the permeation rate of different species [7, 41].

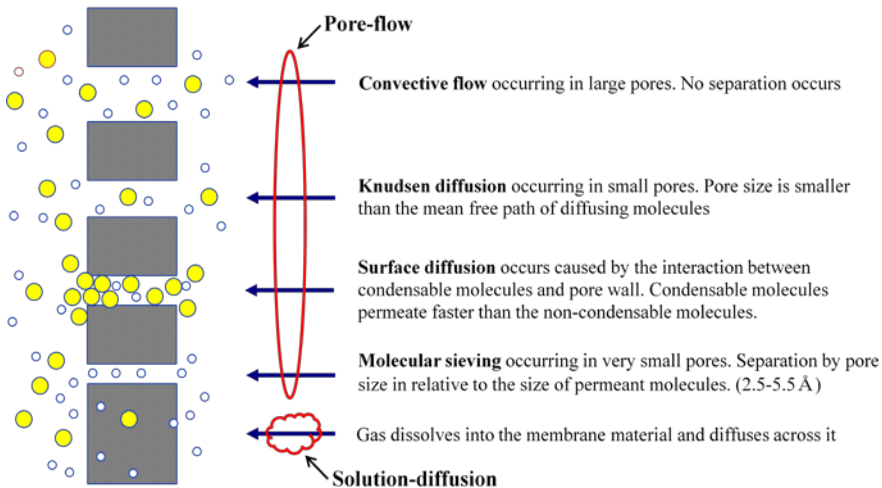


Figure. 1.7. Mechanisms for permeation solutes through porous and dense membranes [7].

To describe the permeation mechanism as shown in Figure 1.7, two different models can be used. One is the pore-flow model and the other model is the solution-diffusion model (Figure 1.8). The transport for the

micro- and macro-porous membranes such as ultrafiltration, microfiltration and Knudsen-flow gas separation occurs by pore-flow. On the other hand, the transport through membranes having a dense polymer layer with no visible pores, such as reverse osmosis, pervaporation and polymeric gas separation membrane are explained by the solution-diffusion model.

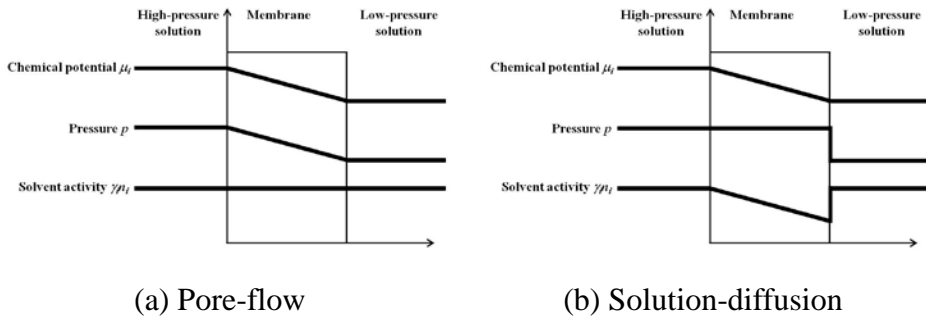


Figure. 1.8. Pressure-driven permeation of one component solution through a membrane according to the (a) pore-flow and (b) solution-diffusion models.

The driving forces of pressure, temperature, concentration, and electromotive force for movement of a permeant in membrane are expressed as the gradient in its chemical potential. Thus, the flux  $J_i$ , of a component,  $i$ , is described by following equation [49]:

$$J_i = -L_i \frac{d\mu_i}{dx} \quad (1.4)$$

where  $d\mu_i/dx$  is the gradient in chemical potential of component  $i$  and  $L_i$  is a coefficient of proportionality (not necessarily constant) linking

this chemical potential driving force with flux.

Restricting ourselves to driving forces generated by concentration and pressure gradients, the chemical potential is described as:

$$d\mu_i = RTd\ln(\gamma_i c_i) + v_i dp \quad (1.5)$$

where  $c_i$  is the molar concentration (mol/mol) of component  $i$ ,  $\gamma_i$  is the activity coefficient linking concentration with activity,  $p$  is the pressure, and  $v_i$  is the molar volume of component  $i$ .

The pore-flow model assumes that the concentrations of solvent and solute within a membrane are uniform and that the chemical potential gradient across the membrane is expressed only as a pressure gradient (Figure 1.8. (a)). By Combining Equation (1.4) and (1.5) the pore-flow model can be expressed as following equation.

$$J_i = -L_v \frac{dp}{dx} \quad (1.6)$$

This equation can be integrated across the membrane to give Darcy's law in which the permeability coefficient ( $k$ ) contains structural factors, like membrane pore size, surface porosity and tortuosity.

$$J_i = \frac{k(p_o - p_l)}{l} \quad (1.7)$$

where  $k$  is the Darcy's law coefficient, equal to  $L_v$ , and  $l$  is the membrane thickness.

The pore-flow model, in which permeants are separated by pressure-driven convective flow through tiny pores, has been proposed and developed by Sourirajan and Matsuura [50]. A separation is achieved between different permeants because one of the permeants is excluded (filtered) from some of the pores in the membrane through which other permeants move. Selectivity results from exclusion, based on incompatibility of molecule parameters such size, shape and charge, with the pores in the membrane [51].

The flow of a solvent through porous membranes which are assumed ideal cylindrical pores aligned normal to the membrane surface can be described in terms of a pore flow model [52].

$$J_v = \frac{\varepsilon_m d_p^2 \Delta p}{32 \mu l_p} \quad (1.8)$$

This equation can be used to describe the relationship between the solvent flux and applied pressure where  $J_v$  is the solvent flux,  $\varepsilon_m$  the membrane porosity,  $d_p$  the average pore diameter,  $\Delta p$  the transmembrane pressure,  $\mu$  the solvent viscosity and  $l_p$  the average pore length.

Some membranes have a structure of closely packed pores. In such cases the above equation might be modified for closed pores to give the Carmen-Kozeny equation [52]:

$$J = \frac{\varepsilon^3}{K \cdot \eta \cdot S^2 \cdot (1 - \varepsilon)^2} \frac{\Delta p}{\Delta x} \quad (1.9)$$

where  $J$  is the solvent flux,  $K$  the Kozeny constant,  $\varepsilon$  the membrane

porosity,  $S$  the surface area per unit volume,  $\Delta p$  the transmembrane pressure,  $\mu$  the solvent viscosity and  $\Delta x$  the membrane thickness, respectively.

The transport mechanism for gas separation can be described by Knudsen-flow. In porous membranes when gas transport takes place by viscous flow, no separation is achieved because the mean free path of the gas molecules is very small relative to the pore diameter. In the pore with the larger diameter the gas molecules have more interaction with each other than the pore diameter. By decreasing the diameter of the pores in the membrane, the mean free path of the gas molecules may become greater than the pore diameter. In the pore with the smaller diameter the gas molecules have more interactions with the pore wall than with each other. This kind of gas flow is called Knudsen-flow. The flux in Knudsen diffusion can be described by the following relation [3].

$$J = \frac{\pi n r^2 D_i^k \Delta p}{RT \tau \Delta z} \quad (1.10)$$

Here  $J$  is the flux through the membrane,  $n$  is the number of pores in the membrane,  $r$  is the pore radius,  $\Delta p$  is the transmembrane pressure,  $\Delta z$  is the thickness of the membrane,  $\tau$  is the tortuosity factor, and  $D_i^k$  is the Knudsen diffusion coefficient.

$$D_i^k = 0.66r \sqrt{\frac{8RT}{\pi M_i}} \quad (1.11)$$

Equation 1.11 shows that the Knudsen diffusion coefficient of a gas molecule is inversely proportional to the square root of its molecular weights. In the porous membrane low separation factors of Knudsen flow are generally obtained [53].

The solution-diffusion model was proposed by Lonsdale et al. [54] and has been revisited by Wijmans and Baker [49]. Basically, this model is useful to describe the transport of a gas, vapor or liquid through a dense (non-porous) membrane. The flux of different components through a membrane is assumed to be by sorption and by diffusion (Permeability (P) = Solubility (S)  $\times$  Diffusivity (D)). According to solution-diffusion theory, transport occurs by following three steps. (a) selective sorption of penetrant from upstream (or feed side) to membrane surface, (b) diffusion through the membrane from upstream to downstream due to the concentration difference, then (c) desorption from membrane to downstream (or permeate side). Solubility is a thermodynamic parameter and a measure of the amount of penetrant sorbed by the membrane under equilibrium conditions. In contrast, the diffusivity is a kinetic parameter which indicates how fast a penetrant is transported through the membrane.

This model assumes that the pressure within a membrane is uniform and that the chemical potential gradient across the membrane is expressed only as a concentration gradient (Figure 1.8. (b)). The flow that occurs down this gradient is again expressed by Equation (1.4), but, because no pressure gradient exists within the membrane, Equation (1.4) can be written, by combining Equations (1.4) and (1.5), as

$$J_i = -\frac{RTL_i}{c_i} \frac{dc_i}{dx} \quad (1.12)$$

This has the same form as Fick's law where the term  $RTL_i/c_i$  can be replaced by the diffusion coefficient  $D_i$ . Thus:

$$J_i = -D_i \frac{dc_i}{dx} \quad (1.13)$$

and integrating over the thickness of the membrane then gives,

$$J_i = \frac{D_i(c_{io(m)} - c_{il(m)})}{l} \quad (1.14)$$

## References

1. M. Mulder, *Basic principles of membrane technology*. 2<sup>nd</sup> ed. 1996, Dordrecht, The Netherlands: Kluwer Academic Publishers.
2. A.I. Schafer, A.G. Fane, and T.D. Waite, *Nanofiltration - Principles and applications*. 2005, Oxford: Elsevier Ltd.
3. H. Strathmann, L. Giorno, and E. Drioli, *An introduction to Membrane Science and Technology*. 2006, Roma: Ufficio Pubblicazioni e Informazioni Scientifiche.
4. M. Ulbricht, *Advanced functional polymer membranes*. *Polymer*, 2006. **47**: p. 2217-2262.
5. J. Wanqin, X. Nanping, and S. Jun, *Progress in inorganic nanofiltration membranes*. *Chinese Journal of Chemical Engineering*, 1998. **6**(1): p. 59-67.
6. M. Ulbricht and H. Susanto, *Porous Flat Sheet, Hollow Fibre and Capsule Membranes by Phase Separation of Polymer Solutions*, in *Membranes for Membrane Reactors*. 2011, John Wiley & Sons, Ltd. p. 491-510.
7. R.W. Baker, *Membrane Technology and Applications*. 2nd ed. 2004, England: John Wiley & Sons Ltd.
8. L.J. Zeman and A.L. Zydney, *Microfiltration and ultrafiltration: Principles and Applications*. 1997, New York: Marcel Dekker, INC.
9. S. Loeb and S. Sourirajan, *Sea Water Demineralization by Means of an Osmotic Membrane*, in *Saline Water Conversion-II*. 1963, American Chemical Society. p. 117-132.
10. K. Scott and R. Hughes, *Industrial Membrane Separation Technology*, K. Scott and R. Hughes, Editors. 1996, Blackie Academic & Professional: Glasgow. p. 1-7.
11. J.O. Kessler and C.D. Moody, *Drinking water from sea water by forward osmosis*. *Desalination*, 1976. **18**(3): p. 297-306.
12. S. Loeb, *Production of energy from concentrated brines by pressure-retarded osmosis : I. Preliminary technical and economic correlations*. *Journal of Membrane Science*, 1976. **1**: p. 49-63.
13. S. Loeb, F.V. Hessen, and D. Shahaf, *Production of energy from concentrated brines by pressure-retarded osmosis : II. Experimental results and projected*



- energy costs*. Journal of Membrane Science, 1976. **1**: p. 249-269.
14. R.W. Baker, *Future Directions of Membrane Gas Separation Technology*. Industrial & Engineering Chemistry Research, 2002. **41**(6): p. 1393-1411.
  15. S. Ramaswamy, A.R. Greenberg, and W.B. Krantz, *Fabrication of poly (ECTFE) membranes via thermally induced phase separation*. Journal of Membrane Science, 2001. **210**: p. 175-180.
  16. P. Witte, P.J. Dijkstra, J.W.A. Berg, and J. Feijen, *Phase separation processes in polymer solutions in relation to membrane formation*. Journal of Membrane Science, 1996. **117**: p. 1-31.
  17. Y.S. Kang, H.J. Kim, and U.Y. Kim, *Asymmetric membrane formation via immersion precipitation method. I. Kinetic effect*. Journal of Membrane Science, 1991. **60**: p. 219-232.
  18. A.J. Reuvers and C.A. Smolders, *Formation of membranes by means of immersion precipitation. Part II. The mechanism of formation of membranes prepared from the system cellulose acetate-acetone-water*. Journal of Membrane Science, 1987. **34**: p. 67-86.
  19. J.H. Kim, B.R. Min, J. Won, H.C. Park, and Y.S. Kang, *Phase behavior and mechanism of membrane formation for polyimide/DMSO/water system*. Journal of Membrane Science, 2001. **187**: p. 47-55.
  20. H.J. Kim, T. Mohammadi, A. Kumar, and A.E. Fouda, *Asymmetric membranes by a two-stage gelation technique for gas separation: formation and characterization*. Journal of Membrane Science, 1999. **161**: p. 229-238.
  21. A.F. Ismail, N. Ridzuon, and S.A. Raahman, *Latest development on the membrane formation for gas separation*. Journal of Science & Technology, 2002. **24**: p. 1025-1043.
  22. C. Barth, M.C. Gonçalves, A.T.N. Pires, J. Roeder, and B.A. Wolf, *Asymmetric polysulfone and polyethersulfone membranes: effects of thermodynamic conditions during formation on their performance*. Journal of Membrane Science, 2000. **169**: p. 287-299.
  23. P.J. Flory, *Principles of polymer chemistry*. 1953, Ithaca, New York: Cornell University Press.

24. H. Tompa, *Polymer solutions*. 1956, London: Butterworths.
25. P. Vandezande, L.E.M. Gevers, and I.F.J. Vankelecom, *Solvent resistant nanofiltration: separating on a molecular level*. Chemical Society Reviews, 2008. **37**: p. 365-405.
26. S.A. McKelvey and W.J. Koros, *Phase separation, vitrification, and the manifestation of macrovoids in polymeric asymmetric membranes*. Journal of Membrane Science, 1996. **112**(1): p. 29-39.
27. L.P. Cheng and C.C. Gryte, *Limitations on compositional changes during the isothermal mass transfer process in systems with limited miscibility*. Macromolecules, 1992. **25**(12): p. 3293-3294.
28. J.G. Wijmans, J.P.B. Baaiji, and C.A. Smolders, *The mechanism of formation of microporous or skinned membranes produced by immersion precipitation*. Journal of Membrane Science, 1983. **14**: p. 263-274.
29. A.F. Ismail and A.R. Hassan, *Effect of additive contents on the performances and structural properties of asymmetric polyethersulfone (PES) nanofiltration membranes*. Separation and Purification Technology, 2007. **55**: p. 98-109.
30. C.A. Smolders, A.J. Reuvers, R.M. Boom, and I.M. Wienk, *Microstructures in phase-inversion membranes. Part 1: Formation of macrovoids*. Journal of Membrane Science, 1992. **73**: p. 259-275.
31. E. Fontananova, J.C. Jansen, A. Cristiano, E. Curcio, and E. Drioli, *Effect of additives in the casting solution on the formation of PVDF membranes*. Desalination, 2006. **192**: p. 190-197.
32. E. Yuliwati and A.F. Ismail, *Effect of additives concentration on the surface properties and performance of PVDF ultrafiltration membranes for refinery produced wastewater treatment*. Desalination, 2011. **273**: p. 226-234.
33. W.-Y. Chuang, T.-H. Young, and W.-Y. Chiu, *The effect of acetic acid on the structure and filtration properties of poly(vinyl alcohol) membranes*. Journal of Membrane Science, 2000. **172**: p. 241-251.
34. M.-J. Han, *Effect of propionic acid in the casting solution on the characteristics of phase inversion polysulfone membranes*. Desalination, 1999. **121**: p. 31-39.
35. A. Mansourizadeh and A.F. Ismail, *Effect of additives on the structure and*

- performance of polysulfone hollow fiber membranes for CO<sub>2</sub> absorption.* Journal of Membrane Science, 2010. **348**: p. 260-267.
36. S.H. Yoo, J.H. Kim, J.Y. Jho, J. Won, and Y.S. Kang, *Influence of the addition of PVP on the morphology of asymmetric polyimide phase inversion membranes: effect of PVP molecular weight.* Journal of Membrane Science, 2004. **236**: p. 203-207.
  37. J.-H. Kim and K.-H. Lee, *Effect of PEG additive on membrane formation by phase inversion.* Journal of Membrane Science, 1998. **138**: p. 153-163.
  38. J.-Y. Lai, F.-C. Lin, C.-C. Wang, and D.-M. Wang, *Effect of nonsolvent additives on the porosity and morphology of asymmetric TPX membranes.* Journal of Membrane Science, 1996. **118**: p. 49-61.
  39. S.C. Pesek and W.J. Koros, *Aqueous quenched asymmetric polysulfone membranes prepared by dry/wet phase separation.* Journal of Membrane Science, 1993. **81**: p. 71-88.
  40. J. Ren, Z. Li, and F.-S. Wong, *Membrane structure control of BTDA-TDI/MDI (P84) co-polyimide asymmetric membranes by wet-phase inversion process.* Journal of Membrane Science, 2004. **241**: p. 305-314.
  41. D. Wang, K. Li, and W.K. Teo, *Relationship between mass ratio of nonsolvent-additive to solvent in membrane casting solution and its coagulation value.* Journal of Membrane Science, 1995. **98**: p. 233-240.
  42. I.-C. Kim, K.-H. Lee, and T.-M. Tak, *Preparation and characterization of integrally skinned uncharged polyetherimide asymmetric nanofiltration membrane.* Journal of Membrane Science, 2001. **183**: p. 235-247.
  43. A.F. Ismail and P.Y. Lai, *Effects of phase inversion and rheological factors on formation of defect-free and ultrathin-skinned asymmetric polysulfone membranes for gas separation.* Separation and Purification Technology, 2003. **33**: p. 127-143.
  44. J. Geens, B.V.d. Bruggen, and C. Vandecasteele, *Characterisation of the solvent stability of polymeric nanofiltration membranes by measurement of contact angles and swelling.* Chemical Engineering Science, 2004. **59**: p. 1161-1164.
  45. C. Linder, M. Perry, M. Nemas, and R. Katraró, *Solvent stable membranes.* 1991.
  46. Y.H.S. Toh, X.X. Loh, K. Li, A. Bismarck, and A.G. Livingston, *In search of a*

- standard method for the characterisation of organic solvent nanofiltration membranes.* Journal of Membrane Science, 2007. **291**: p. 120-125.
47. S.M. Dutczak, M.W.J. Luiten-Olieman, H.J. Zwijnenberg, L.A.M. Bolhuis-Versteeg, L. Winnubst, M.A. Hempenius, N.E. Benes, M. Wessling, and D. Stamatialis, *Composite capillary membrane for solvent resistant nanofiltration.* Journal of Membrane Science, 2011. **372**(1-2): p. 182-190.
  48. P. Vandezande, X. Li, L.E.M. Gevers, and I.F.J. Vankelecom, *High throughput study of phase inversion parameters for polyimide-based SRNF membranes.* Journal of Membrane Science, 2009. **330**: p. 307-318.
  49. J.G. Wijmans and R.W. Baker, *The solution-diffusion model: a review.* Journal of Membrane Science, 1995. **107**: p. 1-21.
  50. S. Sourirajan and T. Matsuura, *Reverse Osmosis/Ultrafiltration Principles.* 1985, Ottawa, Canada: National Research Council of Canada.
  51. D.A. Patterson, A. Havill, S. Costello, Y.H. See-Toh, A.G. Livingston, and A. Turner, *Membrane characterisation by SEM, TEM and ESEM: The implications of dry and wetted microstructure on mass transfer through integrally skinned polyimide nanofiltration membranes.* Separation and Purification Technology, 2009. **66**: p. 90-97.
  52. P. Silva, S. Han, and A.G. Livingston, *Solvent transport in organic solvent nanofiltration membranes.* Journal of Membrane Science, 2005. **262**: p. 49-59.
  53. M.T. Ravanchi, T. Kaghazchi, and A. Kargari, *Application of membrane separation processes in petrochemical industry: a review.* Desalination, 2009. **235**: p. 199-244.
  54. H.K. Lonsdale, *Transport properties of cellulose acetate membranes to selected solutes.* Journal of Applied Polymer Science, 1965. **9**: p. 1341-1362.

## **Chapter 2 Solvent resistant membranes**

### **2.1. Solvent resistant nanofiltration membranes**

Nanofiltration (NF) is similar to ultrafiltration (UF) and to reverse osmosis (RO). In all three membrane process, a hydrostatic pressure is applied as a driving force [1]. In addition, the solvent and low molecular weight solutes can permeate the membrane while high molecular weight molecules are retained by the membrane. The main difference between UF and NF is the pore size of the membrane. NF membranes are the same as RO membranes only the network structure is more open [1-2]. Moreover, it should be noted that the NF and eventually also RO membranes carry positive or negative electric charge at the surface. Brief comparison between the processes is summarized in Table 2.1.

The applications of nanofiltration membranes with molecular weight cut-off (MWCO) ranging 200-1000 g/mol have been increased due to the advantages of low energy consumption and no phase change [3]. Especially, since Sourirajan reported the first application of membranes to non-aqueous system in 1964, major oil company and chemical company began to file patents on the use of polymeric membranes to separate molecules from organic solution [4]. Today, the interests of nanofiltration process have been increased in various industrial sectors such as fine chemical, pharmaceutical, food and petrochemical industries [1, 5-7]. The separation of these substances, which is being done by highly energy-consuming evaporation techniques, could be proposed by membrane processes especially with “SRNF membranes” due to

economical, ecological advantages and safety issues [8-9]. In this case solutes including low molecular-weight are rejected, the solvent is removed, and it can be reused in the process.

Table 2.1 Comparative rejection value of RO, loose RO, NF and UF [8].

Species	RO	Loose RO	NF	UF
Sodium chloride	99%	70-95%	0-70%	0%
Sodium sulfate	99%	80-95%	99%	0%
Calcium chloride	99%	80-95%	0-90%	0%
Magnesium sulfate	>99%	95-98%	>99%	0%
Sulphuric acid	98%	80-90%	0-5%	0%
Hydrochloric acid	90%	70-85%	0-5%	0%
Fructose	>99%	>99%	20-99%	0%
Sucrose	>99%	>99%	>99%	0%
Humic acid	>99%	>99%	>99%	30%
Virus	99.99%	99.99%	99.99%	99%
Protein	99.99%	99.99%	99.99%	99%
Bacteria	99.99%	99.99%	99.99%	99%

The advantages of SRNF application are numerous. In most cases, additives aren't needed, and separations don't involve any phase transition. Thermal damage, resulting in degradation and side reactions, can be minimized during the separation due to the low temperature of operation compared with distillation. Possibilities are created to recycle solvents and/or valuable compounds and to lower losses or exhausts. Energy consumption is low as compared with alternative unit operations like distillation and crystallization. Thermal solvent exchanges can be performed, allowing to swap from a high-boiling to a low-boiling solvent. SRNF can be installed easily as a continuous process, and just like any other membrane separation, it can be combined readily with existing processes into a hybrid process. The latter can be attributed to its modular set-up, which also renders up-scaling relatively simple [9].

In general, there are two main fields of application for SRNF membranes [10].

- Treatment of industrial waste water streams which either contain high concentrations of organic solvents or require higher temperature of extreme pH resistance (e.g. landfill leaches, paint and dye stuff waste waters)

- Treatment of non-aqueous systems, like edible oil separation from solvents, recovery of homogeneous catalysts from organic solvents, separation of oligomers and polymers from solvents, and treatment of lubricating oils

There are, however, a number of problems in developing solvent stable membranes for these fields, i.e., the need to provide: 1) membrane stability, 2) economically favorable fluxes by optimizing a different

membrane for each solvent class, and 3) membrane selectivity that vary from one solvent to another in solvent mixtures.

The origin of the flux and selectivity problems lies in solvent and membrane interactions, the solution-diffusion transport mechanism, and the many different solvents with a wide range of hydrophobicity and hydrophilicity balances, viscosities and surface tension.

The SRNF membranes which can operate in non-aqueous system, including aprotic solvents, require a superior chemical, mechanical and thermal stability with high rejection and high flux [2, 9, 11-13]. For these demands, SRNF membranes have been made from inorganic, polymeric or a combination of the two materials [14-15]. The inorganic membranes (especially ceramic membranes) have been prepared by coating ceramic UF membrane with inorganic nanoparticles, followed by sintering or by a sol-gel process [8, 16]. These membranes are neither dissolve nor swell even slightly in any organic solvent. Also, they do not deform under high pressure and can be easily cleaned. In spite of advantages of inorganic membranes, the use of polymeric membranes for separations in organic solvents has been suggested by a growing number of authors, but practical application is usually limited because of solvent stability and lower rejections of solutes in comparison with the rejections obtained in aqueous solution and low solvent fluxes at enhanced solute concentrations [17]. However, the low cost and easy processability with reproducibility of the membrane fabrication process make polymeric materials very attractive for preparation of SRNF membranes. Several different polymeric materials have been reported for the preparation of organic solvent resistant membranes such as



polyacrylonitrile (PAN), polydimethylsiloxane (PDMS), polybenzimidazole (PBI), polysulfonamide (PSA), poly(*p*-phenylene terephthalamide), poly(imide siloxane), poly(1-(trimethylsilyl)-1-propyn), and polyimides (PIs) [2, 18-25].

Most polymeric SRNF membranes have an asymmetric structure, and can be divided into two types: the integrally skinned asymmetric structure and the thin film composite (TFC) types. As explained in previous chapter, the whole membrane is composed of the same material for integrally skinned asymmetric membrane while the selective layer is made of a different material from the supporting porous matrix for TFC membrane.

### **2.1.1. Materials**

#### **a) Poly(dimethyl siloxane) (PDMS)**

PDMS has been also widely studied for organic solvent application due to its superior properties such as high hydrophobicity, low surface tension, high thermal and chemical stability, high biocompatibility and elastomeric behavior [26-27] than other commonly used polymeric materials. Despite its broad chemical stability and its frequent use in SRNF application, the extensive swelling of PDMS in organic solvents, is an important issue which limits its utility in some polar solvents. The PDMS membranes as a SRNF have been reported from various applications, for example, homogeneous catalyst recovery [28] and the de-acidification of vegetable oil [29].

#### b) Polyimides (PIs)

Polyimides membranes can be easily crosslinked during membrane formation [30-31] and/or after membrane formation through the chemical [12, 31-33], thermal [34] and irradiation [26, 35] methods. Crosslinked membranes show excellent stability in various organic solvents including *N*-methyl-2-pyrrolidone (NMP), dimethylformamide (DMF) and dimethylacetamide (DMAc) used as solvents to dissolve polymer for the preparation of membrane. The SRNF PI membranes have been reported from various applications, for example, developments in oil processing [29, 36-40], separation of amino acids from organic solvents [41], removal of solubilized catalysts from reaction mixtures [28, 42-48], etc.

#### c) Polyamide (PA)

Polyamide membranes are also suitable for the treatment of non-aqueous system. Bhanushali et al. [49] and Yang et al. [50] reported on solvent fluxes through Desal-5, Desal-DK commercial membranes made from PA.

#### d) Polybenzimidazole (PBI)

PBI is a membrane polymer with outstanding chemical resistance. Chemical modification of PBI membranes renders stability in polar solvents. The reaction of PBI with strong polybasic acids dissolved in weak acids, for example perfluoroglutaric acid, sulfuric acid or pyromellitic acid in glacial acetic acid, results in membranes with improved solvent stability [8].

#### e) Polyacrylonitrile (PAN)

PAN is commonly used membrane material for water treatment process, but is also attractive as a material for solvent resistant membranes because it is quite stable in aromatic and aliphatic hydrocarbons, chlorinated solvents, and ketones. However it cannot be used in solvents like DMF, DMAc or NMP. To improve its stability, the prepared PAN membranes can be post-treated by crosslinking process [9]. Then crosslinked PAN-based membranes often used as the solvent resistant UF membrane or support layer for TFC membranes. For instance, Koch Membrane Systems (USA) provides a UF membrane (MWCO 20,000 g/mol), based on crosslinked PAN in flat sheet and spiral wound elements. In addition, it is believed that the MPF series from the same supplier uses crosslinked PAN support to fabricate SRNF membranes [4]. The limited use of PAN as the SRNF membrane is that it is not feasible to reduce pore size in NF range by phase inversion method. Therefore, additional modification process such as heat treatment in the presence of  $ZnCl_2$  is required to transform the UF PAN membrane to NF membranes.

#### f) Poly(1-trimethylsilyl-1-propyn) (PTMSP)

PTMSP, a hydrophobic glassy polymer with an extremely high free-volume (up to 25%), was coated on a commercial cellophane film, showed higher ethanol permeability than two silicone-based, commercially available SRNF-membranes (MPF-50 and Membrane D), while rejection was highly dependent on solute charge [22].

Not only the polymers discussed above but also some more polymeric materials such like polyphosphazenes (PPz), poly(vinyl alcohol)(PVA) and polyetheretherketone (PEEK) are potential materials for solvent stable nanofiltration membranes.

### **2.1.2. Commercial membranes**

Solvent resistant nanofiltration process is relatively new process compare to the membrane process for aqueous system. However, to the best of our knowledge, after extensive research on the development of membrane materials and membrane process for SRNF applications, five companies provide polymeric SRNF membranes.

#### **a) Koch SelRO<sup>®</sup> membranes**

Koch Membrane Systems (USA) was the first company to enter the SRNF market with three different membranes designed for solvent applications [4]. Koch introduced the SelRO<sup>®</sup> membranes which are stable in aqueous solutions with pH between 0 to 14 as well as in most organic solvents at temperatures up to a maximum 70 °C. The hydrophobic MPF60 membranes (MWCO 400 Dalton (Da), based on rejection of Sudan IV (384 Da) in acetone) [2], the hydrophobic MPF50 (MWCO 700 Da, based on rejection of Sudan IV in ethyl acetate (EA)) [3, 51-53] and the hydrophilic MPF44 membrane (MWCO 250 Da, based on rejection of glucose (180 Da) in water) [53] have been studied.

It is not clear which polymers are used for these membranes. However, MPF50 was known as membrane composed a dense silicon-based top layer and has been widely used for examination of transport mechanism

with hydrophobic and dense membrane. Koch also distributes an UF membrane (nominal MWCO 20,000 Da), based on crosslinked PAN, available in both flat sheet (MPF U20S) and spiral-wound (MPS U20S) elements, claimed to be stable in various solvents [9].

#### b) Starmem<sup>TM</sup> membranes

Another important class of commercial SRNF membranes is the Starmem<sup>TM</sup> series, a trademark of W.R. Grace-Davison (USA). Four types of Starmem<sup>TM</sup> series are hydrophobic membranes and all PI based. These membranes are claimed to be stable in alcohols, alkanes, aromatics, ethers, ketones and esters. Starmem<sup>TM</sup> membranes have distinct MWCOs (based on 90% rejection of n-alkanes in toluene) of 200 Da (Starmem<sup>TM</sup> 120) [53], 220 Da (122) [51-52], 280 Da (228) [3] and 400 Da (240) [53]. All membranes are available as flat sheets, pre-cut discs or spiral-wound elements. Starmem<sup>TM</sup> membranes tested in petrochemical industry for recovery of solvent from lube oil dewaxing process [40] and also applied for separation of catalysts [54] in pharmaceutical manufacturing process.

#### c) SolSep membranes

SolSep (The Netherlands) is commercializing several NF membranes with different stabilities and nominal MWCO values (based on 95% rejection) between 300 and 750 Da, and one UF membrane with a MWCO around 10,000 Da. Chemical stability is claimed in alcohols, esters and ketones and for some membranes also in aromatics and chlorinated solvents. SolSep membranes are applicable at pressures and

temperatures up to 40 bar and 150 °C respectively [55].

d) Osmonics Desal-5 and Desal-DK

Desal-5 and Desal-DK, manufactured by GE/Osmonics (USA), are PA based hydrophilic membranes with a relatively dense structure, showing rejections for sucrose (342 Da) around 96%. According to Petersen, Desal-5 is a composite membrane consisting of a poly(piperazine amide) barrier layer on top of a microporous polysulfone (PSf) support between which an additional sulfonated PSf layer has been applied [56]. The chemical stability of Desal-DK in solvents has been reported to be limited, showing severe damage after exposure to EA and toluene. Desal-5 on the other hand remained intact with rejections for Solvent Blue (350 Da) of 9, 28 and 41%, in toluene, EA and methanol respectively [50].

e) DuraMem™

Membrane Extraction Technology (UK, now a division of Evonic) developed integrally asymmetric crosslinked PI-based SRNF membranes. These membranes are available with different MWCO ranges (180-1,200 Da) and show excellent stability in a range of solvents including aprotic solvents such as NMP and DMF. Long term stability of the membrane was tested by continuous operating of the process for 120 hours in DMF THF and the experimental results confirmed the chemical stability and stable performances (stable fluxes and good separation properties) [4].

### **2.1.3. Applications for industry**

The feasibility of using polymeric SRNF membranes for non-aqueous system has been explored for various applications at lab scale [38]. In addition, some of the applications have been scaled up to industrial level [57]. Examples include solvent dewaxing [40, 57], solvent exchange [58], organometallic catalyst recovery [47], and deacidification of vegetable oils [29].

#### **2.1.3.1. Food applications**

Most processes in the food industry are carried out in aqueous system, but in some cases the use of organic solvents is required. For instance, in the vegetable oil industry or in the synthesis of amino acids and their derivatives which are commonly used as the additives.

##### **a) Edible oil processing**

Crude vegetable oils are commonly prepared by pressing the seeds, followed by a solvent extraction, mostly with hexane. The obtained oil fraction contains not only edible oil but also undesirable components such as phospholipids, free fatty acids, pigments and proteins, which should be removed. The membrane separation process can be used for the removal of phospholipids and pigments (degumming), the recovery of extraction solvents and the deacidification of the oil. Also, implementation of membrane separation could lead to significant energy savings. It has been estimated that introduction of membrane technology in edible oil processing could potentially save 15–22 trillion kJ per year of energy in the USA alone, while reducing oil losses by 75%,

improving the oil quality, and minimizing thermal damage [9].

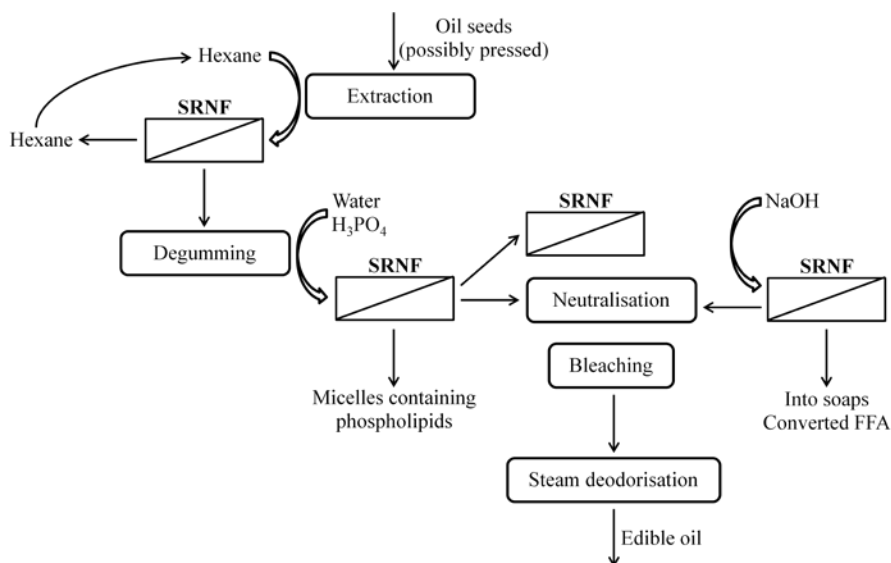


Figure 2.1. General scheme for edible oil processing with possible opportunities to implement SRNF [9].

### 2.1.3.2. Catalytic applications

In general, catalysts are expensive and are often difficult to separate from the reaction products, resulting in the use of intensive energy and generating waste. The separation of homogeneous catalysts is most commonly carried out by distillation, chromatography or extraction. However, SRNF membranes can replace these processes to recover the catalyst from the solvent mixtures. Furthermore, SRNF process does not accompany temperature changes during operation. Because homogeneous catalysts are relatively large (MW 450 Da), and the reaction products substantially smaller, so that separation is feasible with SRNF. Smet et al. [47] revealed the feasibility of the SRNF process



(MPF-60, Koch membrane) for recycling of Ru-Binap and Rh-DUPHOS catalysts dissolved in methanol.

### **2.1.3.3. Petrochemical applications**

The largest NF plant for organic solvent processing is installed in the petrochemical industry.

#### a) Solvent recovery in lube oil dewaxing

A typical solvent dewaxing process (refer to Figure 2.2) involves the addition of a mixture of volatile solvents, usually methyl ethyl ketone (MEK) and toluene, during the chilling process of a waxy oil raffinate. In the chilling section, the precipitated waxes are filtered and solvent in the filtrate is removed by evaporation and reused in the process. However, the cooling and distillation processes for the large amount of solvent result in high energy demands. Methods proposed by Bitter and White is incorporation of membrane in the conventional process. The benefit of this approaches are that filtered solvent doesn't need to be heated. Hence, energy savings are considerable and equipment can be smaller. After then same authors attempted to develop an alternative SRNF based process (shown in Figure 2.3) to recover these solvents, using spiral-wound Grace-Davison PI membranes [40]. By replacing the evaporation step with a SRNF membrane, a 99% pure solvent mixture could be obtained at refrigeration temperature, which could be directly recycled to the chilled feed stream.

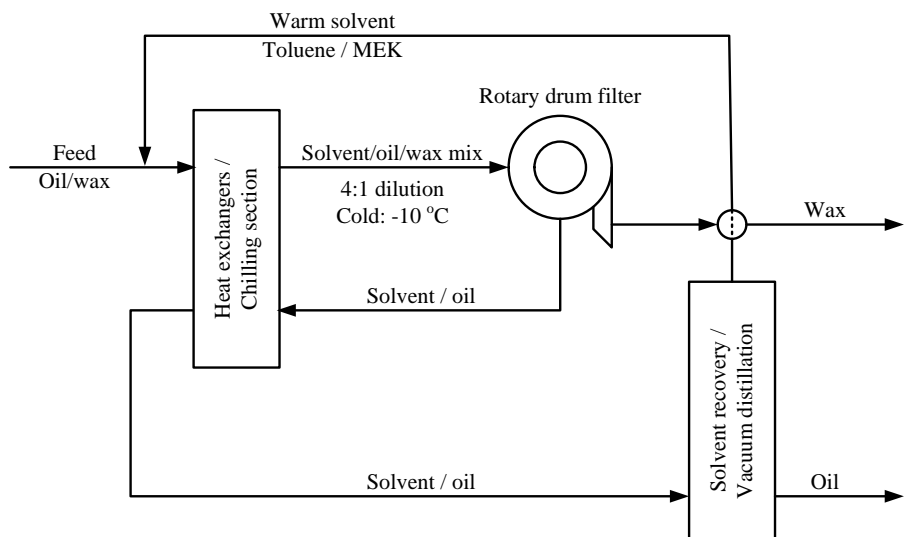


Figure 2.2. Conventional chilled solvent dewaxing.

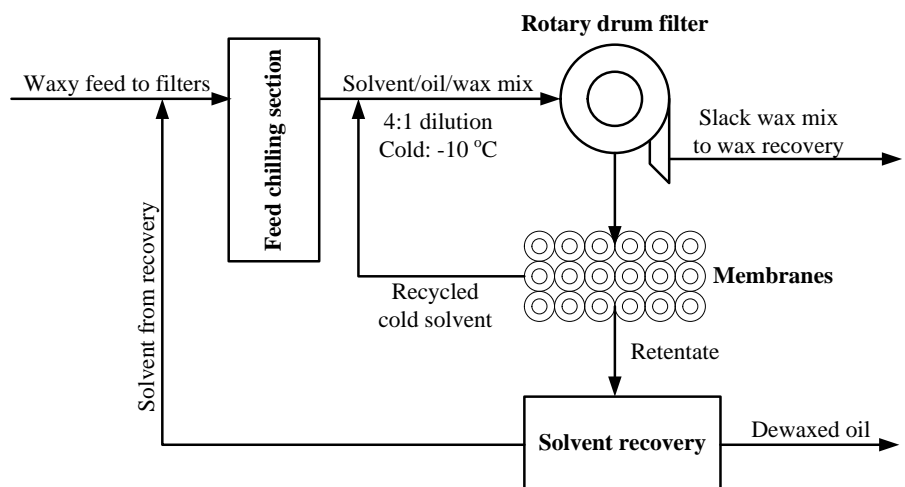


Figure 2.3. Novel solvent dewaxing incorporating a NF unit.

#### **2.1.3.4. Pharmaceutical applications**

SRNF membranes can be applied in drug synthesis process especially in between each reaction steps or in the downstream processing. In case of thermolabile compounds, SRNF has an additional benefit compared to conventional thermal operations such as distillation. In general, SRNF process does not accompany any phase changes which means the thermal damage on the thermolabile compounds can be minimized. In addition, lower operating temperature compare to distillation makes SRNF more an economical process. SRNF can be used to either retain a larger target molecule, or allow the target molecule to permeate while retaining the impurity [9]. A PI based SRNF membrane has been developed for the concentration of the antibiotic Spiramycin, forming a mixture of three compounds with MWs between 830 and 800 Da [59]. Spiramycin is extracted from bacterial broths with butyl acetate, which is traditionally recovered via evaporation. In addition to the energy consumption, this has also a negative influence on the quality of the final product. The membrane showed a stable long-term (35 days) separation performance with excellent solvent resistance and rejections around 99%.

#### **2.1.4. Transport models for SRNF membranes in non-aqueous systems**

NF membranes have a slightly charged surface. Therefore, charge interaction in NF membrane plays a dominant role for separation of components from aqueous systems. The rejection of non-charged solutes through NF membrane usually occurs by sieving effect. The separation of charged ions, on the other hand, is extremely complex.

Kedem and Katchalsky [60] derived the following equation (Spiegler-Kedem model) in the presence of a solute. This model was used to obtain the convective and diffusive contributions. The volumetric solution flux ( $J_v$ ), based on membrane area, is related to the applied pressure ( $\Delta p$ ) and the osmotic pressure ( $\Delta \pi$ ) and solute flux ( $J_s$ ) is related to concentration of solute ( $C$ ).

$$J_v = L_p(\Delta p - \sigma \Delta \pi) \quad (2.1)$$

$$J_s = P(c_f - c_p) + (1 - \sigma)J_v c \quad (2.2)$$

Equation (2.1) and (2.2) indicate that transport across a membrane is characterized by three transport parameters, i.e. the pure water permeability  $L_p$ , the reflection (selectivity) coefficient  $\sigma$ , the solute permeability  $P$ . This model, however, is usually applied when there is no electrostatic interaction between the membrane and the neutral solute.

The extended Nernst-Planck equation with Donnan potential [61-62] has been widely used to describe the performance of nanofiltration membrane in aqueous system. This model describes the transport of ions across the membrane in terms of diffusion, convection and electromigration and yields two membrane parameters; the effective membrane charge density and a structural parameter which combines porosity and membrane thickness.

$$J_i = -D_i^m \left( \frac{dc_i^m}{dx} + c_i^m \frac{z_i F}{RT} \frac{d\psi^m}{dx} \right) + K_{i,c} J_v c_i^m \quad (2.3)$$

with  $J_i$  being the solute flux,  $D$  the diffusion coefficient of  $i$ ,  $c$  the solute concentration in the membrane,  $x$  the coordinate in the flow direction,  $z$  is the electrochemical valence of the solute,  $R$  the gas constant,  $T$  the absolute temperature,  $\psi$  the membrane surface electrical potential,  $F$  the Faraday's constant,  $J_v$  the solvent flux and  $K_{i,c}$  the convective coupling coefficient. The superscript m refers to the membrane phase.

Attempts to understand transport mechanisms in non-aqueous system established different transport models. However, it is still not clear whether transport (both solvent and solute) occurs by viscous flow or diffusion because the mechanism of the separation with polymeric membranes in organic solvents is more complicated from that in aqueous solution by various parameters.

The Hagen-Poiseuille model is commonly used for porous membranes. The solvent flux  $J$  depends on the applied pressure  $\Delta p$ , on the porosity  $\varepsilon$  (defined as the fractional pore area at the membrane surface), the tortuosity  $\tau$  (defined as the path lengthening of the pores compared to cylindrical pores), the membrane thickness  $\Delta x$  and the liquid viscosity  $\mu$ . ( $r$  the average pore radius)

$$J = \frac{\varepsilon r^2 \Delta p}{8\eta\tau \Delta x} \quad (2.4)$$

For organic solvents this model in which the viscosity is the only solvent parameter considered is not enough due to possible interactions between solvent and membrane [63]. Also, pore size of membrane

depends on the type of organic solvent used, due to different swelling of the membrane polymer [64].

Machado et al. [19, 65] have used the viscosity and the superficial tension (polarity) for determination of the permeation of the pure solvents and solvent mixtures. The resistance-in-series model relates the flux of a solvent mixture with easily measurable solvent and membrane properties (surface tension, viscosity and membrane hydrophobicity).

$$J = \frac{\Delta p}{\phi[(\gamma_c - \gamma_L) + f_1\mu] + f_2\mu} \quad (2.5)$$

where  $f_1 = k_M^1/k_M^0$  is a solvent independent parameter characterizing the first NF layer,  $f_2 = k_M^2/(d_p^2)^2$  is a solvent independent parameter characterizing the second UF layer, and  $\phi = k_M^0/(d_p^1)^2$  is a solvent parameter.  $\mu$  the viscosity,  $\gamma_c$  the critical surface tension of the membrane material and  $\gamma_L$  is the surface tension of solvent.

However, this model is not covering the whole area of membranes and solvents because the model is developed for hydrophobic membranes. Moreover, for each solvent-membrane combination, an empirical parameter  $\phi$  must be determined as a measure for the interaction between a solvent and the membrane material.

The solution-diffusion model [66] is applicable both to the solute and solvent in terms of the pressure and concentration difference across the membrane. The flux of a species  $i$  through the membrane is given by:

$$J_i = \frac{D_i K_i}{l} \left[ c_{if} - c_{ip} \exp \left( \frac{-v_i (p_f - p_p)}{RT} \right) \right] \quad (2.6)$$

where  $D_i$  is the diffusion coefficient,  $K_i$  the sorption coefficient,  $l$  the membrane thickness,  $c_{if}$  and  $c_{ip}$  concentration of feed and permeate of species  $i$ ,  $v_i$  the partial molar volume of the  $i$ ,  $p_f$  and  $p_p$  the feed and permeate side pressures, respectively.

Similarly, the flux of the solute  $j$  is:

$$J_j = \frac{D_j K_j}{l} \left[ c_{jf} - c_{jp} \exp \left( \frac{-v_j (p_f - p_p)}{RT} \right) \right] \quad (2.7)$$

According to Bhanushali et al.[49], the viscosity ( $\mu$ ), the molar volume ( $V_m$ , as a measure for molecular size), the surface free energy of the solid membrane material ( $\gamma_{sv}$ ) and the sorption value ( $\phi$ , as a measure for membrane-solvent interactions) are used for determination of the permeation of organic solvents.

$$J \propto A \propto \left( \frac{V_m}{\mu} \right) \left( \frac{1}{\phi^n \gamma_{sv}} \right) \quad (2.8)$$

In this way, Bhanushali et al. were the first to suggest an influence of three parameters: viscosity, molecular size and the affinity between the solvent and the membrane material. The model is appropriate model for the description of solvent transport through dense NF membranes.

However, this model predicts higher fluxes with decreasing hydrophilicity of the membrane surface (i.e. decreasing surface tension) and is only valid for non-polar solvents. Therefore, the more polar solvent will be, the lower fluxes are expected with hydrophobic membranes, which cannot be described by this model.

Darvishmanesh et al. [11, 67] demonstrated that the following parameters control permeation rate through membranes; solvent solubility parameter, dielectric constant (polarity), ratio of surface tension of membrane-solvent ( $\beta$ ), and solvent viscosity ( $\mu$ ). The proportion of each effect on the solvent transport is related to the pore size of membrane (generally expresses as MWCO), as well as, stability of membrane in solvent media. It was shown that permeation through dense membranes is more affected by mutual affinities of membrane and solvent, whereas viscosity is the major transport parameter for porous membranes.

$$Jv = \frac{a_0 \alpha}{\mu \exp(1 - \beta)} (\Delta p - \Delta \pi) + \frac{b_0}{\mu \exp(1 - \beta)} \Delta p \quad (2.9)$$

$\alpha$  (the non-dimensional polarity coefficient) is defined for hydrophilic and hydrophobic membrane separately.  $a_0$  and  $b_0$  are specific diffusivity and permeability values, which are determined using the experimental data and mathematical computing software.

Besides Robinson et al. [64] explained using the polarity of organic solvents which is strongly related to surface tension, for the solvent permeation. Geens et al. [63] made a new model for solvent transport by



the combination of three parameters such as the solvent viscosity, solvent molar volume and the difference in surface tension between the solid membrane material and the liquid solvent.

In conclusion, at least three parameters such as solvent viscosity, molar volume and affinity between membrane and solvent are important to describe transport mechanism in non-aqueous system.

The solvent viscosity is incorporated as a measure for the resistance against pore flow (transport of momentum). This parameter appears in all transport models for transport through porous membranes. The molar volume of the solvent is used as a measure for the molecular size and the steric hindrance effects. It is indeed obvious that the resistance against permeation increases with increasing solvent size: the influence of membrane material (pore wall) is stronger when the ratio of the solvent molecule and the pore diameter is increasing. The membrane-solvent interactions induce a degree of swelling for polymeric membranes in organic solvents. Finally, it contributes to resistance against permeation.

## **2.2. Scope and outline of this study**

Among the discussed polymeric materials, poly(dimethylsiloxane) and polyimide have been selected for preparation of SRNF membranes. The general scope, outline and methodologies are briefly summarized in Figure 2.4.

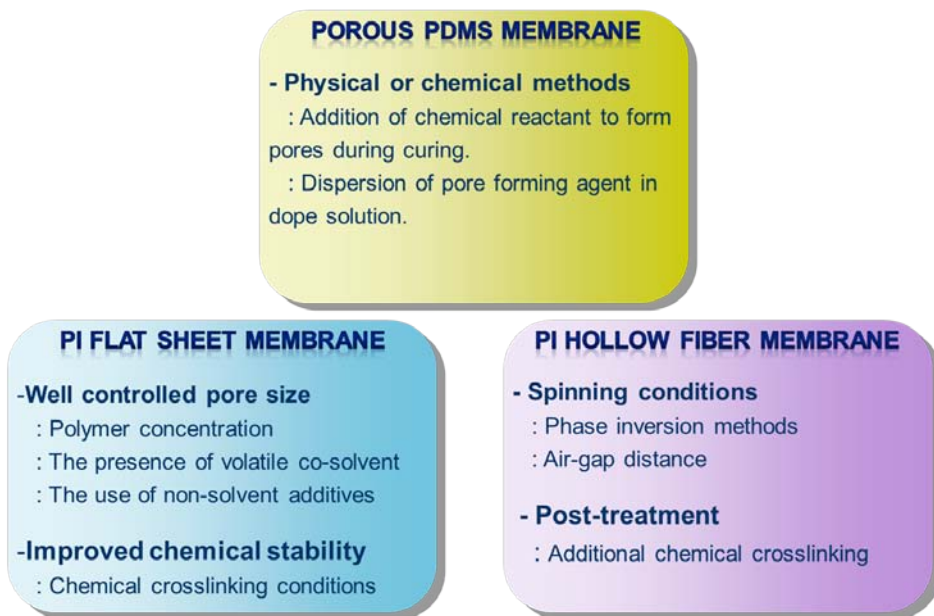


Figure 2.4. Purpose and methodologies of the study.

Porous PDMS flat sheet membranes were prepared by adding chemical or physical additive in casting solution to form the pores in membranes. Chemical additive implies sort of chemical which can induce chemical reaction to form pores in membrane. In this study, several different alcohols and water were employed as the chemical additive. Basically, -OH group in alcohol can react to -SiH group in PDMS crosslinker to form hydrogen gas. The effects of additive concentration, temperature of casting solution and post-treatment on the membrane properties including morphology and permeation properties were investigated. Second approach was to disperse physical additive in polymer solution before the film formation. Finally, additives in membranes can be removed by washing to make porous PDMS film.

1,4-Dioxane was used as a physical additive. The effects of several casting conditions including the concentration of additive, casting temperature and evaporation time, and post-treatment on membrane properties were systematically studied.

As mentioned in previous sections, polyimide is one of the most commonly used membrane material for preparation of solvent resistant membrane. In this study, different pore sized flat sheet and hollow fiber membranes were prepared with polyimide. In order to control the pore size of PI flat sheet membrane, composition of polymer solution including polymer concentration, presence and concentration of volatile co-solvent and non-solvent additives have been carefully changed. In addition, to improve the chemical stability of the membrane, chemical crosslinking conditions have been optimized. Solvent resistant polyimide hollow fiber membranes were prepared by wet or dry-wet phase inversion method. Furthermore, innovative in-line crosslinking of the hollow fiber was attempted by introducing the aqueous crosslinker solution (1,5-Diamino-2-methylpentane, DAMP) as the bore fluid (or inner coagulant). In dry-wet spinning process, air-gap length was varied to control the membrane morphology. The effects of casting conditions and spinning conditions on membrane morphology, solvent flux and rejection of dye were systematically investigated.

## References

1. H. Strathmann, L. Giorno, and E. Drioli, *An introduction to Membrane Science and Technology*. 2006, Roma: Ufficio Pubblicazioni e Informazioni Scientifiche.
2. D. Bhanushali, S. Kloos, and D. Bhattacharyya, *Solute transport in solvent-resistant nanofiltration membranes for non-aqueous systems: experimental results and the role of solute–solvent coupling*. *Journal of Membrane Science*, 2002. **208**: p. 343-359.
3. Y. Zhao and Q. Yuan, *Effect of membrane pretreatment on performance of solvent resistant nanofiltration membranes in methanol solutions*. *Journal of Membrane Science*, 2006. **280**: p. 195-201.
4. L.G. Peeva, M. Sairam, and A.G. Livingston, *Nanofiltration operations in nonaqueous systems*, in *Comprehensive Membrane Science and Engineering*. 2010, Elsevier. p. 91-113.
5. K. Grodowska and A. Parczewski, *Organic solvents in the pharmaceutical industry*. *Acta Poloniae Pharmaceutica - Drug Research*, 2010. **67**: p. 3-12.
6. A.G. Livingston, L.G. Peeva, and P. Silva, *Organic solvent nanofiltration*, in *Membrane technology in the chemical industry*, S.P. Nunes and L.-V. Peinemann, Editors. 2006, WILEY-VCH Verlag GmbH & Co. KGaA: Weinheim. p. 203-228.
7. M.T. Ravanchi, T. Kaghazchi, and A. Kargari, *Application of membrane separation processes in petrochemical industry: a review*. *Desalination*, 2009. **235**: p. 199-244.
8. A.I. Schafer, A.G. Fane, and T.D. Waite, *Nanofiltration - Principles and applications*. 2005, Oxford: Elsevier Ltd.
9. P. Vandezande, L.E.M. Gevers, and I.F.J. Vankelecom, *Solvent resistant nanofiltration: separating on a molecular level*. *Chemical Society Reviews*, 2008. **37**: p. 365-405.
10. K.V. Peinemann, K. Ebert, H.-G. Hicke, and N. Scharnagl, *Polymeric composite ultrafiltration membranes for non-aqueous applications*. *Environmental Progress*, 2001. **20**: p. 17-22.
11. S. Darvishmanesh, A. Buekenhoudt, J. Degrève, and B.V.d. Bruggen, *General*

- model for prediction of solvent permeation through organic and inorganic solvent resistant nanofiltration membranes.* Journal of Membrane Science, 2009. **334**: p. 43-49.
12. Y.H. See-Toh, M. Silva, and A. Livingston, *Controlling molecular weight cut-off curves for highly solvent stable organic solvent nanofiltration (OSN) membranes.* Journal of Membrane Science, 2008. **324**: p. 220-232.
  13. E.S. Tarleton, J.P. Robinson, C.R. Millington, and A. Nijmeijer, *Non-aqueous nanofiltration: solute rejection in low-polarity binary systems.* Journal of Membrane Science, 2005. **252**: p. 123-131.
  14. S. Basu, M. Maes, A. Cano-Odena, L. Alaerts, D.E. De Vos, and I.F.J. Vankelecom, *Solvent resistant nanofiltration (SRNF) membranes based on metal-organic frameworks.* Journal of Membrane Science, 2009. **344**(1-2): p. 190-198.
  15. S. Darvishmanesh, A. Buekenhoudt, J. Degrève, and B. Van der Bruggen, *Coupled series-parallel resistance model for transport of solvent through inorganic nanofiltration membranes.* Separation and Purification Technology, 2009. **70**(1): p. 46-52.
  16. J. Wanqin, X. Nanping, and S. Jun, *Progress in inorganic nanofiltration membranes.* Chinese Journal of Chemical Engineering, 1998. **6**(1): p. 59-67.
  17. B.V.d. Bruggen, J. Geens, and C. Vandecasteele, *Fluxes and rejections for nanofiltration with solvent stable polymeric membranes in water, ethanol and n-hexane.* Chemical Engineering Science, 2002. **57**: p. 2511-2518.
  18. H.-G. Hicke, I. Lehmann, G. Malsch, M. Ulbricht, and M. Becker, *Preparation and characterization of a novel solvent-resistant and autoclavable polymer membrane.* Journal of Membrane Science, 2002. **198**(2): p. 187-196.
  19. D.R. Machado, D. Hasson, and R. Semiat, *Effect of solvent properties on permeate flow through nanofiltration membranes. Part I: investigation of parameters affecting solvent flux.* Journal of Membrane Science, 1999. **163**(1): p. 93-102.
  20. P. Staiti, F. Lufrano, A.S. Aricò, E. Passalacqua, and V. Antonucci, *Sulfonated polybenzimidazole membranes - preparation and physico-chemical characterization.* Journal of Membrane Science, 2001. **188**(1): p. 71-78.
  21. P. Vandezande, X. Li, L.E.M. Gevers, and I.F.J. Vankelecom, *High throughput*

- study of phase inversion parameters for polyimide-based SRNF membranes.* Journal of Membrane Science, 2009. **330**: p. 307-318.
22. A.V. Volkov, D.F. Stamatialis, V.S. Khotimsky, V.V. Volkov, M. Wessling, and N.A. Platé, *Poly[1-(trimethylsilyl)-1-propyne] as a solvent resistance nanofiltration membrane material.* Journal of Membrane Science, 2006. **281**(1-2): p. 351-357.
  23. A.V. Volkov, D.F. Stamatialis, V.S. Khotimsky, V.V. Volkov, M. Wessling, and N.A. Platé, *New membrane material for SRNF applications.* Desalination, 2006. **199**(1-3): p. 251-252.
  24. L. Xue-Ren, G. Cong-Jie, and S. Xiu-Zhen, *Reinforced and dry polysulfonamide membranes.* Desalination, 1985. **54**(0): p. 207-217.
  25. P. Zschocke and H. Strathmann, *Solvent resistant membranes from poly-(p-phenylene-terephthalamide).* Desalination, 1980. **34**(1-2): p. 69-75.
  26. J.S. Kang, J. Won, H.C. Park, U.Y. Kim, Y.S. Kang, and Y.M. Lee, *Morphology control of asymmetric membranes by UV irradiation on polyimide dope solution.* Journal of Membrane Science, 2000. **169**: p. 229-235.
  27. C. Linder, M. Perry, M. Nemas, and R. Katraró, *Solvent stable membranes.* 1991.
  28. J.T. Scarpello, D. Nair, L.M.F.d. Santos, L.S. White, and A.G. Livingston, *The separation of homogeneous organometallic catalysts using solvent resistant nanofiltration.* Journal of Membrane Science, 2002. **203**: p. 71-85.
  29. H.J. Zwijnenburg, A.M. Krosse, K. Ebert, K.V. Peinnemann, and F.P. Cuperus, *Acetone-stable nanofiltration membranes in deacidifying vegetable oil.* Journal of American Oil Chemical Society, 1999. **76**: p. 83-87.
  30. S.-H. Choi, J.C. Jansen, F. Tasselli, G. Barbieri, and E. Drioli, *In-line formation of chemically cross-linked P84<sup>®</sup> co-polyimide hollow fibre membranes for H<sub>2</sub>/CO<sub>2</sub> separation.* Separation and Purification Technology, 2010. **76**: p. 132-139.
  31. K. Vanherck, A. Cano-Odena, G. Koeckelberghs, T. Dedroog, and I. Vankelecom, *A simplified diamine crosslinking method for PI nanofiltration membranes.* Journal of Membrane Science, 2010. **353**(1-2): p. 135-143.
  32. Y.H.S. Toh, F.W. Lim, and A.G. Livingston, *Polymeric membranes for nanofiltration in polar aprotic solvents.* Journal of Membrane Science, 2007. **301**: p. 3-10.

33. K. Vanherck, P. Vandezande, S.O. Aldea, and I.F.J. Vankelecom, *Cross-linked polyimide membranes for solvent resistant nanofiltration in aprotic solvents*. Journal of Membrane Science, 2008. **320**: p. 468-476.
34. N. Tanihara, H. Shimazaki, Y. Hirayama, S. Nakanishi, T. Yoshinaga, and Y. Kusuki, *Gas permeation properties of asymmetric carbon hollow fiber membranes prepared from asymmetric polyimide hollow fiber*. Journal of Membrane Science, 1999. **160**: p. 179-186.
35. S. Behnke and M. Ulbricht. *Membrane for organophilic nanofiltration based on photo-crosslinkable polyimide*. in *XXVII EMS summer school*. 2010. Bucharest, Romania: EMS.
36. K. Ebert and F.P. Cuperus, *Solvent resistant nanofiltration membranes in edible oil processing*. Membrane Technology, 1999. **107**: p. 5-8.
37. S.S. Koseoglu, J.T. Lawhon, and E.W. Lusas, *Membrane processing of crude vegetable oils: pilotplant scale removal of solvent from oil miscellas*. Journal of American Oil Chemical Society, 1990. **67**: p. 315-322.
38. L.P. Raman, M. Cheryan, and N. Rajagopalan, *Deacidification of soybean oil by membrane technology*. Journal of American Oil Chemical Society, 1996. **73**(2): p. 219-224.
39. L.P. Raman, M. Cheryan, and N.R. Urbana, *Solvent recovery and partial deacidification of vegetable oils by membrane technology*. Lipid, 1996. **98**: p. 10-14.
40. L.S. White and A.R. Nitsch, *Solvent recovery from lube oil filtrates with a polyimide membrane*. Journal of Membrane Science, 2000. **179**: p. 267-274.
41. K.K. Reddy, T. Kawakatsu, J.B. Snape, and M. Nakajima, *Membrane concentration and separation of L-aspartic acid and L-phenylalanine derivatives in organic solvents*. Separation Science and Technology 1996. **31**(8): p. 1161-1178.
42. M. Albrecht, N.J. Hovestad, J. Boersma, and G.v. Koten, *Multiple use of soluble metallodendritic materials as catalysts and dyes*. Chemistry - A European Journal, 2001. **7**(6): p. 1289-1294.
43. H. Bahrmann, M. Haubs, W. Kreuder, and T. Muller, *Process for separating organometallic compounds and/or metal carbonyls from their solutions in organic*

- media* 1992, Hoechst Aktiengesellschaft (Oberhausen, DE): U.S.
44. N. Brinkmann, D. Giebel, G. Lohmer, M.T. Reetz, and U. Kragl, *Allylic substitution with dendritic palladium catalysts in a continuously operating membrane reactor*. Journal of Catalysis, 1999. **183**(2): p. 163-168.
  45. D. Nair, J.T. Scarpello, I.F.J. Vankelecom, L.M.F.D. Santos, L.S. White, R.J. Kloetzing, T. Welton, and A.G. Livingston, *Increased catalytic productivity for nanofiltration-coupled Heck reactions using highly stable catalyst systems*. Green Chemistry, 2002. **4**: p. 319-324.
  46. D. Nair, J.T. Scarpello, L.S. White, L.M.F.d. Santos, I.F.J. Vankelecom, and A.G. Livingston, *Semi-continuous nanofiltration-coupled Heck reactions as a new approach to improve productivity of homogeneous catalysts*. Tetrahedron Letters, 2001. **42**(46): p. 8219-8222.
  47. K.D. Smet, S. Aerts, E. Ceulemans, I.F.J. Vankelecom, and P.A. Jacobs, *Nanofiltration-coupled catalysis to combine the advantages of homogeneous and heterogeneous catalysis*. Chemical Communications, 2001: p. 597-598.
  48. I.F.J. Vankelecom, *Polymeric membranes in catalytic reactors*. Chemical Review, 2002. **102**(10): p. 3779-3810.
  49. D. Bhanushali, S. Kloos, C. Kurth, and D. Bhattacharyya, *Performance of solvent-resistant membranes for non-aqueous systems: solvent permeation results and modeling*. Journal of Membrane Science, 2001. **189**: p. 1-21.
  50. X.J. Yang, A.G. Livingston, and L.F.d. Santos, *Experimental observation of nanofiltration with organic solvents*. Journal of membrane Science, 2001. **190**: p. 45-55.
  51. P. Silva, S. Han, and A.G. Livingston, *Solvent transport in organic solvent nanofiltration membranes*. Journal of Membrane Science, 2005. **262**: p. 49-59.
  52. P. Silva and A.G. Livingston, *Effect of solute concentration and mass transfer limitations on transport in organic solvent nanofiltration - partially rejected solute*. Journal of Membrane Science, 2006. **280** p. 889-898.
  53. Y. Zhao and Q. Yuan, *A comparison of nanofiltration with aqueous and organic solvents*. Journal of Membrane Science, 2006. **279**: p. 453-458.
  54. S.S. Luthra, X. Yang, L.M.F.d. Santos, L.S. White, and A.G. Livingston,



- Homogeneous phase transfer catalyst recovery and re-use using solvent resistant membranes.* Journal of Membrane Science, 2002. **201**: p. 65-75.
55. ; Available from: <http://www.solsep.com>.
56. R.J. Petersen, *Composite RO and NF membrane.* Journal of Membrane Science, 1993. **83**: p. 81-150.
57. L.S. White, I. Wang, and B.S. Minhas, *Polyimide membrane for separation of solvents from lube oil.* 1993: U.S.
58. J.P. Sheth, Y. Qin, K.K. Sirkar, and B.C. Baltzis, *Nanofiltration-based diafiltration process for solvent exchange in pharmaceutical manufacturing.* Journal of Membrane Science, 2003. **211**: p. 251-261.
59. D. Shi, Y. Kong, J. Yu, Y. Wang, and J. Yang, *Separation performance of polyimide nanofiltration membranes for concentrating spiramycin extract.* Desalination, 2006. **191**: p. 309-317.
60. O. Kedem and A. Katchalsky, *Thermodynamic analysis of the permeability of biological membranes to non-electrolytes.* Biochimica et Biophysica Acta, 1958. **27**: p. 229-246.
61. W. Bowen and A. Mohammad, *Diafiltration by nanofiltration: prediction and optimization.* AIChE J, 1998. **44**(8): p. 1799-1812.
62. W. Bowen and A. Mohammad, *Characterization and prediction of nanofiltration membrane performance - a general assessment.* Chemical Engineering Research and Design, 1998. **76**(8): p. 885-893.
63. J. Geens, B.V.d. Bruggen, and C. Vandecasteele, *Transport model for solvent permeation through nanofiltration membranes.* Separation and Purification Technology, 2006. **48**: p. 255-263.
64. J.P. Robinson, E.S. Tarleton, C.R. Millington, and A. Nijmeijer, *Solvent flux through dense polymeric nanofiltration membranes.* Journal of Membrane Science, 2004. **230**: p. 29-37.
65. D.R. Machado, D. Hasson, and R. Semiat, *Effect of solvent properties on permeate flow through nanofiltration membranes: Part II. Transport model.* Journal of Membrane Science, 2000. **166**(1): p. 63-69.
66. R.W. Baker, *Membrane Technology and Applications.* 2nd ed. 2004, England: John

Wiley & Sons Ltd.

67. S. Darvishmanesh, J. Degreve, and B.V.d. Bruggen, *Comparison of pressure driven transport of ethanol/n-hexane mixtures through dense and microporous membranes*. Chemical Engineering Science, 2009. **64**: p. 3914-3927.

## Chapter 3 Porous PDMS membranes

### 3.1. Introduction

Porous membranes are widely used in many industrial processes such as water and wastewater treatments, food, pharmaceutical and biotechnological industries due to the high flux, fouling resistance and low energy requirements [1-2]. However, it should be noted that poly(dimethylsiloxane) (PDMS) has rarely been studied for porous membranes in spite of its superior properties such as high hydrophobicity, low surface tension, high thermal and chemical stability, high biocompatibility and elastomeric behavior compare to other polymer materials [3-4]. Most studies with PDMS are concerning the dense membranes and/or composite membranes coated on the porous support membrane for the gas/vapor separation, pervaporation and solvent resistant nanofiltration membrane (SRNF).

Regarding to the porous PDMS membranes, only few researchers have reported the preparation of membranes by different methods and characterization of their properties. Tadashi Uragami [5-7] prepared porous PDMS membranes with aqueous emulsions of organopolysiloxane by freeze-drying method. Khorasani et al. [3] produced porous surfaces of PDMS membrane by two different methods which are irradiation procedure using CO<sub>2</sub>-pulsed laser as an excitation source and salt method by solving of NaCl particles dispersed on the membrane surface. However, these methods for the preparation of porous membrane required special equipment and are more complicated

compared to phase inversion method.

Connal et al. [4] and Kobayashi et al. [3, 8-9] have prepared porous PDMS membranes by phase inversion method. However, Connal also used the special implement like honeycomb grid for the preparation of porous PDMS membranes. On the other hand, Kobayashi suggested two different methods to fabricate porous PDMS membranes. First method is that using of -OH group in alcohol to induce reaction with -SiH group in PDMS for hydrogen generation. However, as the inventers indicated in their publication, the main drawback of this process is the difficulty in controlling of the hydrogen generation conditions such as curing time, curing temperature and membrane thickness which leads to uncontrolled pore size and porosity. The second method which seems simpler and easier than previous method is adding pore forming additives such as 1,4-Dioxane which well dispersed inside the membranes during membrane formation then finally removed to form pores. In this method, concentration of additive (1,4-Dioxane) in the polymer solution is the only parameter to be considered for the controlling of the pore formation.

In this study, porous PDMS membranes have been prepared with commercial PDMS precursor by phase inversion method proposed by Kobayashi et al. with two different methods. The first method is the use of pore forming agents to generate hydrogen during the hydrosilylation reaction of PDMS [10-11] by the reaction between the -SiH group and the -OH group of the additives [8]. The second method is the use of 1,4-Dioxane as a pore forming additive [9]. By washing 1,4-Dioxane with water, pores can be formed in the membrane.

## 3.2. Experimental

### 3.2.1. Materials

Poly(dimethylsiloxane) (PDMS, RTV 615, density of pre-polymer: 1.02 g/cm<sup>3</sup>, viscosity of uncured solution: 4000 mPa.s at 25 °C, GE Bayer Silicones) has been used as a membrane material which consists of two parts; a pre-polymer (Part A, base) and a crosslinker (Part B, curing agent). To obtain satisfactory physical and chemical properties of membranes, the weight ratio of pre-polymer to crosslinker was fixed at 10/1 as recommended by the manufacturer. The PDMS can be cross-linked via hydrosilylation reaction ( $-\text{Si}-\text{CH}_2-\text{CH}_2-\text{Si}$ ) and the chemistry leading to the crosslinked polymer is summarized in Figure 3.1.

Ethylene glycol (EG, anhydrous, Aldrich), isopropanol (IPA, Carlo Erba), methanol (MeOH, Carlo Erba), ethanol (EtOH, Carlo Erba), distilled water and 1,4-Dioxane (Dioxane, Lab Scan) have been used as the pore forming additives without further purification. The physical and chemical properties of the solvents used in this study are summarized in Table 3.1.

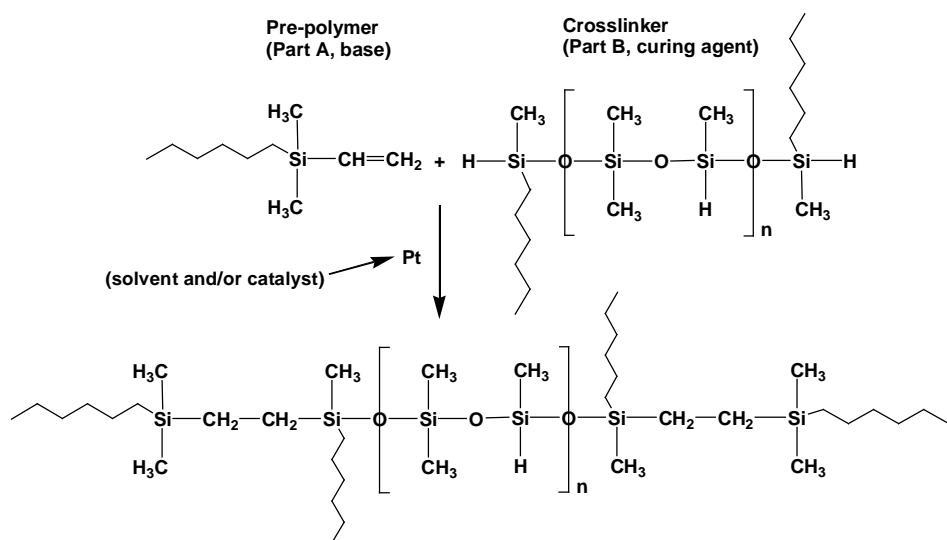


Figure 3.1. Schematic representation of chemical reaction of PDMS membranes [12].

Table 3.1 Chemical and physical properties of solvents used in this study [13-14].

Solvents	Formula	Molecular weight (g/mol)	Density (g/cm <sup>3</sup> )	Viscosity (mPa.s) at 25 °C
Ethylene glycol	C <sub>2</sub> H <sub>4</sub> (OH) <sub>2</sub>	62.10	1.11	13.8
Isopropanol	C <sub>3</sub> H <sub>8</sub> O	60.10	0.786	2.04
Methanol	CH <sub>4</sub> O	32.04	0.7918	0.55
Ethanol	C <sub>2</sub> H <sub>6</sub> O	46.07	0.789	1.26
Water	H <sub>2</sub> O	18.02	1.00	0.89
1,4-Dioxane	C <sub>4</sub> H <sub>8</sub> O <sub>2</sub>	88.11	1.034	1.18
Cyclohexane	C <sub>6</sub> H <sub>12</sub>	84.16	0.779	0.98

### 3.2.2. Preparation of porous PDMS membranes

#### 3.2.2.1. PDMS/Alcohols system

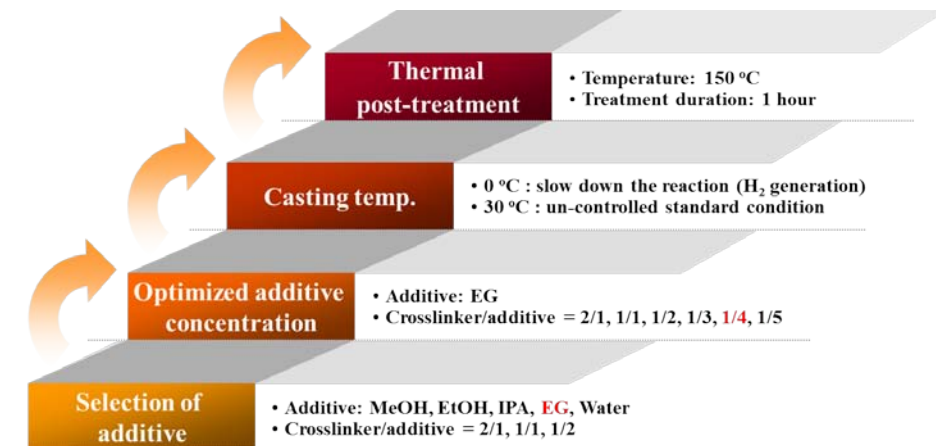


Figure 3.2. Optimization protocols used in this study for preparation of porous PDMS membrane using chemical additives.

As illustrated in Figure 3.2, the first step of the experiment is the selection of the best pore forming additive among the several candidates (MeOH, EtOH, IPA, EG, and water). First, the casting solutions were prepared by adjusting the mixing ratio of PDMS cross-linker and additive (2:1, 1:1, 1:2 mol) at 0 °C, then mixed with PDMS pre-polymer in the presence of cyclohexane. The weight ratio of pre-polymer to cyclohexane was fixed at 100/60. After degassing of solution, it was cast on a glass plate at 500  $\mu\text{m}$  thickness, and then cured at 30 °C for 24 hours. More detailed experimental variables were followed. A series of additives were tested in the same procedures for best pore forming additive.

Then, the effect of the concentration of best pore forming additive in PDMS solution (crosslinker/additive=2/1, 1/1, 1/2, 1/3, 1/4, 1/5) was

intensively investigated. In addition, the effect of temperature of casting solution (0 and 30 °C) and the thermal post-treatment (150 °C for 1 hour) on the membrane morphology and permeation properties were systematically studied.

### **3.2.2.2. PDMS/Dioxane system**

In this system PDMS solution was well-mixed with 1,4-Dioxane having different ratio based on the pre-polymer (pre-polymer/Dioxane parts = 100/30, 100/45, 100/60, 100/80) at 30 °C), and then degassed, finally cast on the glass plate at different thickness (200, 350 or 500 µm) with casting knife. Casting film was exposed to air at different temperature (30 or 40 °C) for different evaporation time (0 min, 10 min, 60 min, or 24 hours). Then the membrane was immersed in water for complete removal of Dioxane from the membrane.

The effects of the temperature of casting solution and evaporation time on the presence of pores in PDMS membranes were investigated. In addition, the effect of post-treatment and casting thickness on the permeation properties was tested. The post-treatment was carried out by applying vacuum to the prepared membrane at 150 °C for 1 hour. Graphical illustration of the protocols for optimization of the preparation of porous PDMS membrane is shown in Figure 3.3.



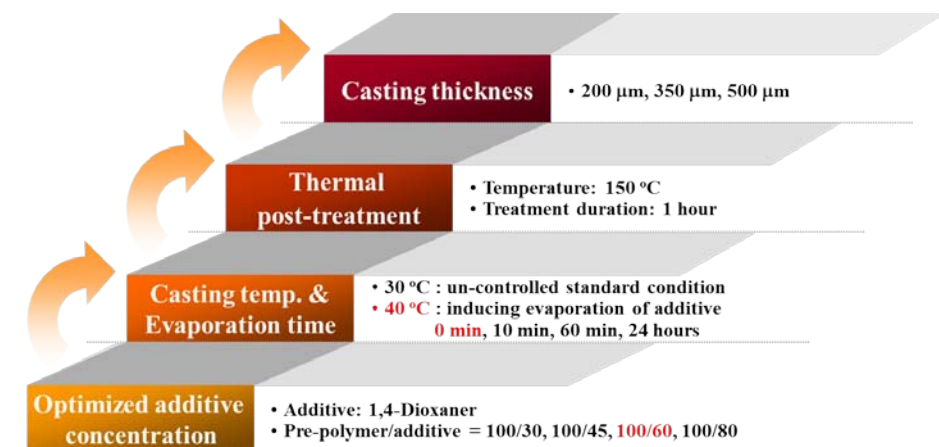


Figure 3.3. Optimization protocols used in this study for preparation of porous PDMS membrane using physical pore forming additives.

### 3.2.3. Membrane characterization

To confirm the presence of pores in the PDMS membrane, water flux measurement and gas permeation test were carried out. For water flux measurement, ultrafiltration cell (Amicon stirred cell 8003, Millipore) with an effective membrane area of 0.9 cm<sup>2</sup> was used. The volume of water passed through the membranes was collected for certain period of time at various pressure ranges under stirring at 350 rpm. The water flux was expressed as volume of water passing per unit membrane area per unit time (m<sup>3</sup>/(m<sup>2</sup>.h)). Gas permeability measurements are frequently used to characterize the presence of pores or to determine the pore size of the membrane. Especially, gas permeation test offers a simple and rapid quality test of membranes [15]. The gas transport properties were determined by single gases permeation measurements at 25±1 °C and 1 bar (1×10<sup>5</sup> Pa) of feed pressure in a fixed volume pressure-increase instrument, constructed by GKSS (Geesthacht, Germany).

The morphology of the prepared membranes was characterized by scanning electron microscopy (SEM, FEI QUANTA 200F). Especially, to observe the cross-sectional membrane, the membrane was dipped in the liquid nitrogen and then broken quickly because of no changing of its structure. The cross-section of membranes was observed at 20 kV under low vacuum without sputter coating.

The pore size and pore size distribution were measured by capillary flow porometer (CFP 1500 AEXL, Porous Materials, Inc., USA).

To determine the swelling degree, a sample is equilibrated in a test solution. After removing the surface access solution, the wet weight ( $W_{wet}$ ) of the swollen membrane is measured. The same sample is then dried at evaluated temperature (often under reduced pressure) until a constant dry weight ( $W_{dry}$ ) is obtained. The swelling is calculated by following equation.

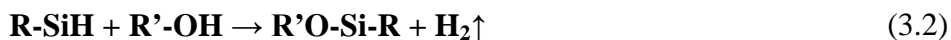
$$\text{Swelling (wt\%)} = \frac{W_{wet} - W_{dry}}{W_{wet}} \times 100 \quad (3.1)$$

### **3.3. Results and discussion**

#### **3.3.1. PDMS/Alcohols system**

##### **3.3.1.1. Screening of effective additives**

The addition of the additive which contains -OH group in it affects consumption of the -SiH group in PDMS crosslinker for the hydrogen generation. Hydrogen generation occurs in accordance with the following reaction.



Water permeation test results confirmed that the membranes prepared from MeOH, EtOH and IPA and water as the additive were non-porous. Therefore, the SEM images were not shown in here. The increase of the alcohols concentration in the casting solution led to an increase of hydrogen generation rate and decrease of viscosity of the casting solution. Consequently, the generated hydrogen gases are diffused to atmosphere more easily before the complete curing of PDMS [8]. Finally, the number of hydrogen remained in the cured membrane is limited.

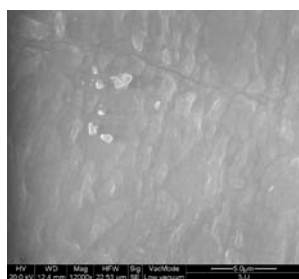
As mentioned above, almost all of the alcohols and water additives showed extremely difficult to control the hydrogen formation process and film curing speed. However, EG containing two -OH group in one molecule showed the possibility to make pores in PDMS membrane at the same preparation condition (Figure 3.4).

In this study, EG was chosen as a good candidate to produce porous PDMS membrane compared with other alcohols and water and further investigation were carried out.

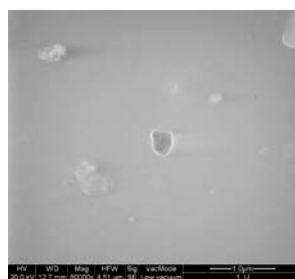
### **3.3.1.2. Effect of EG concentration**

The concentration of EG in PDMS casting solution was carefully controlled based on the crosslinker amount. The molar ratio of crosslinker to EG was varied at 1/3, 1/4 and 1/5 mol. The increase of the EG concentration led to increase the porosity of the membrane (Figure 3.4). Higher EG concentration increased the possibility to react and form H<sub>2</sub> gas. As a result, porosity has been increased. Water flux measurement

was conducted with the membranes which prepared from casting solution containing 1/4 and 1/5 mol. ratio of crosslinker and EG samples. In case of 1/3 mol membrane sample, no water permeation was observed up to 4 bar. Furthermore, gas permeation test confirmed the dense membrane structure.



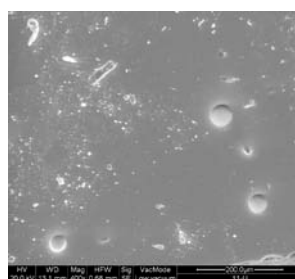
(a) crosslinker/EG=2/1



(b) crosslinker/EG=1/1



(c) crosslinker/EG=1/2



(d) crosslinker/EG=1/4

Figure 3.4. SEM images of PDMS membranes prepared with different concentration of EG.

The experimental results of the water flux measurement were plotted in Figure 3.5. As increase EG content, the water flux increased due to higher hydrogen generation. It should be noted that the membrane sample (1/5 mol) prepared from the casting solution containing higher concentration of EG showed much higher water flux than relatively low

EG contained sample (1/4 mol).

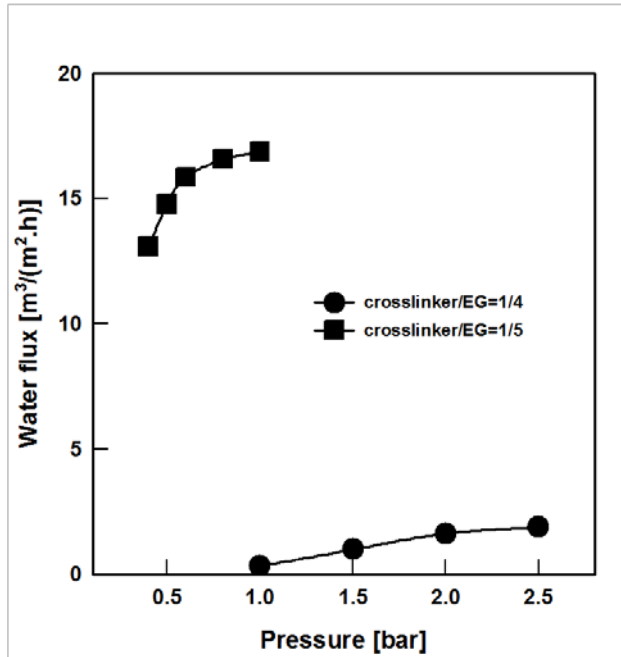


Figure 3.5. The effect of EG concentration on water flux.

### 3.3.1.3. Effects of temperature of the casting solution and the thermal post-treatment

The experiments were performed with composition of Crosslinker/EG=1/4 mol in casting solution at various temperatures and resulting morphology was investigated and illustrated in Figure 3.6. The membrane from casting solution prepared at 0 °C showed lower water flux compared to that of 30 °C because the hydrogen generation is accelerated by increasing the temperature of casting solution. The acceleration of the hydrogen generation can make larger pores [8].

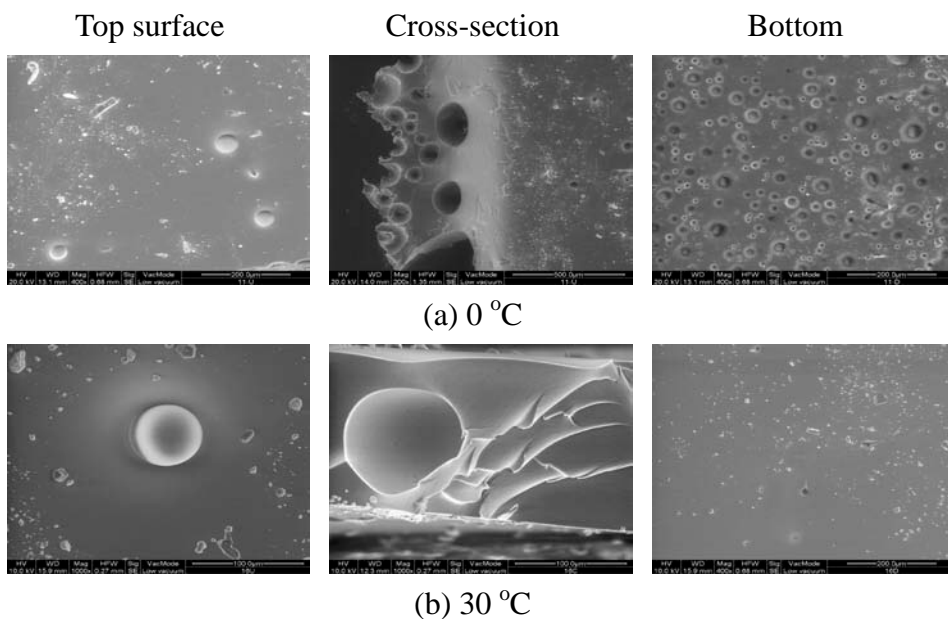


Figure 3.6. SEM images of PDMS membranes from casting solution prepared at (a) 0 °C and (b) 30 °C. (Crosslinker/EG=1/4 mol)

Post-treatment carried out by applying vacuum and annealing (150 °C) to prepared membrane for 1 hour then water permeation properties were investigated. As shown in Figure 3.7, the water flux decreased approximately 20% and 90% for the membrane prepared from casting solutions of 0 °C and 30 °C, respectively. It can be concluded that the suggested post-treatment method was effective to reduce pore size in the membrane. It is commonly observed for polymeric membranes, especially in this case, degree of crosslinking increase by thermal treatment. Also this explanation can be approved from the results of swelling degree measurement and pore size measurement which summarized in Table 3.2.

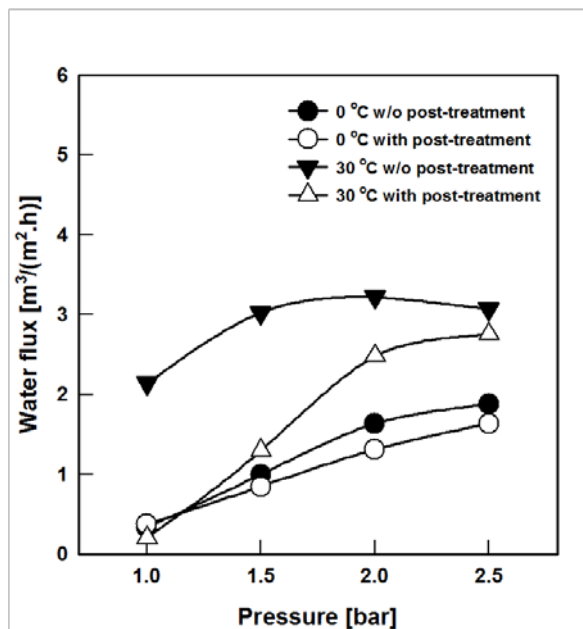


Figure 3.7. The effects of casting temperature and post-treatment on water flux. (Crosslinker/EG=1/4 mol)

Table 3.2 Effect of thermal post-treatment and casting temperature on swelling degree and porosity. (Crosslinker/EG=1/4 mol)

Preparation conditions	Swelling degree (%), g/g in EtOH	Porosity (%)
Casting solution: 0°C Untreated sample	1.65	2.15
Casting solution: 0°C Post-treated sample	1.55	2.02
Casting solution: 30°C Untreated sample	1.59	2.07
PDMS/EG 30°C Post-treated sample	1.48	1.94

### **3.3.2. PDMS/Dioxane system**

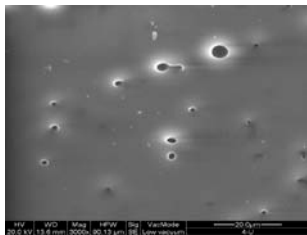
The formation of pores in the PDMS membranes was carried out in the presence of Dioxane as a pore forming additive during curing. After casting, the membrane having certain exposed times was immersed into the water bath to remove the Dioxane.

#### **3.3.2.1. Effect of Dioxane content**

Figure 3.8 shows the SEM images of the top surface and bottom of the membrane which prepared from the PDMS solution containing different weight percent of Dioxane from 30 to 80 wt% and cured at 30 °C. Undoubted clear pores were observed from top surfaces of all membranes, whereas porous bottom surface was observed only for 60 wt% Dioxane contained membrane sample. However, it should be noted that the presence of pores on top and bottom does not imply the porous structure of the membrane. The porous structure can be finally determined through the gas or water permeation test. In this case, to confirm the structure of the prepared membranes, water permeation test was carried out and no water permeation was observed for all the tested samples include the membrane which prepared from the casting solution which contains 60 wt% Dioxane.



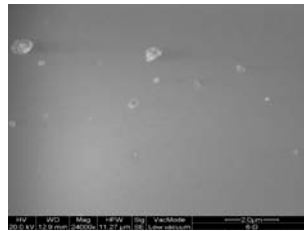
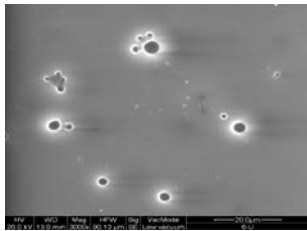
Top surface



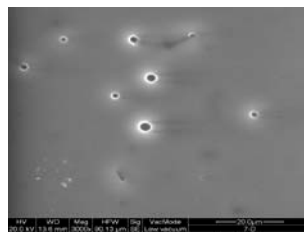
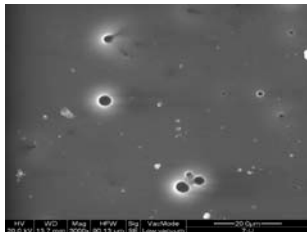
Bottom



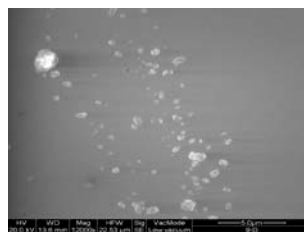
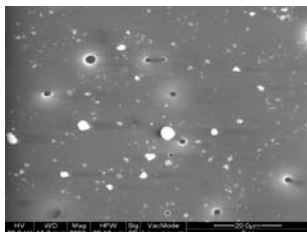
(a) Dioxane 30 wt%



(b) Dioxane 45 wt%



(c) Dioxane 60 wt%



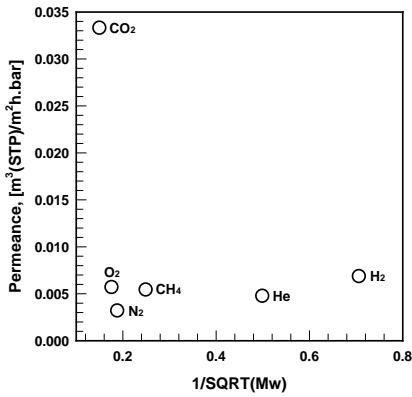
(d) Dioxane 80 wt%

Figure 3.8. SEM image of PDMS membranes prepared with different concentration of Dioxane (evaporation time on the air; 60 min.).

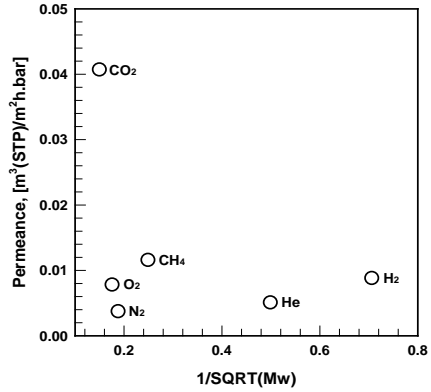
To confirm the presence of pores, gas permeation tests were conducted again. In these measurements, we observed clear time-lag of CO<sub>2</sub> gas in the all membranes and which means dense membranes (non-porous in intermediate layer). However, based on the SEM images, we believed that the casting solution contains 60 wt% Dioxane could be optimized to make porous membrane due to the cast film has clear pores on top and bottom. Therefore, concentration of Dioxane in casting solution was fixed at 60 wt% and further study was carried out to obtain porous structure. To make the porous structure in intermediate layer, the temperature of casting solution and the curing conditions were carefully controlled. The casting solution at two different temperatures (30 °C and 40 °C) was cast on the glass plate. Then the cast films were exposed in the air for different times (0 min, 10 min, 60 min and 24 hr) before immersing into the water bath.

No water flux was observed for the membranes which were cured at 30 °C. Also, the gas permeability measurement which plotted in Figure 3.9 confirmed that the prepared membranes were dense. For instance, the selectivity of CO<sub>2</sub> and N<sub>2</sub> through the typical dense PDMS membranes is 11 and the same value was obtained for the membranes cured at 30 °C. However, it is interesting to note that the membrane which was immersed in water immediately after casting at 40 °C shows porous skin on the surface and bottom. Final confirmation was made based on the gas permeation result. Figure 3.9(c) presents the Knudsen plot, for which the flux is inversely proportional to the square root of the molecular weight of the permeating gases. This indicates that the membranes are basically porous and that the maximum pore size is of the same order of

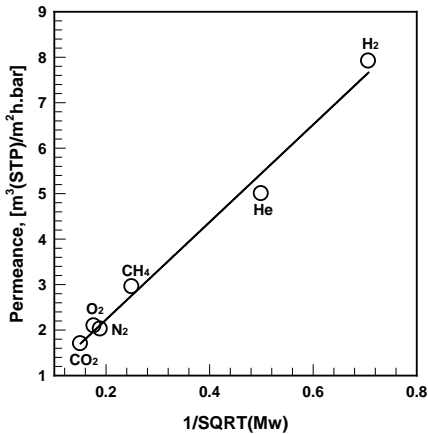
magnitude as the mean free path length of the permeating gas.



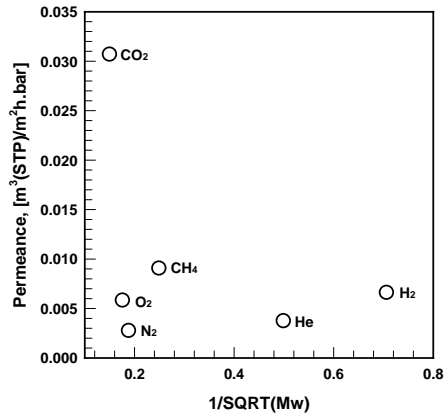
(a) 0 min. @ 30 °C



(b) 60 min. @ 30 °C



(c) 0 min. @ 40 °C



(d) 60 min. @ 40 °C

Figure 3.9. Gas permeation plot of six different gases on the different evaporation time and temperature (CO<sub>2</sub>, O<sub>2</sub>, N<sub>2</sub>, CH<sub>4</sub>, He and H<sub>2</sub>).

Figure 3.10 indicated that the effect of thermal post-treatment on the gas permeation property of porous PDMS membrane. Kindly remind that the membrane was prepared from the casting solution containing 60 wt%

Dioxane at 40 °C and immediate immersion (0 min) to water bath. Thermal post-treatment carried out by same procedure which used for PDMS/EG system (applying vacuum and annealing (150 °C) for 1 hour). As shown in Figure 3.10, the gas permeability decreased approximately 50 wt% to 70 wt% after post-treatment. However, the slope which obtained from the plot of gas permeability vs. square root of the gas molecular weight was linear and it confirmed that the membrane structure remains porous.

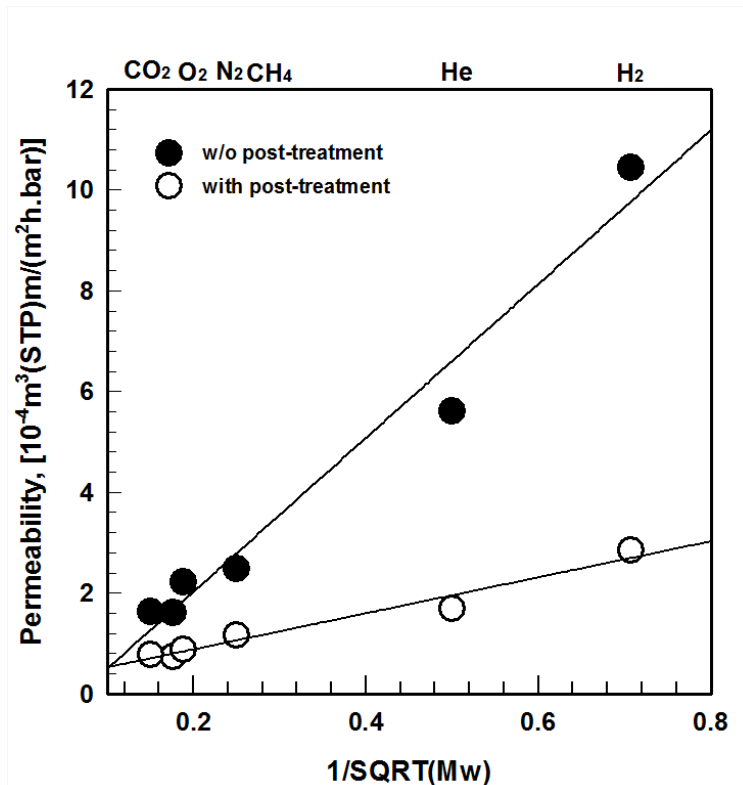


Figure 3.10. Effect of post-treatment on gas permeability through porous PDMS membrane. (Casting solution contains 60 wt% 1,4-Dioxane)

The pore size and pore size distribution of some membranes were measured by capillary flow porometer and presented in Figure 3.11. After post-treatment, pore size distribution became narrow (sharp), and the mean pore size decreased from 0.063  $\mu\text{m}$  to 0.018  $\mu\text{m}$ . From this result, it can be concluded that the thermal post-treatment can be useful tool to adjust pore size distribution and pore size.

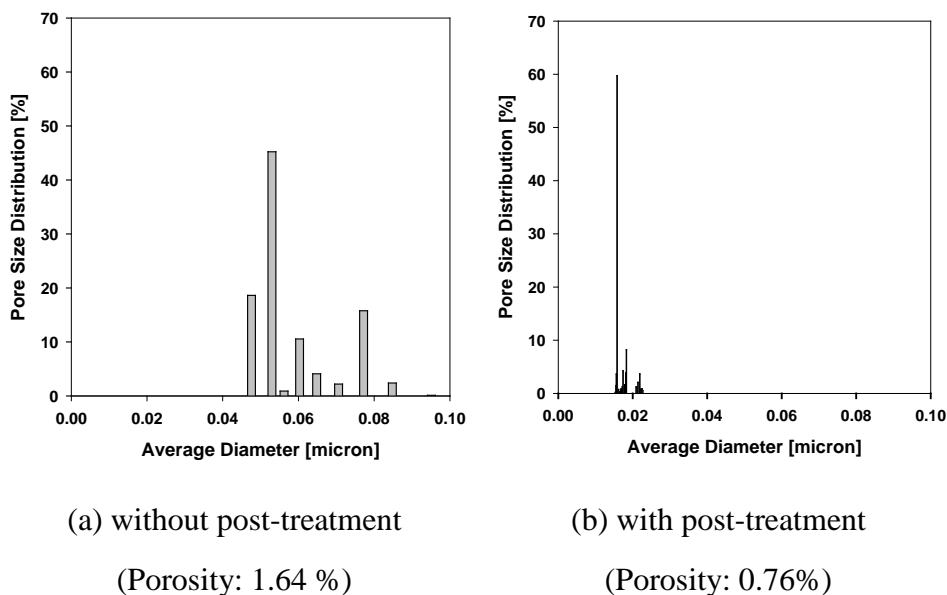


Figure 3.11. The effect of post-treatment on pore size and pore size distribution with porous PDMS membranes with Dioxane 60 wt%.

Finally, the effect of initial thickness of casting film was characterized by gas permeation test (Figure 3.12). PDMS solutions with Dioxane 60 wt% cast on glass plate with three different thicknesses (200, 350 and 500  $\mu\text{m}$ ) at 40  $^{\circ}\text{C}$ . After casting, the membrane was immersed

immediately in the water bath. As a result, the membranes cast at the thickness of 200 and 350  $\mu\text{m}$  were dense (Figure 3.12), whereas 500  $\mu\text{m}$  cast membrane was porous (Figure 3.9 (c)). Gas permeation test confirmed the presence of pores through the membrane.

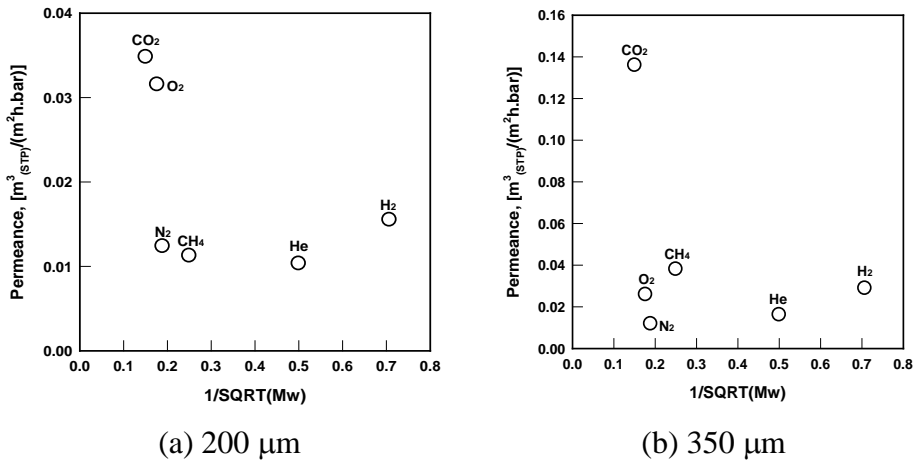


Figure 3.12. The effect of initial thickness of casting film.

### 3.4. Conclusions

For the preparation of porous asymmetric PDMS membranes, two different methods were used. One is to introduce several different alcohols (MeOH, EtOH, IPA and EG) and water as a pore forming agents to form hydrogen gases by reaction with vinyl group in PDMS. During the cure of PDMS generated hydrogen gases make pores in the PDMS membrane. The increase of the concentration of alcohols and water in the casting solution accelerate the hydrogen formation. Nevertheless, addition of the additives led to decrease the viscosity of the solution,

results in high diffusivity of the formed hydrogen to atmosphere. Finally, the number of hydrogen remains inside the membrane film for making pores can be limited. However, in the aspect of the viscosity EG has the higher viscosity compared to other additives (MeOH, EtOH, IPA and water). In addition, it contains two -OH group in a molecule. For the reason, we can prepare the porous PDMS membranes with controlled concentration of EG and temperature of the casting solution.

Physical pore forming additive, 1,4-Dioxane, was dispersed in PDMS casting solution. After the curing of the PDMS membrane, Dioxane was removed by washing with water. Casting conditions such as the concentration of additive, temperature of casting solution and evaporation time on the membrane morphology and permeation properties were systematically investigated. In this study, it was found that there is a critical concentration of 1,4-Dioxane (physical additive, 60 wt%) to make porous PDMS membrane. Also elevated temperature (40 °C) and immediate immersion of casting film were useful method to create pores through the membrane not only on the top surface and bottom of the membrane. The presence of pores in the membranes was confirmed not only by the SEM analysis but also by gas permeation test. Especially, gas permeation test was useful tool to evaluate the porous structure. Finally, the thermal post-treatment could reduce the pore size and pore size distribution.

Porous PDMS membranes have been successfully prepared by adding chemical or physical additive in casting solution. However, controlling the pore size and pore size distribution were extremely difficult. Especially for chemical additives added PDMS system, it was difficult in

to control the curing speed of PDMS and pore forming speed. Moreover, prepared membranes showed too low permeation properties and porosity for PDMS/1,4-Dioxane system.

Therefore, for further study, polyimide was selected as a new membrane material for preparation of the solvent resistant membranes.



## References

1. H. Susanto and M. Ulbrichta, *Characteristics, performance and stability of polyethersulfone ultrafiltration membranes prepared by phase separation method using different macromolecular additives*. Journal of Membrane Science, 2009. **327**: p. 125-135.
2. R.W. Baker, ed. *Membrane Technology and Applications*. second ed. 2004.
3. M.T. Khorasani, H. Mirzadeh, and Z. Kermani, *Wettability of porous polydimethylsiloxane surface: morphology study*. Applied Surface Science, 2005. **242**: p. 339-345.
4. L.A. Connal and G.G. Qiao, *Preparation of porous poly(dimethylsiloxane)-based honeycomb materials with hierarchal surface features and their use as soft-lithography templates*. Advanced Materials, 2006. **18**: p. 3024-3028.
5. T. Uragami, Y. Tanaka, M. Ozaki, and T. Nakamura, *Process for fabrication porous silicone product*. 1994: U.S.
6. T. Uragami, *Structural design of polymer membranes for concentration of bio-ethanol*. Polymer Journal, 2008. **40**(6): p. 485-494.
7. T. Uragami, *Concentration of aqueous ethanol solutions by porous poly(dimethylsiloxane) membranes during temperature difference controlling evaporation*. Desalination, 2006. **193**: p. 335-343.
8. T. Kobayashi, H. Saitoh, N. Fujii, Y. Hoshino, and M. Takanashi, *Porous membrane of polydimethylsiloxane by hydrosilylation cure: Characteristic of membranes having pores formed by hydrogen foams*. Journal of Applied Polymer Science, 1993. **50**: p. 971-979.
9. T. Kobayashi, H. Saitoh, and N. Fujii, *Porous polydimethylsiloxane membranes treated with aminopropyltrimethoxysilane*. Journal of Applied Polymer Science, 1994. **51**: p. 483-489.
10. H.Y. Wang, T. Kobayashi, H. Saitoh, and N. Fujii, *Porous polydimethylsiloxane membranes for enzyme immobilization*. Journal of Applied Polymer Science, 1996. **60**: p. 2339-2346.
11. D.J. Campbell, K.J. Beckman, C.E. Calderon, P.W. Doolan, R.M. Ottosen, A.B.

- Ellis, and G.C. Lisensky, *Replication and compression of bulk and surface structures with polydimethylsiloxane elastomer*. Journal of Chemical Education, 1999. **75**(4): p. 537-541.
12. I.F.J. Vankelecom, *Polymeric membranes in catalytic reactors*. Chemical Reviews, 2002. **102**(10): p. 3779-3810.
13. D.R. Lide, *Handbook of chemistry and physics*. Vol. 84. 2003-2004: CRC Press.
14. J. Brandrup, E.H. Immergut, and E.A. Grulke, *Polymer handbook*. 4th ed. 1999: Jon Wiley.
15. M.G. Buonomenna, A. Figoli, J.C. Jansen, and E. Drioli, *Preparation of asymmetric PEEK-WC flat membranes with different microstructures by wet phase inversion*. Journal of Applied Polymer Science, 2003. **92**: p. 576-591.

## Chapter 4 Polyimide asymmetric membranes

### 4.1. Introduction

Solvent resistant membranes need to be characterized by a high durability in organic solvents, as well as an efficient separation for various molecules [1]. Several authors have attempted to control the molecular weight cut-off (MWCO) from macroporous to microporous membranes with polyimide material by changing membrane formation parameters such as the type of solvent [2-5], coagulants composition [4], additives [6] and polymer concentration [4, 7]. In addition, to improve the stability of PI membranes, post-treatments have been carried out by employing chemical crosslinking procedures [3, 5, 8-9], irradiation [10] or thermal treatment [2] after the membrane formation.

In the present chapter, we mainly focused on the improvement of solvent resistant membranes performances by controlling the membrane formation parameters, including polymer concentration, concentration of volatile solvent, solvent type and concentration of non-solvent additives. Furthermore, a systematic study has been conducted to test the feasibility of the chemical crosslinking for improving chemical stability of P84<sup>®</sup> co-polyimide membranes.

The performances of the prepared membranes were evaluated through permeation experiments principally with organic solutions containing low molecular weight dyes or catalysts. Several organic solvents such as acetonitrile, ethanol, methanol, DMF and chloroform has been chosen because they have been widely used as solvent in the pharmaceutical

industry [11-13]. Moreover, several dyes and catalysts with various molecular weights and charges in order to understand their effect on membrane performances were examined.

## 4.2. Experimental

### 4.2.1. Materials

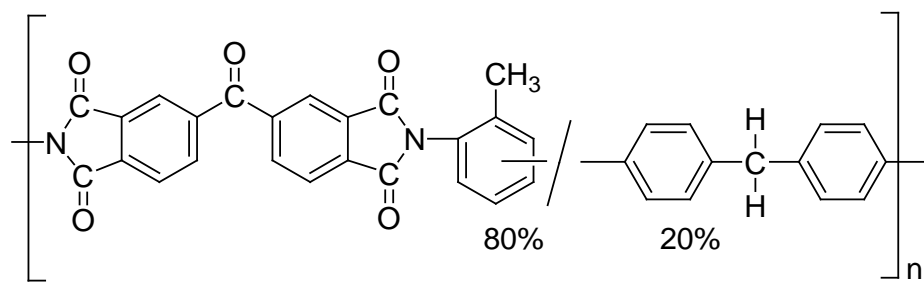


Figure 4.1. Chemical structure of Lenzing P84<sup>®</sup> (BTDA-TDI/MDI) co-polyimide [14].

Lenzing P84<sup>®</sup> co-Polyimide (hereafter denoted as PI) was purchased from HP polymer GmbH (Figure 4.1). *N*-Methyl-2-pyrrolidone (NMP), *N,N*-Dimethylformamide (DMF) and 1,4-Dioxane (Dioxane) were used as solvent for polymer solution. Ethanol (EtOH) and ultrapure water were used as non-solvent additive. Methanol (MeOH), acetonitrile (CH<sub>3</sub>CN) and chloroform (CHCl<sub>3</sub>) were used as solvent for permeation test. Organic solvents reagents were purchased from Carlo Erba. 1,5-Diamino-2-methylpentane (DAMP, from Sigma-Aldrich) was used as chemical crosslinker (Figure 4.2). Dyes and two catalysts with different molecular weights were purchased from Sigma-Aldrich and used to

characterize membrane performances. The chemical structure and some properties of dyes and catalysts were summarized in Table 4.1. All the solvents and chemicals were of analytical grade and used as received without any further purification.

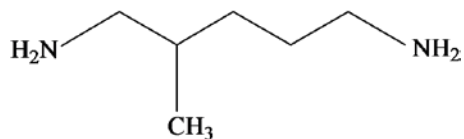
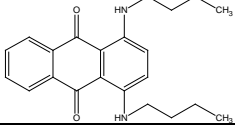
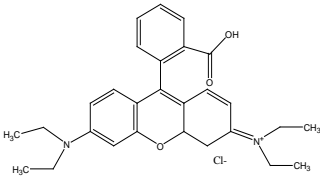
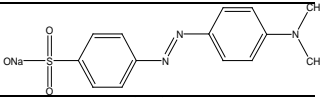
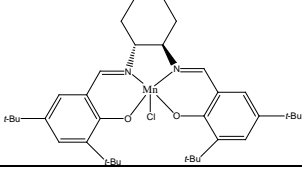
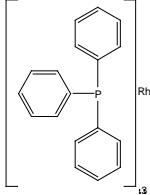
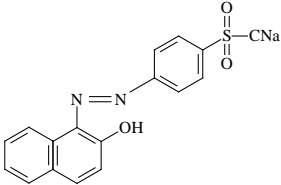
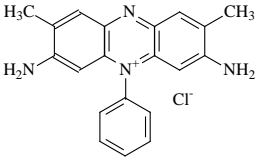
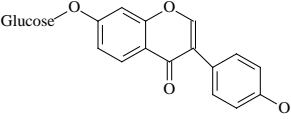


Figure 4.2. Structure of 1,5-Diamino-2-methylpentane crosslinker.

Table 4.1 Some properties of the dyes and the catalysts used in this study.

Name	Molecular weight (g/mol)	Charge	UV absorption wavelength (nm)	Chemical structure
Solvent blue 35	350.45	neutral	641	
Rhodamine B	479.01	positive	556	
Methyl orange	327.33	negative	422	
Jacobsen's catalyst	635.22	positive	500	
Wilkinson's catalyst	925.22	positive	325	
Orange II	350.33	negative	479	
Safranin O	350.85	positive	527	
Soybean daidzin	416.38	neutral	HPLC analysis	

#### 4.2.2 Membranes preparation

Asymmetric PI membranes were prepared from ternary mixtures comprising a polymer (PI), a solvent (NMP or DMF), and a volatile co-solvent (Dioxane) /or a non-solvent additive (water or EtOH) by phase inversion technique. Homogeneous solutions were prepared by adding PI powder into the solvents mixture in a glass Erlenmeyer flask under magnetic stirring.

The properties of the casting solution were modulated by changing the polymer concentration, the ratio of the solvent and the volatile co-solvent, the solvent type and the non-solvent concentration. Table 4.2 summaries the composition of the casting solutions and the membrane samples codes.

The polymer solutions were cast at 250  $\mu\text{m}$  thickness on a glass plate using a casting knife and an automatic film applicator at the speed 2 cm/sec. The liquid film was firstly left to evaporate for 60 seconds at  $24\pm 3$   $^{\circ}\text{C}$  and  $50\pm 5\%$  of relative humidity and then it was immersed into water coagulation bath at  $24\pm 3$   $^{\circ}\text{C}$  for at least 24 hours. Finally, the rinsed membranes were stored in water until their chemical crosslinking treatment.

The effect on the membrane properties of the crosslinking conditions, such as the concentration of the crosslinker and crosslinking time, was also investigated. In Table 4.3, detailed crosslinking conditions were summarized.

If not otherwise indicated, the chemical crosslinking was carried out with 10 v/v% DAMP/MeOH solution for 24 hours at  $24\pm 3$   $^{\circ}\text{C}$ . The chemically modified films were washed with fresh methanol to wash

away any residual crosslinker un-reacted. Then, crosslinked membranes were stored in an aqueous solution containing 5 wt% of ethanol to minimize the potential growth of microorganisms on the membrane.

Table 4.2 Composition of the casting solution and sample code.

Investigated parameters	Composition of the casting solution (wt%)	Membrane codes
	PI/NMP/additive	
Polymer concentration	19.00/20.25/60.75 <sup>a</sup>	PI19
	21.00/19.75/59.25 <sup>a</sup>	PI21
	23.00/19.25/57.75 <sup>a</sup>	PI23
	25.00/18.75/56.25 <sup>a</sup>	PI25
Concentration of volatile solvent	21/79/0 <sup>a</sup>	PI/Dioxane0
	21/59/20 <sup>a</sup>	PI/Dioxane20
	21/49/30 <sup>a</sup>	PI/Dioxane30
	21/39/40 <sup>a</sup>	PI/Dioxane40
	21/29/50 <sup>a</sup>	PI/Dioxane50
	21/19/60 <sup>a</sup>	PI/Dioxane60
Solvent type	21/39/40 <sup>a</sup>	PI/NMP39/Dioxane40
	21/39 <sup>b</sup> /40 <sup>a</sup>	PI/DMF39/Dioxane40
Concentration of non-solvent additives	21/79/0 <sup>c</sup>	PI/additive0
	21/78/1 <sup>c</sup>	PI/water1%
	21/77/2 <sup>c</sup>	PI/water2%
	21/75/4 <sup>c</sup>	PI/water4%
Concentration of non-solvent additives	21/78/1 <sup>d</sup>	PI/EtOH1%
	21/77/2 <sup>d</sup>	PI/EtOH2%
	21/75/4 <sup>d</sup>	PI/EtOH4%
	21/69/10 <sup>d</sup>	PI/EtOH10%

<sup>a</sup> Dioxane was used as the volatile co-solvent additive for this membrane.

<sup>b</sup> DMF was used as the solvent for this membrane.

<sup>c</sup> Water was used as the non-solvent additive for this membrane.

<sup>d</sup> Ethanol was used as the non-solvent additive for this membrane.



Table 4.3 Chemical crosslinking conditions.

Crosslinker and solvent	Concentration of crosslinker (v/v%)	Crosslinking time
	1	
	5	24 hr
	10	
		5 min
DAMP in MeOH		30 min
		1 hr
	10	3 hr
		5 hr
		7 hr
		24 hr

#### 4.2.3. Membrane permeation experiments

Pure solvent flux of the crosslinked membranes was evaluated in a laboratory scale dead-end NF cell with an effective membrane area of 14.6 cm<sup>2</sup>. Before the tests, each membrane was first soaked in the target solvent for at least 24 hours and then placed in NF cell. The loaded membrane was compacted with solvent at fixed transmembrane pressure, until the permeation flux reached a steady state (about 1 hour). After measuring pure solvent flux, rejection of solute was carried out.

Rejection was calculated by the Equation 4.1. The experimental protocol to determine rejection was the following: 100 ml of dyes or catalysts solutions (100 mg/L) were used as a feed solution, 50 ml of permeate solution was collected and the concentration of solute in the feed, retentate and permeate was analyzed by UV spectrometer (Lambda 650S UV/Vis spectrometer, PerkinElmer, USA). During the experiment,

the feed solution was stirred using a magnetic stirrer at high speed to prevent concentration polarization.

$$R (\%) = \left( 1 - \frac{C_p}{C_r} \right) \times 100 \quad (4.1)$$

where  $R$  is the rejection of membrane,  $C_p$  and  $C_r$  represent permeate and retentate concentrations, respectively. In all rejections, a mass balance (Equation 4.2) was used to check any loss during the experiment.

$$\text{Mass balance } (\%) = \left( \frac{(V_p \times C_p + V_r \times C_r)}{V_f \times C_f} \right) \times 100 \quad (4.2)$$

where  $C_f$ ,  $C_p$  and  $C_r$  represent concentrations of feed, permeate and retentate and  $V_f$ ,  $V_p$  and  $V_r$  are volumes of feed, permeate and retentate, respectively.

#### **4.2.4. Membrane characterization**

For the characterization of solvent resistant membranes, SEM observation, FT-IR/ATR and dimensional swelling were tested.

The membrane morphology was observed by scanning electron microscopy (SEM, FEI QUANTA 200F) at 20 kV under low vacuum. For the observation of the membrane cross-section, the samples were fractured in liquid nitrogen.

PerkinElmer Spectrum One FT-IR/ATR Spectrophotometer was used to monitor the chemical changes in the membranes. The spectra were collected in the attenuated total reflection (ATR) mode, directly from the

outer membrane surface. The spectra were recorded at a resolution of 4  $\text{cm}^{-1}$  as an average of eight scans.

The dimensional swelling was determined by measuring the increase of dimensions of a membrane sample after 24 hours of immersion in a solvent:

$$\text{Dimensional swelling (\%)} = \left( \frac{A_{wet} - A_{dry}}{A_{dry}} \right) \times 100 \quad (4.3)$$

where  $A_{dry}$  and  $A_{wet}$  represent areas of dry and wet membranes, respectively.

#### **4.2.5. Ternary phase diagrams**

Ternary phase diagrams were determined by cloud point measurement at  $22 \pm 2$  °C. Homogeneous solutions with different composition of PI/NMP/Dioxane were prepared, and then non-solvent (water) was added slowly until changing turbidity of the casting solution.

### **4.3. Results and discussion**

#### **4.3.1. Effect of the polymer concentration**

In order to control the membrane morphology, the concentration of the polymer in the casting solution was changed from 19 to 25 wt%. The SEM images of the membranes (Figure 4.3) showed that as increasing the polymer concentration, membrane morphologies were changed to sponge-like structure and the formation of macrovoids were suppressed.

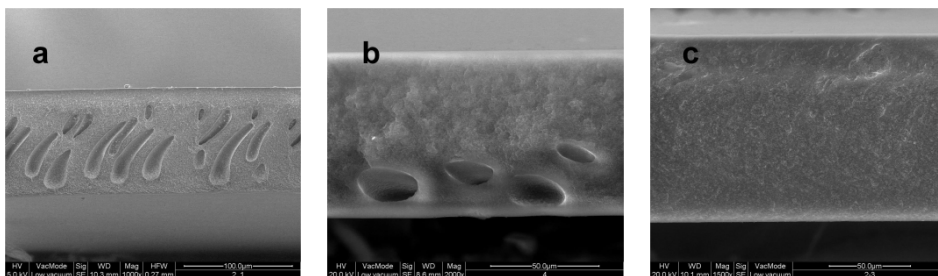


Figure 4.3. SEM images of the cross-section of PI membranes prepared from different concentration of polymer; (a) PI19, (b) PI21, (c) PI23.

As expected, acetonitrile flux decreased with the increasing of the polymer concentration (Table 4.4). It should be noted that the membranes prepared from polymer concentration of 23 wt% or over, showed extremely low flux, therefore, PI23 and PI25 membranes were excluded for the further characterization (i.e. rejection test). Viscosity of casting solution increases with the increase of polymer content, inducing delay of the liquid-liquid demixing. As a result, more dense top layer and less porous sublayer without macrovoids, were formed [4].

Table 4.4 Pure solvent flux and rejection of dyes in the membranes prepared from different polymer concentration.

Sample codes	CH <sub>3</sub> CN flux [L/(m <sup>2</sup> .h)]	Rejection [%]	
		Solvent blue 35	Rhodamine B
PI19	20 ± 1	98	>99
PI21	12 ± 0.5	98	>99
PI23	Too low	-	-

### 4.3.2. Effect of the concentration of volatile co-solvent

Figure 4.4 shows ternary phase diagram of PI membranes prepared using different concentrations of the Dioxane. As increase the concentration of Dioxane in the casting solution, the miscibility line is shifted toward the polymer-solvent axis in the ternary diagram. It means that increasing Dioxane concentration, less water is necessary for the liquid-liquid demixing. However, in the phase inversion induced by a non-solvent, the final morphology of the membranes depends not only from the thermodynamic miscibility of the ternary solutions, but also from kinetic phenomena, strongly influenced by the mutual affinity of solvent/non-solvent.

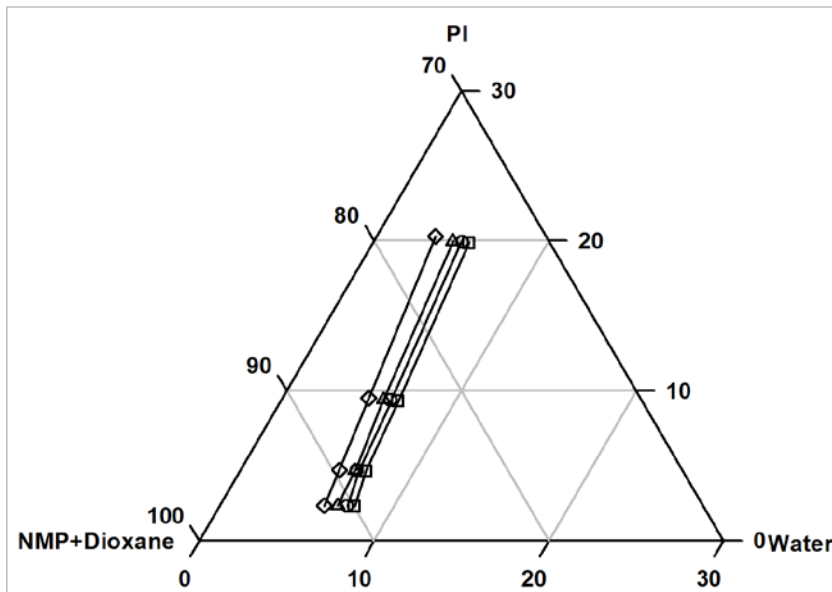


Figure 4.4. Ternary phase diagram of the PI membranes prepared from different concentration of Dioxane;  $\square$ : Dioxane0%,  $\circ$ : Dioxane20%,  $\triangle$ : Dioxane40%,  $\diamond$ : Dioxane60%.

The membrane prepared without Dioxane had a typical finger-like structure (Figure 4.5). However, as increase the concentration of Dioxane, membrane morphologies were changed to more sponge-like structure. The increase of Dioxane concentration means relative reduction of solvent (NMP) concentration in the casting solution. As a result, exchange rate of solvents and non-solvent is decreased due to the poorer affinity between Dioxane and water and induces the delay of the liquid-liquid demixing. Dioxane has in fact a lower affinity for water than NMP, as confirmed by comparison of their solubility parameters (Table 4.5; when the affinity decreases, the difference in the solubility parameters ( $\Delta\delta$ ) increases. The difference in the solubility parameters ( $\Delta\delta$ ) is the absolute value of (solubility parameter of target material I) - (solubility parameter of target material II)). Thus more sponge-like structure was obtained.

Furthermore, vapour pressure of Dioxane (27 mmHg at 20 °C) is much higher than NMP (0.29 mmHg at 20 °C). This means that the solvent evaporation from casting solutions, before immersion in the coagulation bath, is easier and a denser skin layer is formed (Figure 4.5). As a consequence, the acetonitrile flux decreased with the increasing of the concentration of Dioxane and also rejection of dyes increased (Figure 4.6).

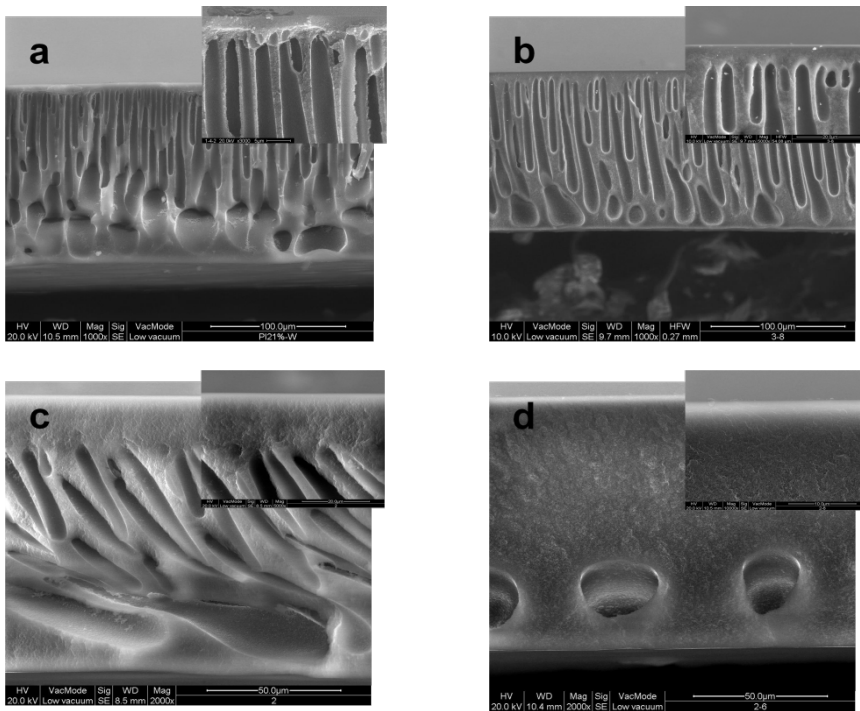


Figure 4.5. Cross-sections and particular of the top layer of membranes obtained from the casting solution prepared increasing the Dioxane concentration; (a) PI/Dioxane0, (b) PI/Dioxane20, (c) PI/Dioxane40 and (d) PI/Dioxane60.

Table 4.5 Solubility parameters of the polymer and liquids used [15-16].

	Hansen solubility parameter (MPa) <sup>1/2</sup> at 25°C			
	$\delta_d$	$\delta_p$	$\delta_h$	$\delta_t$
PI(P84)	*	*	*	26.8
NMP	18.0	12.3	7.20	22.9
DMF	17.4	13.7	11.3	24.8
1,4-Dioxane	19.0	1.80	7.40	20.5
Water	15.5	16.0	42.4	47.9
Ethanol	15.8	8.80	19.4	26.6
Acetonitrile	15.3	18.0	6.10	24.6
Methanol	15.1	12.3	22.3	29.7
Chloroform	17.8	3.10	5.70	19.0



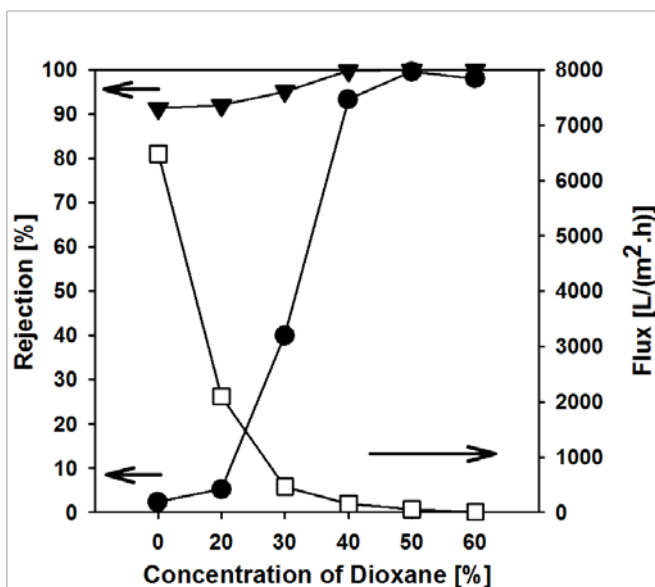


Figure 4.6. Pure acetonitrile flux (□) and Solvent blue 35 (●) and Rhodamine B (▼) rejection in acetonitrile of membranes prepared with different Dioxane concentration.

#### 4.3.3. Permeation flux of pure solvents

The fluxes of pure organic solvents through the membranes were investigated (Figure 4.7). The flux of pure solvents decreased in the following order:  $\text{CH}_3\text{CN} > \text{MeOH} > \text{DMF}$ .

Such results depend from solvent viscosity [17-20] and the mutual interactions between membrane material and solvents [21]. As the viscosity of solvents increased (Table 4.6), the flux of pure solvents decreased (Figure 4.7 (a)). High affinity of PI and DMF (Table 4.5,  $\Delta\delta_{\text{PI-solvent}}$ ) leads to increase of swelling degree of membrane. As a result, pores of membrane in the DMF reduced and also flux of DMF was lower than flux of other solvents (Figure 4.7 (b) and Table 4.7).

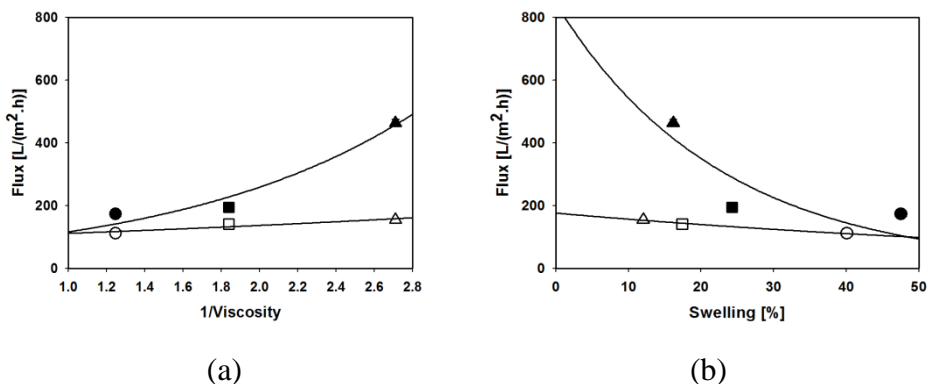


Figure 4.7. The effect of solvent viscosity (a) and swelling (b) on the flux of pure solvents through the PI/Dioxane30 membranes (solid symbols) and the PI/Dioxane40 membrane (open symbols).

Table 4.6 Some chemical-physical properties measured at 25°C of the liquids used [16, 22].

Solvents	Molecular weight (g/mol)	Molar volume (cm <sup>3</sup> /mol)	Viscosity (mPa.s)
NMP	99.13	96.50	1.67
DMF	73.09	77.00	0.80
1,4-Dioxane	88.11	85.70	1.18
Water	18.02	18.00	0.89
Ethanol	46.10	58.50	1.08
Acetonitrile	41.05	52.60	0.37
Methanol	32.04	40.70	0.54
Chloroform	119.38	80.70	0.54

Table 4.7 Degree of dimensional swelling of membranes in the different solvents.

Sample codes	Dimension swelling [%]		
	In CH <sub>3</sub> CN	In MeOH	In DMF
PI/Dioxane30	16.15	24.28	47.58
PI/Dioxane40	12.02	17.39	40.11

#### 4.3.4. Effect of the ionic charge, molecular weight and solvent type on membrane rejection

The effect of molecule charge on rejection was also investigated (Table 4.8).

Table 4.8 Rejection of molecules with different ionic charge.

Sample codes	Neutral	Positive	Neutral	Negative	
	Solvent blue 35 in CH <sub>3</sub> CN	Rhodamine B in CH <sub>3</sub> CN	Solvent blue 35 in MeOH	Methyl orange in MeOH	Methyl orange in DMF
PI/Dioxane30	40	95	-	92	95
PI/Dioxane40	89	>99	93	98	98

By reason of poor solubility of Methyl orange in acetonitrile, the solvents used with Methyl orange were methanol and DMF.

Membranes showed higher rejection in acetonitrile for Rhodamine B and Methyl Orange, than for Solvent blue 35. These results can be

explained by the charge effect [13, 23-24]. When the molecular size is much smaller than the membrane pores, the molecular charge can be the decisive factor in determining retention of the molecule. And charged molecules are usually better retained than uncharged molecules because they have bigger hydration sphere and effective diameter.

The rejection of Methyl orange in DMF was higher than in methanol. The reason is the higher swelling degree of the membrane in DMF which reduces the membrane pore size [25-26], increasing the rejection.

Table 4.9 Rejection of catalysts in different solvents.

Sample codes	Jacobsen's catalyst in CH <sub>3</sub> CN	Jacobsen's catalyst in CHCl <sub>3</sub>	Wilkinson's catalyst in CH <sub>3</sub> CN
PI/Dioxane30	16	-	-
PI/Dioxane40	67	90	97
PI/Dioxane50	97	-	-

The performance of the PI membranes was also investigated for separation of catalysts of interest (Table 4.9). As increase Dioxane concentration from 30 to 50%, rejection of Jacobsen's catalyst in acetonitrile increased due to reduction of membrane pores. Also the type of solvents, in which the molecules to be retained are dissolved, affects the rejection. The catalyst rejection in chloroform was higher than in acetonitrile, accordingly with the lower flux in chloroform (Figure 4.8).

Though the Jacobsen's and Wilkinson's catalysts have higher

molecular weight compared to Rhodamine B, their rejections in acetonitrile were lower compared to Rhodamine B because of intrinsic difference in the structure of the molecules and their interactions with the functional groups of the membrane material.

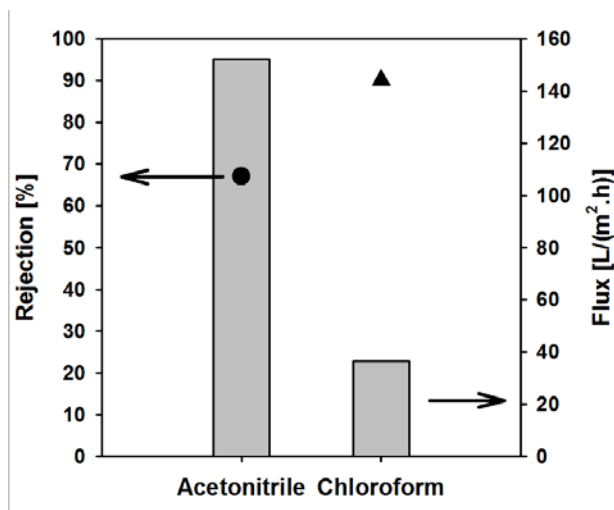


Figure 4.8. Pure solvents flux (grey columns) and Jacobsen's catalyst rejection (● and ▲) in different solvents for the PI/Dioxane40 membrane.

#### 4.3.5. Effect of solvent type in the casting solution

The diffusion rates of solvent and non-solvent during the phase inversion process, is a very important factor to control membrane morphology and transport property. Low mutual affinity between solvent and non-solvent has been usually known to suppress macrovoids and make more sponge-like structure in the membrane preparation [27]. In this work, the effect of two different solvents (NMP and DMF) was examined.

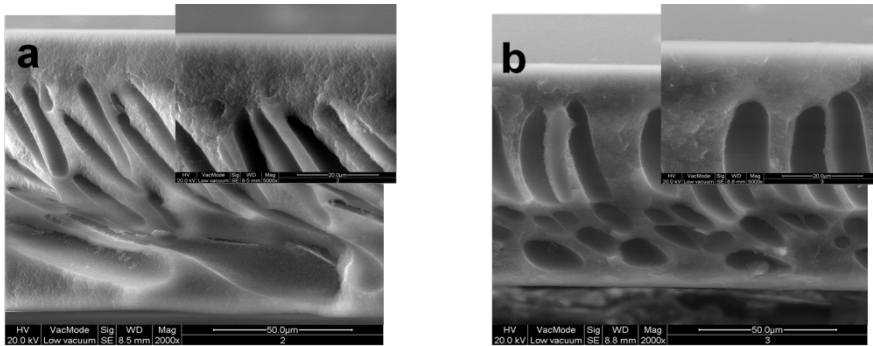


Figure 4.9. SEM images of cross-section for PI membranes prepared from different solvents; (a) PI/NMP39/Dioxane40, (b) PI/DMF39/Dioxane40.

Less macrovoids and more sponge-like structure were observed in the morphology of DMF-based membranes, despite of the higher affinity of DMF with water compared to NMP (Figure 4.9 and Table 4.5) and the general observation that macrovoids formation is favored by a higher affinity solvent/non-solvent [28].

A similar behavior has been observed in literature for PES/DMAc/water and PES/NMP/water ternary systems [29-30]. Membranes prepared from the first system have less macrovoids than those prepared from the second one, despite the affinity DMAc/water is higher than that NMP/water. This has been attributed to the vitrification boundary which intersects the binodal at lower polymer concentration for the first system compared to the second one, inducing an earlier vitrification of the polymer rich phase, which suppressed the macrovoids formation.

Moreover, DMF is a better solvent for PI than NMP (Table 4.5) and this contributes to delay the phase separation process.

However, solvent flux through DMF-based PI membrane was higher than that of NMP-based PI membrane (Table 4.10). This tendency can be explained by the nodular structure in the skin layer formed by rapid demixing and more interconnection of nodular structure occur increase of permeation [4, 28, 31].

Table 4.10 Pure solvent flux and rejection of dyes in the membranes prepared with different solvents.

Sample codes	CH <sub>3</sub> CN flux [L/(m <sup>2</sup> .h)]	Solvent blue 35 Rejection [%]	Rhodamine B Rejection [%]
PI/NMP39/Dioxane40	155±20	89	>99
PI/DMF39/Dioxane40	570±20	16	96

In order to evaluate the performance of our membrane for non-aqueous applications, a comparison with commercial membranes was summarized in Table 4.11. The membranes selected were Starmem<sup>TM</sup> series (120, 122, 228 and 240, hydrophobic) membranes from Membrane Extraction Technology, Desal-DK and Desal-5 membranes (hydrophilic) from GE OSMONICS, MPF44 (negative charged hydrophilic) and MPF60 (silicone uncharged hydrophobic) membranes from Koch Membrane Systems, and UTC-20 (positive charged hydrophilic) from Toray. The nominal molecular weight cut-off (MWCO) of the membranes given by the manufacturer are indicated in Table 4.11.

Starmem<sup>TM</sup> series, Desal-DK and UTC-20 membranes are made of polyimide, polyamide and polyamide, respectively. Polyimide and

polyamide materials have a similar solubility parameter value ( $26.2 \text{ (MPa)}^{1/2}$  and  $23.2\text{--}26.8 \text{ (MPa)}^{1/2}$ , respectively). For this reason, we can expect that these membranes have a similar affinity toward target solvent like methanol.

Methanol solution flux and rejection of solvent blue 35 (neutral), soybean daidzin (neutral), safranin O (positively charged) and Orange II (negatively charged) in methanol were tested for this study. These three molecules except soybean daidzin have similar molecular weight at 350 Da and so close to the nominal MWCO range (200–400) of the selected solvent resistant commercial membranes.

The PI/NMP39/Dioxane40 is characterized by higher flux and higher rejection of solute than commercial membranes except rejection of Orange II. However, Methyl orange which has similar molecular weight with Orange II, in methanol showed high rejection of 98% as shown in Table 4.8. These results confirm the interest for the membranes prepared in optimized conditions in this work.



Table 4.11 Comparison of permeation properties of SRNF membranes prepared in this work from (PI/NMP39/Dioxane40) and some commercial membranes\*.

Name of solute	Solvent blue 35	Soybean daidzin	Safranin O	Orange II
MW of solute	350.46	416.38	350.85	350.33
Performance	MeOH solution flux [L/(m <sup>2</sup> .h)] / Dye rejection [%]			
PI/NMP39 /Dioxane40	161 / 89	-	226 / 93	363 / 33
Desal-DK (MW 300)	26 / 49 [24]	41 / 71 [13]	32 / 60 [24]	48 / 54 [24]
Desal-5 (MW 350)	188 / 28 [24]	-	178 / 38 [24]	210 / 31 [24]
Starmem120 (MW 200)	-	170 / 53 [13]	-	-
Starmem122 (MW 220)	-	320 / 20 [13]	-	-
Starmem228 (MW 280)	-	22 / 79 [13]	-	-
Starmem240 (MW 400)	-	164 / 51 [13]	-	-
MPF44 (MW 200)	5.6 / 85 [24]	7.4 / 72 [13]	8.6 / 92 [24]	6.3 / 88 [24]
MPF60 (MW 400)	3.9 / 81 [24]		5.9 / 92 [24]	6.2 / 94 [24]
UTC-20 (MW 180)	53 / 79 [24]		64 / 94 [24]	56 / 94 [24]

\*Experimental conditions:

- Transmembrane pressure: 30 bar for all
- Dyes concentration: 100 mg/L for Ref.[24] and this work; 10 mg/L for Ref.[13]
- Temperature: 18-20°C for Ref.[24]; 20°C for Ref.[13]; 23±3°C for this work
- Active membrane area: 16.9 cm<sup>2</sup> for Ref.[24]; 14.6 cm<sup>2</sup> for Ref.[13] and this work
- Feed volume and permeate volume: from 50 to 300 ml and the corresponding half volume for Ref.[24]; 200 mL and 100 mL for Ref.[13]; 100 mL and 50 mL for this work

#### 4.3.6. Effect of non-solvent additives

To evaluate the effect of type and concentration of non-solvent additive on membrane properties, polymer concentration in the casting solutions was fixed at 21 wt%. Water has strong non-solvent power. Even small amount of water such like 4% cause increase viscosity of solution compared to same concentration of EtOH. Therefore the available maximum concentration of additive in polymer solution was controlled by the viscosity of polymer solution and solubility of polymer in the solvent/additive mixture.

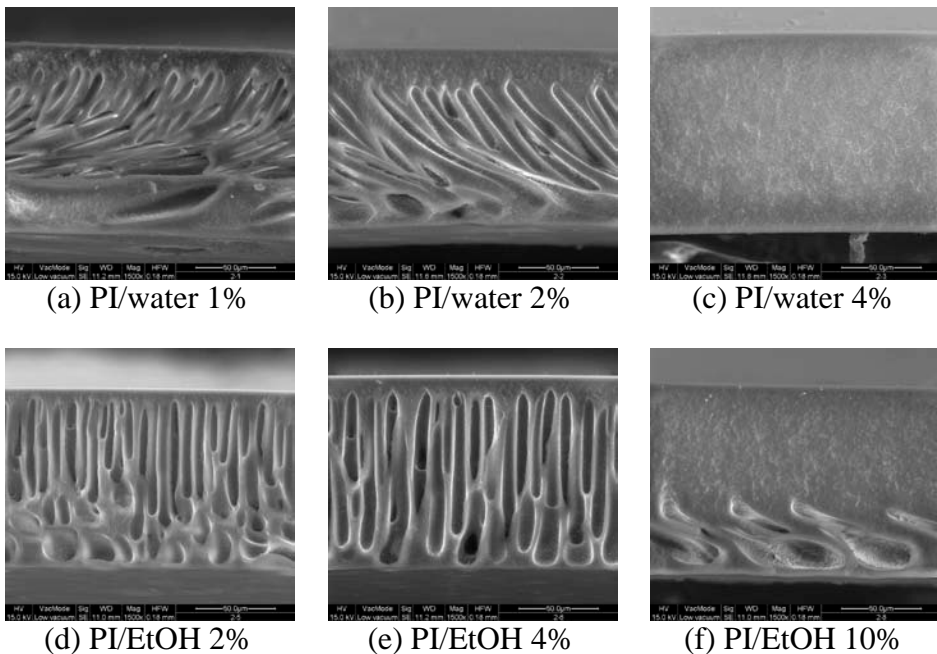


Figure 4.10. Cross-sectional SEM images of membrane prepared from different type and different concentration of non-solvent additive in casting solution.

Figure 4.10 shows the effect of different additives, as water and ethanol, in casting solution on the morphology of asymmetric membranes. The cross-sectional images reveal that the number of macrovoids gradually disappears as additives concentration is increased. The thickness of sponge-like structure was enriched from skin layer to bottom of membrane. The non-solvent additives can reduce thermodynamic miscibility of casting solution and eventually faster precipitation of cast film tends to form macrovoids with finger-like membrane structure (thermodynamic effect). Whereas slow phase inversion results in sponge-like structure membrane [32-33]. The additives also increase the viscosity of casting solution which results in decrease of mutual diffusion between solvent in casting solution and non-solvent in coagulation bath. Therefore, they induce a phase separation delay (kinetic effect). A combination of both effects determines the final membrane morphology.

Table 4.12 shows the effect of concentration of non-solvent additives on pure water with PI/Dioxane membranes.

Table 4.12 Comparison of water permeation properties of membranes prepared with non-solvent additives or volatile co-solvent.

Membranes	Water permeance [L/(m <sup>2</sup> .h.bar)]	Water permeability [10 <sup>3</sup> L.m/(m <sup>2</sup> .h.bar)]
PI/additive0	217.7	22.89
PI/water1%	106.9	14.86
PI/water2%	97.63	13.08
PI/water4%	121.3	16.01
PI/EtOH1%	98.87	13.20
PI/EtOH2%	72.13	10.25
PI/EtOH4%	51.31	7.016
PI/EtOH10%	143.5	15.33
PI/Dioxane20%	30.71	4.831
PI/Dioxane30%	8.670	1.085
PI/Dioxane40%	4.020	0.481

Water fluxes of PI/water membranes were higher than those of PI/ethanol membranes prepared with same concentration of ethanol, even though PI/water membranes have more thick sponge structure (Figure 4.10). This behavior may be caused by faster evaporation of ethanol during dry-wet phase inversion process. Ethanol induces denser skin layer which causes the polymer-rich phase to undergo rapid vitrification. As a result, few pores or defects are formed, consequently, the water flux is lower. By same reason, the increase of Dioxane concentration shows the decrease of water flux. (Vapour pressure of

solvents (Ethanol - 43.7 mmHg, water - 17.5 mmHg, Dioxane - 27 mmHg) at 20 °C)

For evaluation the performance of crosslinked PI/additive membranes to acetonitrile and ethanol, the membranes were tested with solvents and Rhodamine B solutions.

Table 4.13 Pure solvent permeation and rejection of membranes prepared with non-solvent additives or volatile co-solvent.

Membranes	Solvent permeability [10 <sup>3</sup> L.m/(m <sup>2</sup> .h.bar)]		Rejection of Rhodamine B [%] in	
	CH <sub>3</sub> CN	EtOH	CH <sub>3</sub> CN	EtOH
PI/additive0	98.89	21.30	98.79	36.91
PI/water1%	55.25	20.99	94.83	45.75
PI/water2%	52.18	17.82	95.02	33.98
PI/water4%	45.64	14.88	96.25	31.76
PI/EtOH1%	75.34	18.52	91.39	35.85
PI/EtOH2%	64.02	17.54	94.88	42.79
PI/EtOH4%	62.20	14.52	97.88	42.48
PI/EtOH10%	43.82	14.32	96.21	15.82
PI/Dioxane20%	12.10	-	92.01	-
PI/Dioxane30%	2.186	0.961	95.16	24.10
PI/Dioxane40%	0.557	0.908	99.80	37.10

As shown in Table 4.13, pure solvents permeability was decreased as the additives concentration is increased. The increase of Dioxane concentration also exhibits the decrease of solvent permeation. This showed different trend compared to water permeation. Moreover, the permeability of ethanol was much lower than acetonitrile. This behavior can be attributed to membrane-solvent interaction [19] to be able to cause membrane structural changes (such as swelling) and the development of surface forces adding to the viscous transport of solvent [17, 25, 34]. The swelling of prepared membrane in various organic solvents can be characterized using the difference of PI-solvent solubility parameter ( $\Delta\delta_{PI-solvent}$ ). As can be derived from Table 4.5, ethanol and PI membrane have obviously higher mutual affinity than acetonitrile and PI membrane. This means that porous PI membrane could be swollen more in ethanol, consequently, pore size of membrane reduced. Finally, the flux of ethanol became much lower than acetonitrile. Also, the high viscosity of ethanol also affected the decrease of permeability of pure solvent. (Table 4.6)

In order to understand effects of organic solvent, rejection of dye in organic solvents was needed. The decrease of solvent flux is expected to increase the rejection of molecule. As shown Table 4.13, Rhodamine B in acetonitrile solution showed higher rejection above 90% in spite of high acetonitrile flux. On the other hand, rejection of Rhodamine B in ethanol solution was less than 50%. These behaviors can be explained by the solvent-solute coupling effect [24, 35]. The hydrophilic nature of Rhodamine B produced a high affinity with ethanol compared to acetonitrile. Consequently, Rhodamine B goes together with ethanol

through the membrane, resulting in low rejection of Rhodamine B in ethanol solution.

#### **4.3.7. Effect of different crosslinking conditions**

Though PI material has intrinsically good chemical property, uncrosslinked PI membranes as well as PI polymer can be easily dissolved in aprotic polar organic solvents. However, after crosslinking with diamine solution PI membranes were stable in various solvents including aprotic solvents such as NMP, DMF and DMAc, which are generally used as the solvents to prepare polymer solution.

The effect of the crosslinking conditions on the PI membranes was evaluated in terms of flux and rejection. The effect of crosslinker concentration in diamine solution was investigated for membranes prepared from PI21/NMP39/Dioxane40 solution. Different concentrations (1, 5 and 10 v/v%) of crosslinking solution were prepared by dissolving DAMP in methanol, and then immersing the membranes in diamine solution for 24 hours (Table 4.3).

Before and after crosslinking, the morphologies of membranes were not particularly changed as shown in Figure 4.11. However, the stability of membrane was remarkably improved after crosslinking.

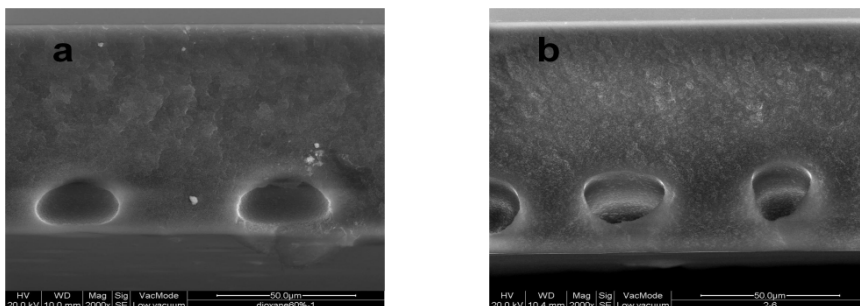


Figure 4.11. SEM images of cross-section for PI/NMP/Dioxane60 membranes (a) before and (b) after chemical crosslinking using 10 v/v% DAMP solution.

The permeation properties of crosslinked membranes depend from the crosslinking conditions (Figure 4.12). The fluxes of the membranes crosslinked with solutions of DAMP at concentration of 1% and 5% were quite similar, however, the rejection of membranes showed a big gap between 1% and 5%. In short, PI membranes crosslinked using more concentrated solutions, showed higher rejection and lower flux than less crosslinked samples. When the crosslinker concentration was high, more crosslinker can react with the polymer to form a compact crosslinked network and reducing the mobility of the polymer chains.



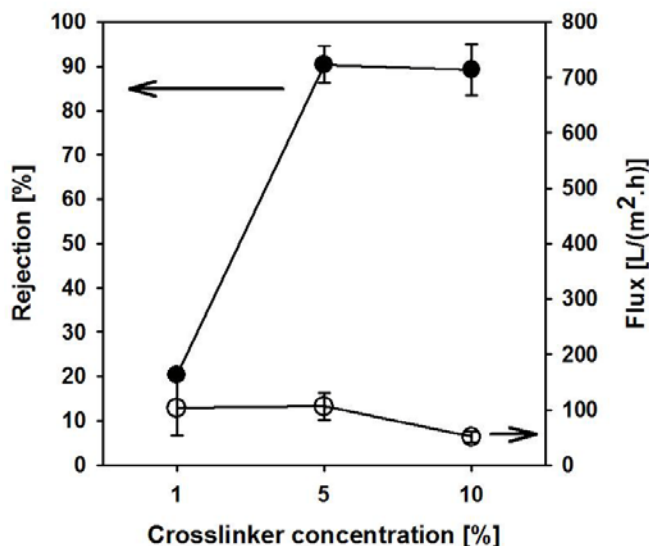


Figure 4.12. Rejection and flux of Solvent blue solution in acetonitrile of PI/NMP39/Dioxane40 membranes as a function of the crosslinker concentration.

The increasing of the degree of cross-linking with the increasing of the DAMP concentration and crosslinking time, was confirmed by FT-IR/ATR analysis (Figure 4.13). Typical imide bands in uncrosslinked PI membrane were identified at  $1778\text{ cm}^{-1}$  (asymmetric stretch of C=O imide group),  $1714\text{ cm}^{-1}$  (symmetric stretch of C=O imide group) and  $1360\text{ cm}^{-1}$  (C-N stretch). As increasing crosslinker concentration (Figure 4.13 (a)) or crosslinking time (Figure 4.13 (b)), imide peaks are reduced. Especially, imide band after 3 hours of crosslinking time was completely disappeared. While two strong peaks at  $1638\text{ cm}^{-1}$  and  $1533\text{ cm}^{-1}$  appeared for crosslinked membranes which are assigned to the stretching vibration of C=O and C-N group of amide, respectively.

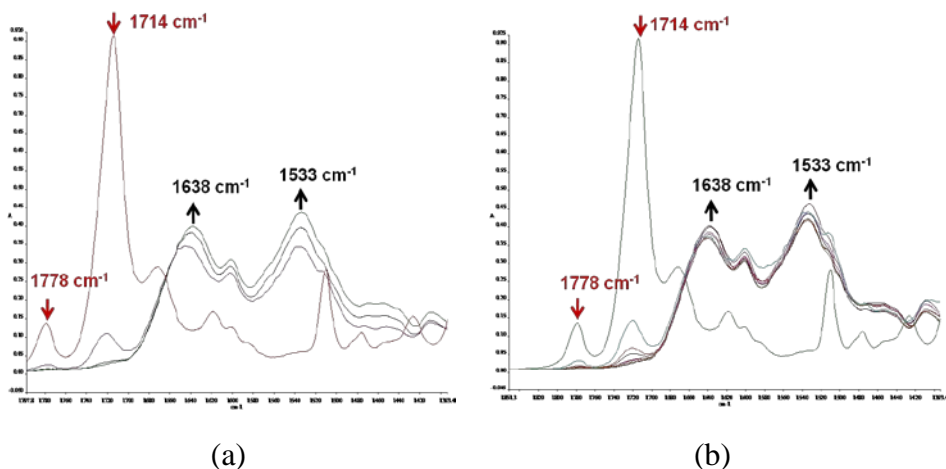


Figure 4.13. FT-IR/ATR spectra of PI membranes crosslinked from different concentration of crosslinking solution (a) red: uncrosslinked PI membrane, violet: 1%, black: 5%, green: 10%, and for different times (b) green: uncrosslinked PI membrane, sky blue: 5 min, red: 30 min, gray: 1 hr, pink: 3 hr, brown: 5 hr, light green: 7 hr, black: 24 hr.

The effect of different crosslinking times (5 min, 30 min, 1 hr, 3 hr, 5hr, 7 hr and 24 hr) on permeation properties has been also analyzed and summarized in Figure 4.14. In this case, the concentration of the crosslinker was fixed at 10%. Even 5 minutes of crosslinking with 10% provides more than 90% of rejection for Solvent blue 35 in acetonitrile. This means that the crosslinking reaction between the polymer and diamine (DAMP) is very fast and effective to increase the rejection and stability of the membrane [9, 36]. Despite the initial performance of the membranes crosslinked only for 5 minutes was good, these membranes did not result stable in water over long time because of a decrease of membrane strength. However, membranes crosslinked for more than 7 hours have been shown excellent stability in water more than 1 year.

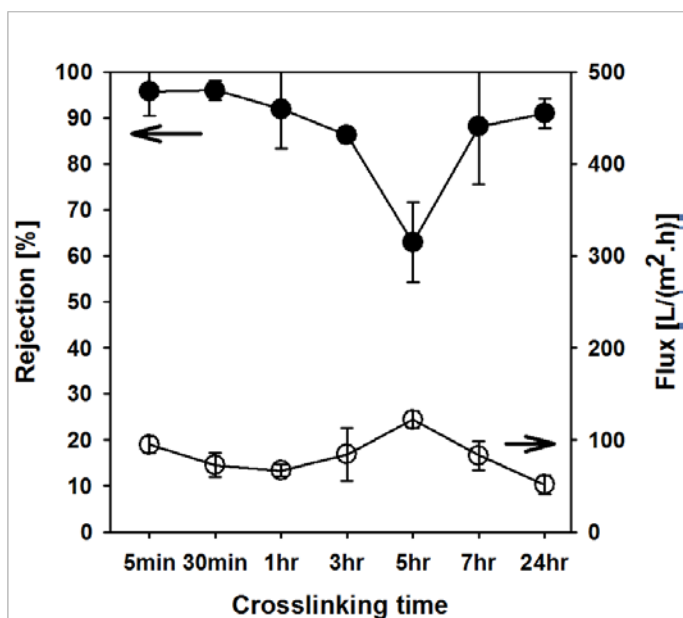


Figure 4.14. Rejection and fluxes of Solvent blue 35 in acetonitrile for PI/NMP39/Dioxane40 membrane as a function of the crosslinking times.

#### 4.4. Conclusions

Membrane morphology and transport properties of asymmetric membranes prepared from co-polyimide (PI) polymer, were efficiently controlled by an appropriate choice of the polymer concentration, concentration of volatile co-solvent and non-solvent additive, and solvent type.

The effect of the crosslinking conditions by using 1,5-Diamino-2-methylpentane (DAMP) as crosslinking reagent, was also investigated in order to improve the membranes chemical stability and to enhance separation properties.

From rejection tests carried out using various dyes and catalysts, it has been identified the membrane prepared from a solution containing 21 wt% of PI in a NMP/Dioxane mixture (39 and 40 wt%, respectively), crosslinked with DAMP (10 v/v%) in methanol for 24 hours, as a promising system having superior performance compared to other SRNF commercial membranes.

## References

1. P. Vandezande, L.E.M. Gevers, and I.F.J. Vankelecom, *Solvent resistant nanofiltration: separating on a molecular level*. Chemical Society Reviews, 2008. **37**: p. 365-405.
2. D.A. Patterson, A. Havill, S. Costello, Y.H. See-Toh, A.G. Livingston, and A. Turnerc, *Membrane characterisation by SEM, TEM and ESEM: The implications of dry and wetted microstructure on mass transfer through integrally skinned polyimide nanofiltration membranes*. Separation and Purification Technology, 2009. **66**: p. 90-97.
3. Y.H. See-Toh, M. Silva, and A. Livingston, *Controlling molecular weight cut-off curves for highly solvent stable organic solvent nanofiltration (OSN) membranes*. Journal of Membrane Science, 2008. **324**: p. 220-232.
4. P. Vandezande, X. Li, L.E.M. Gevers, and I.F.J. Vankelecom, *High throughput study of phase inversion parameters for polyimide-based SRNF membranes*. Journal of Membrane Science, 2009. **330**: p. 307-318.
5. K. Vanherck, P. Vandezande, S.O. Aldea, and I.F.J. Vankelecom, *Cross-linked polyimide membranes for solvent resistant nanofiltration in aprotic solvents*. Journal of Membrane Science, 2008. **320**: p. 468-476.
6. J. Ren, Z. Li, and F.-S. Wong, *Membrane structure control of BTDA-TDI/MDI (P84) co-polyimide asymmetric membranes by wet-phase inversion process*. Journal of Membrane Science, 2004. **241**: p. 305-314.
7. Y.H. See-Toh, F.C. Ferreira, and A.G. Livingston, *The influence of membrane formation on functional performance of organic solvent nanofiltration membranes*. Desalination, 2006. **199**: p. 242-244.
8. Y.H.S. Toh, F.W. Lim, and A.G. Livingston, *Polymeric membranes for nanofiltration in polar aprotic solvents*. Journal of Membrane Science, 2007. **301**: p. 3-10.
9. K. Vanherck, A. Cano-Odenaa, G. Koeckelberghsb, T. Dedrooga, and I. Vankelecoma, *A simplified diamine crosslinking method for PI nanofiltration membranes*. Journal of Membrane Science, 2010. **353**: p. 135-143.

10. J.S. Kang, J. Won, H.C. Park, U.Y. Kim, Y.S. Kang, and Y.M. Lee, *Morphology control of asymmetric membranes by UV irradiation on polyimide dope solution*. Journal of Membrane Science, 2000. **169**: p. 229-235.
11. K. Grodowska and A. Parczewski, *Organic solvents in the pharmaceutical industry*. Acta Poloniae Pharmaceutica - Drug Research, 2010. **67**: p. 3-12.
12. B. Sesto, *Acetonitrile*, in *Chemical industries newsletter*. 2008, SRI Consulting.
13. Y. Zhao and Q. Yuan, *A comparison of nanofiltration with aqueous and organic solvents*. Journal of Membrane Science, 2006. **279**: p. 453-458.
14. J.N. Barsema, N.F.A.v.d. Vegt, G.H. Koops, and M. Wessling, *Carbon molecular sieve membranes prepared from porous fiber precursor*. Journal of Membrane Science, 2002. **205**: p. 239-246.
15. P. Silva, S. Han, and A.G. Livingston, *Solvent transport in organic solvent nanofiltration membranes*. Journal of Membrane Science, 2005. **262**: p. 49-59.
16. J. Brandrup, E.H. Immergut, and E.A. Grulke, *Polymer handbook*. Fourth ed. 1999: Jon Wiley.
17. D. Bhanushali, S. Kloos, C. Kurth, and D. Bhattacharyya, *Performance of solvent-resistant membranes for non-aqueous systems: solvent permeation results and modeling*. Journal of Membrane Science, 2001. **189**: p. 1-21.
18. D.R. Machado, D. Hasson, and R. Semiat, *Effect of solvent properties on permeate flow through nanofiltration membranes. Part I: investigation of parameters affecting solvent flux*. Journal of Membrane Science, 1999. **163**: p. 93-102.
19. N. Stafie, D.F. Stamatialis, and M. Wessling, *Insight into the transport of hexane-solyte systems through tailor-made composite membranes*. Journal of Membrane Science, 2004. **228**: p. 103-116.
20. L.S. White, *Transport properties of a polyimide solvent resistant nanofiltration membrane*. Journal of Membrane Science, 2002. **205**: p. 191-202.
21. B.V.d. Bruggen, J. Geens, and C. Vandecasteele, *Fluxes and rejections for nanofiltration with solvent stable polymeric membranes in water, ethanol and n-hexane*. Chemical Engineering Science, 2002. **57**: p. 2511-2518.
22. D.R. Lide, ed. *Handbook of chemistry and physics*. ed. 84. 2003-2004, CRC Press.
23. B.V.d. Bruggen, J. Schaep, D. Wilms, and C. Vandecasteele, *Influence of molecular*

- size, polarity and charge on the retention of organic molecules by nanofiltration. *Journal of Membrane Science*, 1999. **156**: p. 29-41.
24. X.J. Yang, A.G. Livingston, and L.F.d. Santos, *Experimental observations of nanofiltration with organic solvents*. *Journal of Membrane Science*, 2001. **190**: p. 45-55.
  25. J.P. Robinson, E.S. Tarleton, C.R. Millington, and A. Nijmeijer, *Solvent flux through dense polymeric nanofiltration membranes*. *Journal of Membrane Science*, 2004. **230**: p. 29-37.
  26. E.S. Tarleton, J.P. Robinson, C.R. Millington, and A. Nijmeijer, *Non-aqueous nanofiltration: solute rejection in low-polarity binary systems*. *Journal of Membrane Science*, 2005. **252**: p. 123-131.
  27. K. Kimmerle and H. Strathmann, *Analysis of the structure-determining process of phase inversion membranes*. *Desalination*, 1990. **79**: p. 283-302.
  28. N. Leblanc, D.L. Cerf, C. Chappey, D. Langevin, M. Me'tayer, and G. Muller, *Influence of solvent and non-solvent on polyimide asymmetric membranes formation in relation to gas permeation*. *Separation and Purification Technology*, 2001. **22-23**: p. 277-285.
  29. J. Barzin and B. Sadatnia, *Theoretical phase diagram calculation and membrane morphology evaluation for water/solvent/polyethersulfone systems*. *Polymer*, 2007. **48**: p. 1620-1631.
  30. J. Barzin and B. Sadatnia, *Correlation between macrovoid formation and the ternary phase diagram for polyethersulfone membranes prepared from two nearly similar solvents*. *Journal of Membrane Science*, 2008. **325**: p. 92-97.
  31. H. Yanagishita, T. Nakane, and H. Yoshitome, *Selection criteria for solvent and gelation medium in the phase inversion process* *Journal of Membrane Science*, 1994. **89**: p. 215-221.
  32. A.F. Ismail and A.R. Hassan, *Effect of additive contents on the performances and structural properties of asymmetric polyethersulfone (PES) nanofiltration membranes*. *Separation and Purification Technology*, 2007. **55**: p. 98-109.
  33. D. Wang, K. Li, and W.K. Teo, *Relationship between mass ratio of nonsolvent-additive to solvent in membrane casting solution and its coagulation value*. *Journal*

- of Membrane Science, 1995. **98**: p. 233-240.
34. J. Geens, B.V.d. Bruggen, and C. Vandecasteele, *Transport model for solvent permeation through nanofiltration membranes*. Separation and Purification Technology, 2006. **48**: p. 255-263.
  35. D. Bhanushali, S. Kloos, and D. Bhattacharyya, *Solute transport in solvent-resistant nanofiltration membranes for non-aqueous systems: experimental results and the role of solute-solvent coupling*. Journal of Membrane Science, 2002. **208**: p. 343-359.
  36. L. Shao, L. Liu, S.X. Cheng, Y.D. Huang, and J. Ma, *Comparison of diamino crosslinking in different polyimide solutions and membranes by precipitation observation and gas transport*. Journal of Membrane Science 2008. **213**: p. 174-185.



## **Chapter 5 Solvent resistant hollow fiber membranes**

### **5.1. Introduction**

Systems based on hollow fiber membrane can make chemical plants more compact, more energy efficient, clean, and safe by providing a lower equipment size-to-production capacity ratio, by reducing energy requirements, by improving efficiency, and by lessening waste generation, with the correct choice of membrane material [1]. For that reason, the possibility of hollow fiber membrane in the industrial fields has increased.

The fabrication of a hollow fiber membrane with a desirable pore size distribution and performance is not a trivial process. There are many factors controlling fiber morphology during the phase inversion. In general, the mechanism for asymmetric hollow fiber formation is much more complicated than that for asymmetric flat membranes [2]. For example, it is a known fact that it is very difficult to simulate the hollow fiber spinning process by adopting the process conditions developed for asymmetric flat membranes. The controlling factors for hollow fiber morphology are different from those of flat membranes. There are two coagulations taking place in hollow fiber spinning (internal and external surfaces), while there is only one major coagulation surface for an asymmetric flat sheet membrane. When liquids are used as bore fluids, the internal coagulation process for a hollow fiber starts immediately after extrusion from a spinneret and then the fiber goes through the external coagulation, where there is usually a waiting period for an

asymmetric flat membrane before immersion into a coagulant. Depending on the membrane wall thickness and solvent exchange rate, the formations of inner and outer skins of a hollow fiber are more inter-related than that of a flat membrane. In addition, the spinning dopes suitable for hollow fiber fabrication generally have a much greater viscosity and elasticity than those for flat membranes [3]. This high viscosity retards solvent exchange rates and introduces complexity during the precipitation. Since hollow fiber formation usually takes place non-isothermally under tension, the Gibbs free energies for the states of spinning solutions (for hollow fibers) and casting solutions (for flat membranes) are different.

In this chapter, we focused on the preparation and characterization of solvent stable polyimide hollow fiber membrane with improved membrane performances and chemical stability using P84<sup>®</sup> co-polyimide. For the solvent stable membranes, flat sheet configuration was commonly employed, and only few research groups have reported the use of hollow fiber module [4-6]. Generally, the polyimide membranes in hollow fiber configuration have mainly utilized in pervaporation [7-8] as well as gas separation [9-12].

Furthermore, in-line chemical crosslinking of polyimide hollow fiber for SRNF applications has been firstly attempted. In this innovative method, the chemical crosslinking was included during the phase inversion process by feeding the aqueous diamine (crosslinker) solution as the bore fluid. Permeation properties (flux and rejection), chemical stability and mechanical strength of the membranes prepared by the innovative in-line crosslinking method were investigated and compared

to that of the membranes crosslinked after their formation.

## **5.2. Experimental**

### **5.2.1. Materials**

Lenzing P84<sup>®</sup> co-polyimide was purchased from HP polymer GmbH, Austria. *N*-Methyl-2-pyrrolidone (NMP, Carlo Erba, Italy) has been purchased and used as the solvent for preparation of dope solution. The solubility parameters of polymer, solvents and non-solvent are summarized in Table 5.1. Ultrapure water or an aqueous solution of 1,5-Diamino-2-methylpentane (DAMP, Sigma-Aldrich) has been used as the bore fluid. Isopropanol (IPA, Carlo Erba) has been used to prepare chemical crosslinking solution for post-synthesis chemical crosslinking of as spun fiber (conventional method). Acetonitrile (CH<sub>3</sub>CN) and ethanol (EtOH) have been purchased from Carlo Erba, Italy and used as the solvents to characterize the permeation properties of the prepared membranes. Chemical and physical properties of solvents used in this study are summarized in Table 5.2. Rhodamine B (molecular weight: 479.01g/mol, Sigma-Aldrich) has been used as a probe molecule for rejection of the hollow fiber membranes. All the solvents used are of analytical reagent grade and has been used as received without any further purification. Two component epoxy resin (Stycast 1266, Emerson & Cuming, Belgium) has been used for potting the membrane in the module.

Table 5.1. Solubility parameters of polymer, solvents and non-solvent.

		Hansen solubility parameter (MPa) <sup>1/2</sup> at 25°C [13]			
		$\delta_d$	$\delta_p$	$\delta_h$	$\delta_t$
Polymer	PI (P84)	*	*	*	26.8 [14]
Solvents	NMP	18.0	12.3	7.2	22.9
Additive & Non-solvent	Water	15.5	16.0	42.4	47.9
Tested solvents	CH <sub>3</sub> CN	15.3	18.0	6.1	24.6
	EtOH	15.8	8.8	19.4	26.6

Table 5.2. Chemical and physical properties of solvents used in this study at 25°C [13, 15].

Solvents	Molecular weight (g/mol)	Molar volume (cm <sup>3</sup> /mol)	Viscosity (mPa.s)
NMP	99.13	96.50	1.67
Water	18.02	18.00	0.89
CH <sub>3</sub> CN	41.05	52.60	0.37
EtOH	46.10	58.50	1.08

### 5.2.2. Spinning of hollow fiber membranes

Dope solution was prepared by mixing the polymer (PI), solvent (NMP) and non-solvent additive (water) in a glass flask under mechanical stirring for 1 day until the solution became homogeneous. The dope solution was transferred into the dope tank then kept at 30 °C for 24 hours to remove air bubbles. Hollow fiber membranes were spun by the wet or dry-wet phase inversion technique with the spinning

apparatus showed in Figure 5.1. The spinning conditions and parameters are summarized in Table 5.3. The dope solution and the bore liquid (water or DAMP/water solution) were co-extruded by a precision gear pump and by a peristaltic pump, respectively. The extruded fiber was coagulated in a coagulation bath with continuous circulation to avoid local build-up of the solvent concentration. The fiber was pulled out of the coagulation bath by take-up rolls rotating at an adjustable speed and transferred on the collection spool, immersed in a water bath for further washing. Then the hollow fiber membranes were cut and stored in water bath for 2 days to remove residual solvents.

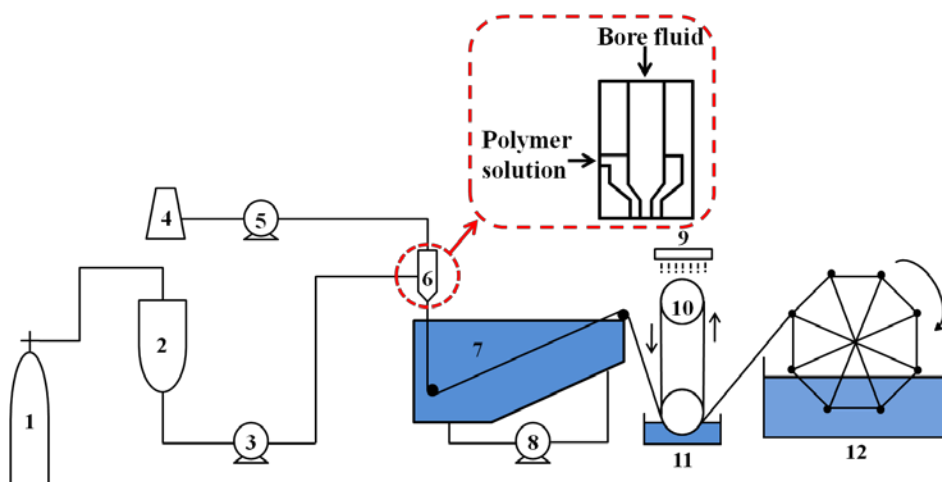


Figure 5.1. Schematic diagram of the spinning apparatus.

1: N<sub>2</sub> gas cylinder, 2: dope solution tank, 3: gear pump, 4: bore fluid reservoir, 5: bore fluid pump, 6: nozzle, 7: external coagulation bath, 8: circulation pump, 9: water spray, 10: take-up rollers, 11: water bath, 12: spool.

Table 5.3 Spinning conditions and parameters for preparation of PI hollow fiber membranes.

Sample code	A-30	A-0	B-30	B-0
Dope composition (wt%)	PI / NMP / Water = 20 / 76 / 4			
Bore fluid composition (wt%)	Pure water = 100		DAMP / Water = 10 / 90	
Dope temperature (°C)	30.0			
Bore temperature (°C)	25.0			
Dope flow rate (g/min)	2.30			
Bore fluid flow rate (g/min)	1.35			
Air-gap (cm)	30	0	30	0
External coagulant	Water			
Coagulant temperature (°C)	25.0			
Room temperature (°C)	25.0 ± 0.2			
Relative humidity (RH%)	40 ± 2			

- Take-up speed (m/min): 4-5

- Dimensions of spinneret (mm): 0.2 (bore), 0.4 (inner diameter of dope channel), 0.8 (outer diameter dope channel)

### **5.2.3. Chemical crosslinking (post-treatment) and module preparation**

Hollow fiber membranes spun using pure water as the bore fluid require post-synthesis crosslinking process to improve their chemical stability in organic solution. Chemical crosslinking (post-treatment) was carried out by immersing the virgin fibers into the 10 v/v% DAMP/IPA crosslinking solution for 1 day at room temperature. In addition, the effect of post-treatment (further chemical crosslinking) on chemical, mechanical and permeation properties of simultaneously crosslinked and coagulated hollow fiber has been evaluated. The post-treated membranes were washed repeatedly with pure IPA to remove any unreacted or residual crosslinker (diamine, DAMP). To prevent pore collapsing, the membranes were stored in 40 v/v% glycerol/IPA solution for 48hr then dried at room temperature before using.

The hollow fiber modules were prepared by potting both ends of a stainless steel tube module with epoxy resin. Each module contains 4 fibers with an effective fiber length of 8 cm.

### **5.2.4. Characterization of hollow fiber membranes**

#### **5.2.4.1. Membrane morphology and chemical/mechanical properties**

The cross section and the surface structure of hollow fiber membranes were characterized by scanning electron microscopy (SEM, FEI QUANTA 200F). The cross section of the fibers was obtained after freeze-fractured in liquid nitrogen.

The Fourier Transform Infrared (FT-IR) spectra of the virgin P84<sup>®</sup> hollow fiber were compared with the in-line crosslinked hollow fiber

membranes to monitor any chemical changes using a PerkinElmer Spectrum One FT-IR/ATR Spectrophotometer. The spectra were collected in the attenuated total reflection (ATR) mode, directly from the outer or inner surface of the hollow fiber membrane. The spectra were recorded at a resolution of  $4\text{ cm}^{-1}$  as an average of four scans.

Before and after chemical crosslinking, tensile strength of the dried fibers was measured by a Zwick/Roell single column Universal Testing Machine (model Z2.5) at room temperature. The clamps were coated with rubber tape to improve their grip on the samples. Sample specimens with an effective length of 5 cm (distance between the clamps) were tested at a deformation rate of 5 mm/min. The average value and the standard deviation of the Young's modulus, the break strength and the maximum deformation were determined on a series of at least 5 samples.

#### **5.2.4.2. Nanofiltration test**

Performances of the prepared hollow fiber membranes were evaluated in terms of solvent flux and solute rejection. All experiments were conducted in a dead-end filtration set-up at 3 bar at  $23\pm 3\text{ }^{\circ}\text{C}$  (Figure 5.2). Prepared membrane modules were firstly immersed in pure ethanol for 2-3 hours and then washed with pure ethanol to remove the glycerol which was used to prevent pore collapse. Before the actual testing, membranes in module were equilibrated (pre-conditioning) in the solvent in which they were going to be tested for at least 24 hours.



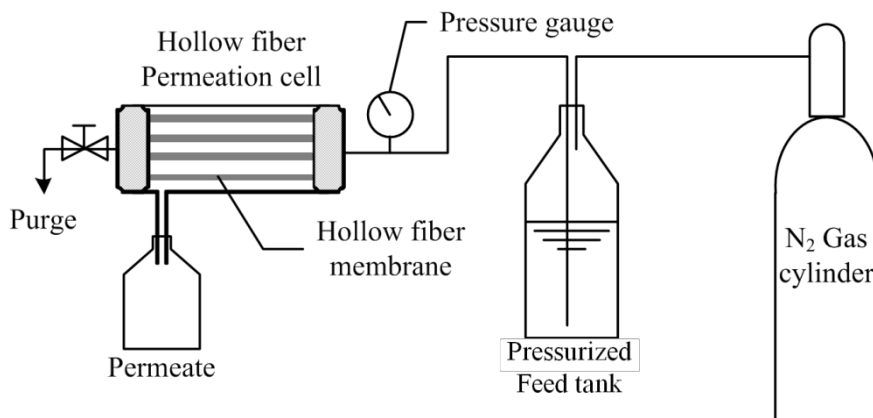


Figure 5.2. Schematic diagram of the SRNF permeation apparatus for hollow fiber membranes. (dead-end mode)

Hollow fiber membrane modules may operate in either an “inside-out” or “outside-in”. However, in this study, inside-out mode was adopted. The feed solution (or pure solvent) was placed in a feed tank and N<sub>2</sub> gas was used to apply pressures up to 3 bar. Then it was filtered through the fiber wall and collected from outside of the fiber. Pure solvent flux was measured at steady state using the following equation (5.1).

$$J = \frac{V}{A \times T} \quad (5.1)$$

where  $J$  (L/(m<sup>2</sup>h)) is flux of solvent;  $V$  (L) the volume of permeate;  $A$  (m<sup>2</sup>) the effective surface area of hollow fiber membrane;  $T$  (h) time. The effective membrane area was calculated using measured effective membrane length, number of fiber and membrane diameter.

Rejection tests were carried out using 0.01 wt/v% Rhodamine B in

target solvents (CH<sub>3</sub>CN or EtOH) at 3 bar and calculated by the following equation.

$$R (\%) = \left( 1 - \frac{C_p}{C_f} \right) \times 100 \quad (5.2)$$

where  $R$  is the rejection of membrane,  $C_f$  and  $C_p$  represent the concentration of Rhodamine B in the feed and permeate, respectively.

The concentrations of feed and permeate solution were analyzed by a UV spectrometer (Lambda 650S UV/Vis spectrometer, PerkinElmer, USA).

### **5.3. Results and Discussion**

#### **5.3.1. Membrane morphology**

The fibers prepared in the present work have a typical asymmetric structure; sponge-like structures are formed near the lumen and the shell edge, while finger-like macrovoids are formed in the middle of the fiber. The presence of a sponge-like structure near the shell and lumen side can be explained by the presence of water as a non-solvent additive, which increased the viscosity of spinning solution dramatically due to the formation of NMP:H<sub>2</sub>O hydrogen-bonding complex. In addition, viscosity of the solution increases more rapidly when in contact with non-solvent, or as a result of solvent evaporation, as the polymer phase is closer to its precipitation point. However, slowly but continuous solvent

and non-solvent exchange induced viscous fingering which formed finger-like macrovoids in the middle of the fiber [16].

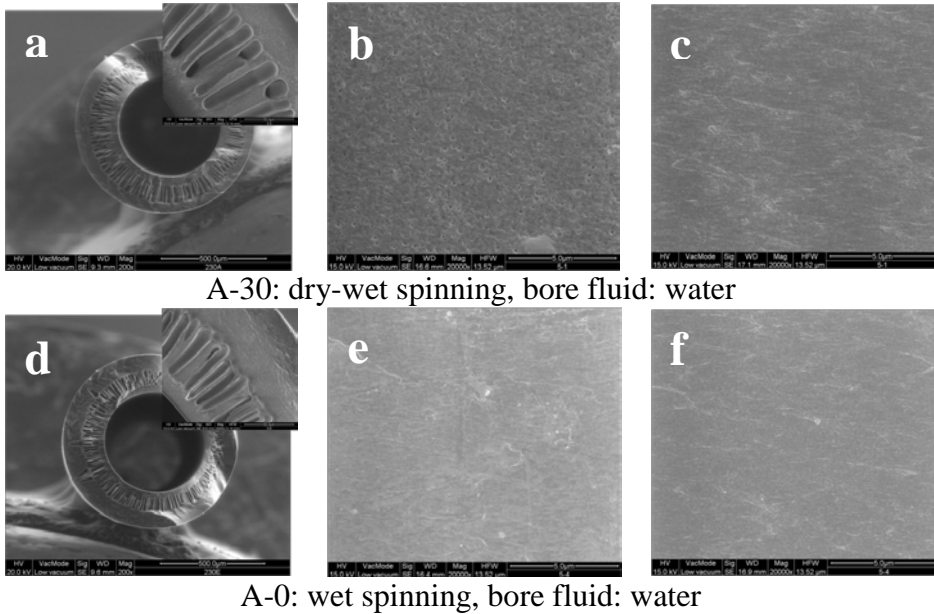
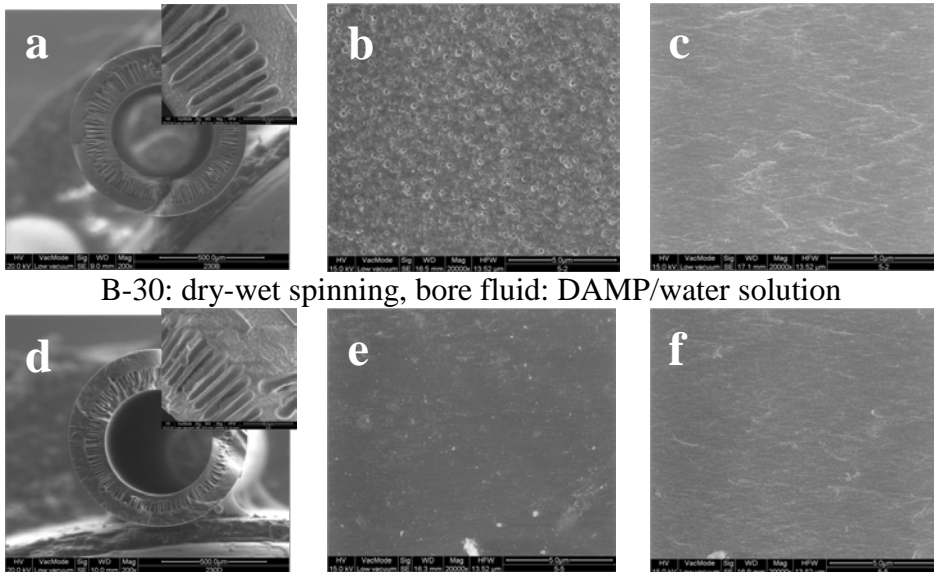


Figure 5.3. SEM images of P84 co-polyimide A series hollow fibers prepared by dry-wet (a: cross-section, b: shell surface, c: lumen surface) and wet (d: cross-section, e: shell surface, f: lumen surface) phase inversion.

Regarding to the surface structure of lumen and shell side, it should be noted that the morphology of the lumen surface was not affected by the composition of the bore fluid or by the phase inversion method. However, a remarkable morphological change was observed on the surface of the shell side by changing the phase inversion method.



B-30: dry-wet spinning, bore fluid: DAMP/water solution

B-0: wet spinning, bore fluid: DAMP/water solution

Figure 5.4. SEM images of P84 co-polyimide B series hollow fibers prepared by dry-wet (a: cross-section, b: shell surface, c: lumen surface) and wet (d: cross-section, e: shell surface, f: lumen surface) phase inversion.

In wet spinning, no obvious pores were observed on the shell side surface of the fiber due to the instantaneous liquid-liquid demixing in water. However, in dry-wet spinning (air gap length of 30 cm), porous shell surface was obtained for both membranes spun from water or DAMP/water solution used as the bore fluid. Of course, it is well known that the surface morphology near the shell side can be strongly affected by the external environment including temperature and relative humidity. Especially water vapour intake from the air is an important factor to be considered. In general, as the nascent membrane is exposed longer to the humid atmosphere, the water content in the top layer increases resulting in more porous structures and higher permeation rates. In other words,

the utilization of an air gap during spinning could be considered as equivalent to the well-known method of adding small amounts of water to the dope in order to increase porosity [17]. In case of wet spinning, the shell surfaces resulted to be dense because of the instantaneous demixing.

### **5.3.2. Chemical and mechanical properties**

Post-synthesis chemical crosslinking of P84<sup>®</sup> co-polyimide membranes with diamine solution is one of the most commonly used methods to increase the chemical (long-term) stability. However, in this study, in-line crosslinking of hollow fiber membrane during spinning process has been attempted to simplify the process and save time and cost. As mentioned earlier, the membranes of series A (A-30 and A-0) were prepared by conventional method which means chemical crosslinking was conducted after spinning the co-polyimide fibers while series B (B-30 and B-0) are prepared by newly proposed method and expected to be crosslinked during spinning procedure. Therefore, to briefly evaluate the effectiveness of the proposed simplified in-line crosslinking method, four different as spun fibers (A-30, A-0, B-30 and B-0) were immersed in pure NMP. A-30 and A-0 samples were totally dissolved in NMP, as expected. However, B-30 and B-0 samples which were spun from an aqueous DAMP solution as the bore fluid, resulted to be stable.

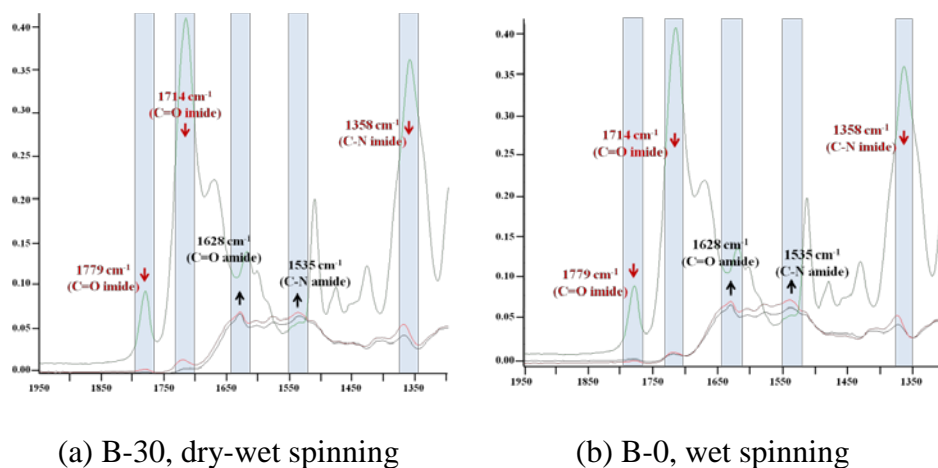


Figure 5.5. FT-IR/ATR spectra of in-line crosslinked samples (series B) without additional post-treatment prepared by dry-wet (a) and wet (b) phase inversion. (green: uncrosslinked fiber, red: shell surface, black: lumen surface)

The influence of in-line crosslinking on the chemical structure of the membrane was monitored by FT-IR/ATR spectra for series B samples (Figure 5.5-Red (shell) and black line (lumen)) and compared to uncrosslinked fiber (Figure 5.5-Green line). Typical imide bands in original polyimide membrane were identified at  $1779\text{ cm}^{-1}$  (asymmetric stretch of C=O imide group),  $1714\text{ cm}^{-1}$  (symmetric stretch of C=O imide group) and  $1358\text{ cm}^{-1}$  (C-N stretch). As can be seen in these figures, amide groups start to form in both lumen and shell side after spinning.

The imide bands are detected only in the shell side of dry-wet spun fiber. On the other hands, the presence of imide bands in lumen and shell side indicates that the in-line crosslinking was partially conducted in wet spun fiber. Moreover, intensity of the imide bands on the shell side is

higher than on the lumen side because of the non sufficient diffusion rate of the diamine from the lumen to the shell side on the nascent hollow fibers. This is more evident for wet spun fiber than for dry-wet. However, simple chemical stability test which was carried out by putting the as spun fiber in NMP confirmed that these in-line crosslinked fibers still have sufficient chemical stability.

The mechanical strength of as spun series B samples were characterized and summarized in Figure 5.6. In addition, the effect of the additional chemical crosslinking (post-treatment with 10 v/v% DAMP/IPA solution for 1 day) on the mechanical property of same samples was carried out. In both, before and after post-treatment, wet spun fibers (B-0) show higher Young's modulus than dry-wet spun fibers (B-30) because of the porous structure of the shell surface of B-30. It is noteworthy to mention that no significant effect of post-treatment on Young's modulus (Figure 5.6-Left) was observed. However, pronounced effect was observed on the tensile properties of the material after crosslinking (Figure 5.6-Right). Stress-strain curve demonstrates the rigidity of the crosslinked fibers, resulting in rupture of samples at lower tensile stress for both samples.

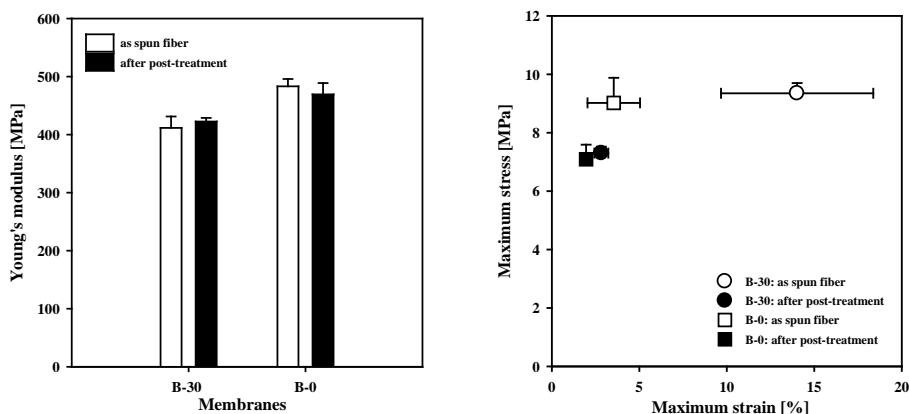


Figure 5.6. Mechanical properties of in-line crosslinked samples (series B) before and after post-treatment. (Post-treatment: 10 v/v % DAMP/IPA solution for 1 day)

In Figure 5.7, the effect of spinning conditions on mechanical properties of fiber spun from four different conditions were characterized and compared after post-treatment. Sample A-0 and B-0 showed higher Young's modulus than A-30 and B-30, respectively. Wet spun fibers have relatively dense shell surface while dry/wet spun fibers have lots of pores on shell surface which decrease Young's modulus. In addition, the in-line chemical crosslinked by aqueous diamine solution increases Young's modulus. As a consequence, sample B-0 showed the highest Young's modulus. The stress vs. strain curve revealed that after post-treatment all samples increased rigidity. One interesting result shown on Figure 8 is that series A samples showed higher stress as well as a higher strain than sample B series. It is possibly due to the effect of the crosslinker during phase inversion process. Chemical crosslinking and



phase inversion took place at the same time for sample B-30 and B-0 which provided more chance to crosslink the polymer matrix and finally become more rigid. On the other hand, for sample A-30 and A-0, once they formed a solid membrane structure, crosslinking is more limited which leads to increased flexibility of the fibers.

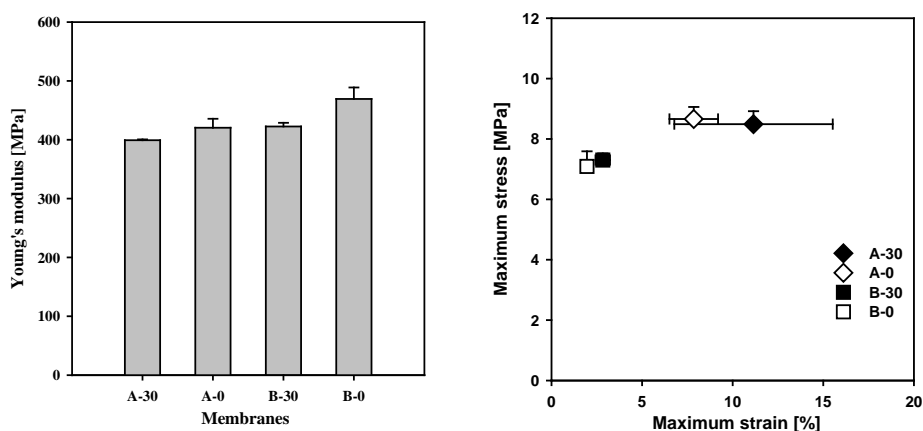


Figure 5.7. Mechanical properties of PI hollow fibers after post-treatment. (post-treatment: 10 v/v % DAMP/IPA solution for 1 day)

### 5.3.3. Permeation properties

Table 5.4 shows permeation properties of the prepared hollow fiber membranes. For both the organic solvents used, acetonitrile and ethanol, the fluxes through dry-wet spun fibers were higher than those of wet spun fibers. These results are consistent with the denser shell surface of the wet-spun fiber. However, surprisingly, the dry-wet spun fiber has not only higher solvent flux but also shows higher solute rejection. It could be explained by the resistance model [18]. Originally, this model was

developed to explain the correlation between the support resistance and coating thickness on the ideal selectivity of the gases and/or vapors through composite membrane. However, this model can be extended to the transport through solvent resistant nanofiltration membranes. According to this model, to have high performance (high flux with high selectivity) composite membranes, it is important to minimize the thickness of the selective layer. However, the minimum coating thickness in a composite membrane having the intrinsic selectivity is limited by the resistance of the porous support layer. It means the support must be highly permeable otherwise thicker coating layer is needed to obtain an ideal selectivity. In this case, of course, permeate flux decreased significantly. Applying this theory in our system, dry-wet spun fiber consists in dense selective layer in lumen side while it has porous support with porous skin surface on the shell side. The single selective layer with porous support led high flux and high solute rejection. On the other hand, solution resistance in wet spun fiber increases by having two dense skin layer in both lumen and shell sides. Finally, dry-wet spun fibers show not only high flux but also high rejection.

It should be mentioned that the as spun fiber of series A, without in-line crosslinking, showed poor chemical resistance in target solvents. Therefore, the solvent flux and rejection test were carried out only after the post-treatment while series B sample remains very stable in same target solvents even in aprotic solvent such as NMP.

Table 5.4 Solvent flux and Rhodamine B rejection in two different systems. (operating pressure: 3 bar)

		Solvent flux		Rejection of Rhodamine B in	
		CH <sub>3</sub> CN	EtOH	CH <sub>3</sub> CN	EtOH
As spun fiber	A-30	<sub>a)</sub>	<sub>a)</sub>	<sub>a)</sub>	<sub>a)</sub>
	A-0	<sub>a)</sub>	<sub>a)</sub>	<sub>a)</sub>	<sub>a)</sub>
	B-30	25.1	5.72	93.0	22.6
	B-0	9.11	1.52	89.0	18.5
Post-treated sample <sup>b)</sup>	A-30	22.5	22.2	84.0	23.6
	A-0	9.90	4.38	73.6	16.2
	B-30	53.6	20.2	77.8	25.9
	B-0	8.54	1.43	52.9	20.3

<sup>a)</sup> Measurements were not carried out due to the low chemical stability.

<sup>b)</sup> Post-treatment condition: 10 v/v % DAMP/IPA solution for 1 day.

Solvent flux and rejection of Rhodamine B in two different solvents (acetonitrile and ethanol) were measured at 3 bar of trans-membrane pressure and summarized in Table 5.4. In general, it was observed that the flux of acetonitrile is higher than ethanol because of different affinity of the solvents with the membrane. Lower affinity between the membrane and acetonitrile compared to that of membrane and ethanol (Table 5.1, difference of PI-solvent solubility parameter,  $\Delta\delta_{PI-solvent}$ ) leads to the increase of acetonitrile flux. Moreover, among the solvent properties (Table 5.2), the decrease of viscosity and molar volume induced the increase of the flux [19-21].

The rejection of Rhodamine B in acetonitrile solution was much higher than that of in ethanol solution in spite of high acetonitrile flux.

Rejection of Rhodamine B in ethanol solution was less than 30% while it showed much higher than 50% in acetonitrile system. These behavior can be explained by the coupling effect of mutual interaction between solute and solvent [22-23]. Rhodamine B is a hydrophilic molecule and has higher affinity with ethanol than acetonitrile. Therefore, molecule and solvent can penetrate the membrane together. Especially, the B series membranes could be more hydrophilic compared to series A due to the usage of DAMP as the bore fluid. Therefore, the decrease of affinity between acetonitrile and B-30 membrane lead to the increase of acetonitrile flux and decrease of Rhodamine B rejection in acetonitrile. On the other hand, the solvents flux of wet spun fiber is not much different, but Rhodamine B rejection in each solvent show quite different.

After post-treatment, B-30 sample shows the increase of acetonitrile flux due to the decrease of affinity between membrane and acetonitrile with the increase of hydrophilicity of membrane. The crosslinker penetrate more easily through porous shell side of the dry-wet spun fiber during post-treatment. The post-treated polyimide hollow fiber became more hydrophilic and finally B-30 membrane exhibits the highest flux among series B membranes. However, the effect of post-treatment on flux of wet spun fiber was not observed because of the double dense skin layers in wet spun fiber which limit the access of the crosslinker. The series B samples for rejections of Rhodamine B in acetonitrile solution showed the decrease from around 90% to less than 80%. This effect is due to the increase of solvent flux because of the increase of hydrophilicity of the membrane. In case of ethanol, the post-treated membranes prepared from dry-wet and wet phase inversion were

observed to increase the rejection. High interaction between solute and solvent may be decreased by post-treatment, resulting in the increase of interaction between solute and membrane. It should be pointed out that in-line crosslinked fibers showed higher Rhodamine B rejection in acetonitrile solution even without the additional post-treatment.

#### **5.4. Conclusions**

In this study, a new method to prepare solvent resistant nanofiltration hollow fiber membranes has been proposed for ensuring membrane stability during spinning process and saving time and cost for additional post-treatment. The hollow fiber membranes were prepared by dry-wet or by wet phase inversion method while pure water or aqueous diamine (DAMP) solution was used as the bore fluid. Dense layers were formed both in lumen and shell side for the wet spun fibers while dry/wet spun fibers have porous shell surface. In-line crosslinked membranes showed higher Young's modulus than the fiber which spun without crosslinker in bore fluid. However, the rigidness of the in-line crosslinked membranes has increased. The post-treated membranes showed good chemical stability in various solvents as well as ethanol and acetonitrile. Especially, in-line crosslinked fibers showed good chemical stability in the harsh conditions like aprotic solvents even without additional post-treatment. Moreover, in-line crosslinked membranes (as spun fibers) show higher rejection of Rhodamine B in acetonitrile (approximately 90%) solution compared to that obtained in ethanol solution (around 20%). However, after additional chemical crosslinking, rejection

decreased from 93% to 78% for dry-wet spun fiber and from 89 to 52% for wet spun fiber because of the increase of hydrophilicity of the membrane. Although in-line crosslinked hollow fiber membranes showed superior chemical stability even in the aprotic solvent such as NMP, FT-IR/ATR analysis revealed that the chemical crosslinking was not completed. Therefore, further optimization of the combined spinning and cross-linking process is required.

## References

1. P. Anil Kumar and S. Ana Maria, *Hollow Fiber Membrane-Based Separation Technology*, in *Solvent Extraction and Liquid Membranes*. 2008, CRC Press. p. 91-140.
2. T.S. Chung and E.R. Kafchinski, *The effects of spinning conditions on asymmetric 6FDA/6FDAM polyimide hollow fibers for air separation*. Journal of Applied Polymer Science, 1997. **65**(8): p. 1555-1569.
3. T.-S. Chung, *The limitations of using Flory-Huggins equation for the states of solutions during asymmetric hollow-fiber formation*. Journal of Membrane Science 1997. **126**: p. 19-34.
4. S. Darvishmanesh, F. Tasselli, J.C. Jansen, E. Tocci, F. Bazzarelli, P. Bernardo, P. Luis, J. Degreève, E. Drioli, and B. Van der Bruggen, *Preparation of solvent stable polyphenylsulfone hollow fiber nanofiltration membranes*. Journal of Membrane Science, 2011. **384**(1-2): p. 89-96.
5. S.M. Dutczak, M.W.J. Luiten-Olieman, H.J. Zwijnenberg, L.A.M. Bolhuis-Versteeg, L. Winnubst, M.A. Hempenius, N.E. Benes, M. Wessling, and D. Stamatiadis, *Composite capillary membrane for solvent resistant nanofiltration*. Journal of Membrane Science, 2011. **372**(1-2): p. 182-190.
6. P.B. Kosaraju and K.K. Sirkar, *Interfacially polymerized thin film composite membranes on microporous polypropylene supports for solvent-resistant nanofiltration*. Journal of Membrane Science, 2008. **321**(2): p. 155-161.
7. R. Liu, X. Qiao, and T.S. Chung, *The development of high performance P84 co-polyimide hollow fibers for pervaporation dehydration of isopropanol*. Chemical Engineering Science, 2005. **60**: p. 6674-6686.
8. X. Qiao and T.S. Chung, *Fundamental characteristics of sorption, swelling, and permeation of P84 co-polyimide membranes for pervaporation dehydration of alcohols*. Industrial and Engineering chemistry Research, 2005. **44**: p. 8938-8943.
9. S.-H. Choi, A. Brunetti, E. Drioli, and G. Barbieri, *H<sub>2</sub> separation from H<sub>2</sub>/N<sub>2</sub> and H<sub>2</sub>/CO mixtures with co-polyimide hollow fibre module*. Separation Science and Technology, 2011. **46**: p. 1-13.

10. Y. Liu, R. Wang, and T.S. Chung, *Chemical cross-linking modification of polyimide membranes for gas separation*. Journal of Membrane Science, 2001. **189**: p. 231-239.
11. M. Peer, M. Mahdeyarfar, and T. Mohammadi, *Investigation of singas ratio adjustment using a polyimide membrane*. Chemical Engineering Progress, 2009. **48**: p. 755-761.
12. P.S. Tin, T.S. Chung, Y. Liu, and R. Wang., *Separation of CO<sub>2</sub>/CH<sub>4</sub> through carbon molecular sieve membranes derived from P84 polyimide*. Carbon, 2004. **42**: p. 3123-3131.
13. J. Brandrup, E.H. Immergut, and E.A. Grulke, *Polymer handbook*. Fourth ed. 1999: Jon Wiley.
14. P. Silva, S. Han, and A.G. Livingston, *Solvent transport in organic solvent nanofiltration membranes*. Journal of Membrane Science, 2005. **262**: p. 49-59.
15. D.R. Lide, ed. *Handbook of chemistry and physics*. ed. 84. 2003-2004, CRC Press.
16. J. Ren, Z. Li, and F.-S. Wong, *Membrane structure control of BTDA-TDI/MDI (P84) co-polyimide asymmetric membranes by wet-phase inversion process*. Journal of Membrane Science, 2004. **241**: p. 305-314.
17. G.C. Kapantaidakis, G.H. Koops, and M. Wessling, *Effect of spinning conditions on the structure and the gas permeation properties of high flux polyethersulfone-polyimide blend hollow fibers*. Desalination, 2002. **144**: p. 121-125.
18. I. Pinnau, J.G. Wijmans, I. Blume, T. Kuroda, and K.V. Peinemann, *Gas permeation through composite membranes*. Journal of Membrane Science, 1988. **37**: p. 81-88.
19. D. Bhanushali, S. Kloos, C. Kurth, and D. Bhattacharyya, *Performance of solvent-resistant membranes for non-aqueous systems: solvent permeation results and modeling*. Journal of Membrane Science, 2001. **189**: p. 1-21.
20. J. Geens, B.V.d. Bruggen, and C. Vandecasteele, *Transport model for solvent permeation through nanofiltrationmembranes*. Sep. Purif. Technol., 2006. **48**: p. 255.
21. J.P. Robinson, E.S. Tarleton, C.R. Millington, and A. Nijmeijer, *Solvent flux through dense polymeric nanofiltration membranes*. Journal of Membrane Science,



2004. **230**: p. 29-37.

22. X.J. Yang, A.G. Livingston, and L.F.d. Santos, *Experimental observation of nanofiltration with organic solvents*. Journal of membrane Science, 2001. **190**: p. 45-55.
23. D. Bhanushali, S. Kloos, and D. Bhattacharyya, *Solute transport in solvent-resistant nanofiltration membranes for non-aqueous system: experimental results and the role of solute-solvent coupling*. Journal of Membrane Science, 2002. **208**: p. 343-359.

## General Conclusions

This study mainly focused on the preparation of solvent resistant polymeric membranes with controlled pore size (microfiltration, ultrafiltration and nanofiltration). Polydimethylsiloxane (PDMS) and P84<sup>®</sup> co-polyimide, which have an excellent chemical stability in various organic solvents, have been used as the membrane materials. In order to control the membrane morphology and properties various formation parameters (i.e., concentration of polymer concentration, solvent type, type and concentration of additives, evaporation time and phase inversion methods) have been carefully modulated.

Porous PDMS membranes have been prepared by two different approaches, and the permeation properties and morphology were characterized. Firstly, chemical additive which contains hydroxyl (-R-OH) functional group (i.e., methanol, ethanol, isopropanol, ethylene glycol and water) was added in PDMS crosslinker (-R'-Si-H) then mixed with PDMS pre-polymer. As the result of the chemical reaction between hydrogen terminated crosslinker and hydroxyl group in the additive, hydrogen (H<sub>2</sub>) gas was formed and diffused to air through the membrane. Porous PDMS films were successfully fabricated from a casting solution which contained more than 4 moles of ethylene glycol (EG) to 1 mole of crosslinker and cast at two different temperatures (0 or 30 °C). EG was the most suitable additive to make porous PDMS membranes because of the high viscosity of EG added casting solution which resulting in the decrease of diffusivity of H<sub>2</sub> gas. In addition, it should be noted that EG contains two -OH groups in a molecule which can form more H<sub>2</sub> gas in

the same casting condition. However, in this method, formation of porous in the membrane depends on the crosslinking speed of PDMS and H<sub>2</sub> formation rate which was extremely difficult to control. The second approach involves the use of physical additive (1,4-Dioxane) which can be dispersed in the casting solution and entrapped in membrane by curing of PDMS. To make porous structure, PDMS film was prepared at the temperature of 40 °C from casting solution which contains 60 wt% of 1,4-Dioxane. And then, it was immersed in water bath immediately to wash out the physical additive. Although porous PDMS membranes were successfully prepared by attempted two methods (i.e., addition of chemical or physical additive in casting solution), however, low porosity (less than 3%) and difficulty in pore size control make this technique unusable for the further study.

As a result of these drawbacks mentioned above, P84® co-polyimide as a new membrane material was alternated and prepared flat sheet and hollow fiber configuration. The effect of polymer concentration in polymer solution and additives on membrane properties was investigated. Especially, permeation properties were characterized in terms of solvents flux and solute (dyes and catalysts with different molecular weights) rejection in non-aqueous system. The increase of concentration of polymer and additives such as volatile solvent (1,4-Dioxane) and non-solvent (water or ethanol) additives induced sponge-like structure by delayed liquid-liquid demixing. This is mainly due to the increase of viscosity of casting solution and evaporation of additive solvents. The resultant membranes showed high solvent flux and high solute rejection compared to permeation properties of commercial membranes in

literatures. It is worthy of note that the membrane permeation properties were influenced not only by the membrane morphology but also by the affinity between membrane, solvent and solute. Furthermore, physical properties such as molar volume of solute, viscosity of solvent and charge of solute and membrane surface must take into account to explain and/or predict permeation properties. For instance, in this study, it was observed that the low rejection rate of Rhodamine B in ethanol solution compared to in acetonitrile solution.

The effect of the crosslinking conditions such as the concentration of crosslinker (1,5-Diamino-2-methylpentane; DAMP) and crosslinking time on membrane stability and permeation properties was investigated. FT-IR/ATR analysis was used to confirm and to optimize the chemical crosslinking of membranes. As increase the DAMP concentration and longer crosslinking time, imide bands were gradually disappeared and amide bands were appeared. Even the initial performance of the membranes crosslinked only for 5 minutes was good due to fast crosslinking reaction between the membrane and DAMP, crosslinking condition was proposed with 10 wt% of DAMP concentration for more than 7 hours for long-term durability in organic solvents.

The solvent resistant nanofiltration (SRNF) hollow fiber membranes have been prepared by different type of bore fluid in wet or in dry/wet phase inversion method. Especially, in-line chemical crosslinking was conducted by introducing an aqueous DAMP solution as the bore fluid to improve the chemical stability of the membrane during spinning process. Permeation properties of prepared hollow fiber were characterized by measuring the solvent flux and solute (Rhodamine B) rejection in

acetonitrile and ethanol. Dry/wet spun fibers showed higher solvents fluxes and higher rejection than wet spun fibers even though their porous shell surface which can be explained by resistant model.

In-line crosslinked fibers showed high acetonitrile flux and high solute rejection in acetonitrile solution with excellent chemical stability in various organic solvents without further post-treatment.

After post-treatment, the rejection of in-line crosslinked membranes in acetonitrile solution has been decreased from around 90% to less than 80%. It is due to the increase of hydrophilicity of the membrane by additional crosslinking. In case of ethanol solution, the solute rejection has been increased because of the strong interaction between membrane and solute compare to the interaction between solvent and membrane.